Report No. FAA-NA- 75-151

FLIGHT TEST INVESTIGATION OF THE VORTEX WAKE CHARACTERISTICS BEHIND A BOEING 727 DURING TWO-SEGMENT AND NORMAL ILS APPROACHES

L. J. Garodz - NAFEC
M. R. Barber - NASA FRC
R. L. Kurkowkski - NASA ARC

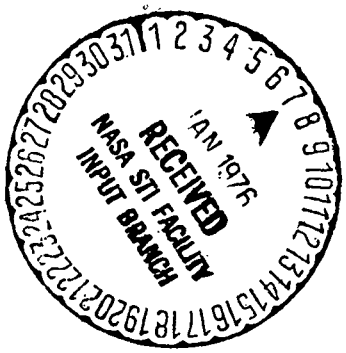

OCTOBER 1975

FINAL REPORT

U. S. DEPARTMENT OF TRANSPORTATION
FEDERAL AVIATION ADMINISTRATION
National Aviation Facilities Experimental Center
Atlantic City, New Jersey 08405

NOTICE

This document is disseminated under the sponsorship of the Department of Transportation in the interest of information exchange. The United States Government assumes no liability for its contents or use thereof.

1. Report No.	2. Government Accession No.	3. Recipient's Catalog No.
FAA-NA-75-151		

4. Title and Subtitle

Flight Test Investigation of the Vortex Wake Characteristics Behind a Boeing 727 During Two-Segment and Normal ILS Approaches

5. Report Date
October 1975

6. Performing Organization Code

7. Author(s) L. J. Garodz - NAFEC
M. R. Barber - NASA FRC
R. L. Kurkowkski - NASA ARC

8. Performing Organization Report No.
NA-75-151

9. Performing Organization Name and Address

Federal Aviation Administration
National Aviation Facilities Experimental Center
Atlantic City, New Jersey 08405

10. Work Unit No.
768-80-01

11. Contract or Grant No.

12. Sponsoring Agency Name and Address
U.S. Department of Transportation
Federal Aviation Administration
Systems Research and Development Service
Washington, D. C. 20590

13. Type of Report and Period Covered
Final Report

14. Sponsoring Agency Code

15. Supplementary Notes The Tests and evaluations presented in this Final Report are the results of a combined effort of the following Agencies: NASA FRC, CA.; NASA ARC, Moffett Field, CA.; FAA Western Region Los Angeles CA.; and FAA Flight Standards, Washington, D.C.

16. Abstract

A series of flight tests were performed to evaluate the vortex wake characteristics of a Boeing 727 (B727-200) aircraft during conventional and two-segment ILS approaches. Twelve flights of the B727, equipped with smoke generators for vortex marking, were flown wherein its vortex wake was intentionally encountered by a Lear Jet model 23 (LR-23) or a Piper Twin Comanche (PA-30); and its vortex location during landing approach was measured using a system of photo-theodolites.

The tests showed that at a given separation distance there were no readily apparent differences in the upsets resulting from deliberate vortex encounters during the two types of approaches. Timed mappings of the position of the landing configuration vortices showed that they tended to descend approximately 91 meters (300 feet) below the flight path of the B727. The flaps of the B727 have a dominant effect on the character of the trailed wake vortex. The clean wing produces a strong, concentrated vortex. As the flaps are lowered, the vortex system becomes more diffuse. Pilot opinion and roll acceleration data indicate that 4.5 nautical miles would be a minimum separation distance at which roll control could be maintained during parallel encounters of the B727's landing configuration wake by small aircraft. This minimum separation distance is generally in scale with results determined from previous tests of other aircraft using the same roll control criteria.

17. Key Words (Suggested by Author(s))		18. Distribution Statement
Trailing vortices	Vortex wake effects	Document is available to the public through the National Technical Information Service, Springfield, Virginia 22151
Wake turbulence	Airway spacing	
Aircraft wakes	Two-segment approach	

19. Security Classif. (of this report)	20. Security Classif. (of this page)	21. No. of Pages	22. Price*
Unclassified	Unclassified	138	

*For sale by the National Technical Information Service, Springfield, Virginia 22151

TABLE OF CONTENTS

SYMBOLS

A_n	Normal acceleration, g units
A_x	Longitudinal acceleration, g units
A_y	Lateral acceleration, g units
C_L	Airplane lift coefficient
C_{h_e}	Elevator hinge moment coefficient
C_l	Rolling moment coefficient
$C_{l_{\delta_a}}$	Lateral control effectiveness derivative, per degree
$C_{m_{\delta_e}}$	Pitch control effectiveness derivative, per degree
C_Y	Side force coefficient
$C_{Y_{\delta_r}}$	Side force control effectiveness derivative, per degree
$\dot{P}_{\delta_{a_{max}}}$	Maximum roll control acceleration, rad/sec^2
$\dot{P}_{vortex}$	Roll acceleration induced by vortex, rad/sec^2
P	Roll rate, rad/sec or deg/sec
q	Pitch rate, rad/sec
r	Yaw rate, rad/sec
α	Angle of attack, deg
β	Angle of sideslip, deg
θ	Airplane pitch angle, deg
ϕ	Airplane roll angle, deg
ψ	Airplane yaw angle, deg
δ_a	Aileron deflection, deg
δ_e	Elevator deflection, deg

δ_f	Flap deflection, deg
δ_r	Rudder deflection, deg
γ	Glide slope angle, deg
$\Delta()$	Change in value of the parameter

A dot over a quantity denotes the time derivative of that quantity.

SUMMARY

A series of flight tests were performed to evaluate the vortex wake characteristics of a Boeing 727 (B727-200) aircraft during conventional and two-segment ILS approaches. Twelve flights of the B727, equipped with smoke generators for vortex marking, were flown wherein its vortex wake was intentionally encountered by a Lear Jet model 23 (LR-23) or a Piper Twin Comanche (PA-30); and its vortex location during landing approach was measured using a system of photo-theodolites.

The tests showed that at a given separation distance there were no readily apparent differences in the upsets resulting from deliberate vortex encounters during the two types of approaches. Timed mappings of the position of the landing configuration vortices showed that they tended to descend approximately 91 meters (300 feet) below the flight path of the B727. The flaps of the B727 have a dominant effect on the character of the trailed wake vortex. The clean wing produces a strong, concentrated vortex. As the flaps are lowered, the vortex system becomes more diffuse. Pilot opinion and roll acceleration data indicate that 4.5 nautical miles would be a minimum separation distance at which roll control could be maintained during parallel encounters of the B727's landing configuration wake by small aircraft. This minimum separation distance is generally in scale with results determined from previous tests of other aircraft using the same roll control criteria.

INTRODUCTION

Results of NASA, FAA and airline flight tests and on-line evaluations of two-segment approaches indicated this to be an operationally effective means for noise abatement (Reference 1, 2). However, because of the terminal area mixture of two-segment traffic with normal ILS traffic, concern has been expressed that the wake vortex resulting from a two-segment approach may present a problem to other aircraft, especially light general aviation aircraft making a standard ILS approach. The purpose of this program was to assess the severity of vortices trailing a typical narrow-body jet with aft-mounted engines on a two-segment approach and to assess the impact, if any, on existing and/or proposed IFR separation standards.

A joint NASA/FAA Test Team was organized to investigate wake turbulence characteristics associated with operation of a Boeing 727 (B727) aircraft during conventional and two-segment ILS approaches. An Inter-agency Agreement (DOT-FA73-WAI-384) was established between NASA and DOT/FAA on September 25, 1973. A series of flight tests were conducted at the NASA Flight Research Center during the time period of October 31, 1973 through November 5, 1973.

The objectives of these flight tests were as follows: (a) obtain qualitative and quantitative evaluations of the upset responses of two

general aviation aircraft (Lear Jet LR-23 and Piper PA-30) resulting from deliberate encounters of the vortex wake behind a B727 (landing configuration) during two-segment and conventional approaches (most of these were simulated approaches at high altitude), (b) measure the drift and persistence of the B727's wake during two-segment and conventional ILS approaches, (c) measure the effect of different flap deflections, thrust settings, etc., on the wake characteristics, and (d) compare the vortex shed by the B727 with those shed by other aircraft.

This report describes the flight tests and test equipment, and presents the results of the study.

TEST AIRCRAFT AND EQUIPMENT

Wake Vortex Generator Aircraft

The B727 was selected as the wake vortex generator aircraft because it constitutes a large portion of the current air carrier service fleet, it is expected to continue in airline service in significant numbers well into the 1980's, and its vortex wake characteristics were not well documented. The aircraft was equipped with corvus oil smoke generators for vortex marking. Figure 1 is a photograph of the generating aircraft and figure 2 is a closeup photograph of the vortex markers. The aircraft's pertinent physical characteristics are contained in Table I.

A B727-200 aircraft was leased from United Airlines. The aircraft had just been used in a six-month operational flight evaluation of a two-segment approach guidance system. The evaluation included 65 approaches in actual IFR weather. The aircraft was equipped with both a two-segment approach avionics system and a digital data recording system. Detailed descriptions of the avionics and data systems are contained in reference 2. A DME transmitter/antenna was co-located with the glide slope antenna at Edwards AFB to provide information needed for the two-segment guidance.

Wake Vortex Probe Aircraft

A Lear Jet Model 23 (LR-23) and a Piper Twin Comanche (PA-30) were used to probe the B727's wake. Figures 3 and 4 present photographs of the two aircraft respectively. Both aircraft were instrumented to measure vortex-induced upset characteristics. Both aircraft were also equipped with air-to-air ranging DME using a beacon system which was mounted in the B727. The DME range was displayed to the probe aircraft pilots and recorded on the data systems. The LR-23 was equipped with a three-component hot-wire anemometer which was mounted on a nose boom in close proximity to the airspeed and angles-of-attack and sideslip sensors. The anemometer was used for measuring the velocities in the vortex flow field. The data from these measurements will be contained in a subsequent NASA report.

It should be noted that the LR-23 control system is equipped at the factory with autopilot, yaw damper, stick shaker and stick pusher. For the purposes of this test program, the autopilot and yaw damper were deactivated. For stall protection, the stick shaker and pusher remained active and were activated on occasion during the penetration probes.

Table I presents the pertinent physical characteristics of the LR-23 and the PA-30.

Supporting Aircraft

A Lockheed F-104 military fighter aircraft was utilized to probe the B727's vortex prior to probes by the LR-23 and PA-30. These probes were performed as a safety precaution because calculations had indicated that the LR-23 and PA-30 might experience severe loads during the probes. The F-104 probes showed that the calculations were too conservative and the tests were continued as planned.

A Cessna 402-B (C-402) aircraft was used for airborne meteorological surveys during this flight. The instrument package for meteorological determinations consisted of an ambient air temperature sensor, a dew point hygrometer, a barometer, altimeter, airspeed indicators and an inertial navigation system used to provide geographical location and to derive local horizontal wind fields. An inertial subrange turbulence meter (epsilon meter) was used to establish the levels of atmospheric turbulence. Altitude surveys were made for every flight condition. The survey aircraft flew in the vicinity for all vortex probes and vortex mapping runs, in order to document the atmospheric conditions.

Photo chase aircraft were a North American T-28 and a Grumman Gulfstream.

Wake Vortex Mapping System

A photo-theodolite vortex mapping system was utilized to track the vortex as visualized by the smoke. Figure 5 presents the conventional and two-segment approach geometries and points out the location of the photo-theodolites. By placing the photo-theodolites on both sides of the runway, the horizontal and vertical drift of the vortex could be determined.

TEST DESCRIPTION

The test program is outlined in Table II. It consisted of 12 flights of the B727 vortex generator, during which the probe aircraft were utilized to evaluate (1) vortex upset characteristics by in-trail probes and (2) wake vortex velocity by cross-track probes. The crew of the LR-23 consisted of a NASA pilot, a FAA pilot and a NASA flight test engineer. The crew of the PA-30 consisted of two NASA pilots for initial flights. During later

flights the PA-30 was crewed by a NASA pilot and a FAA pilot. The B727 was flown by a United Airlines crew with NASA and FAA pilot observers on board. The photo-theodolite system was used to measure the vortex position relative to the two-segment and conventional approach paths during landing approach. Meteorological information (winds, turbulence, humidity and temperature gradients) was documented for each test flight condition, using the instrumented C-402.

A summary of the separation distances at which data were obtained during in-trail penetrations of the vortex wake of the B727's landing configuration is shown in Table III. Deliberate in-trail wake encounters were attempted for a larger range of distances; however, these attempts were not always successful due to the inherent difficulty in locating the vortex core precisely in the diffused smoke trail. The information is grouped for probes (a) in level flight at altitude (3,658 meters (12,000 ft.) m.s.l.), (b) for simulated 3 and 6 degree approach descents at altitude, and (c) for a limited sequence of low altitude approach runs.

RESULTS AND DISCUSSIONS

In the following section, the flight test results are summarized. The vortex wake characteristics during two-segment and conventional approaches are compared on the basis of upset responses for deliberate wake encounters by the probe aircraft, and vortex wake drift. The effect of flap configuration on the vortex wake is discussed. Finally, a comparison is made of the results of this investigation with those from previous tests of other transport aircraft.

I. Comparison of Vortex Wake Characteristics Generated During Two-Segment and Conventional Approaches

The vortex wake behind the B727 in a landing configuration with 30° flaps was evaluated. Evaluations were made first in level flight, and then for both 3° and 6° descending flight paths. The descending flight paths correspond to the conventional and the upper segment of a two-segment approach, respectively. A time history of the probe aircraft response is presented for a typical encounter and the maximum disturbances from all encounters are summarized. This is followed by a discussion of separation distances based on roll control criteria and pilot comments.

Lear Jet Vortex Encounters

Typical Response Dynamics.- Figures 6a and 6b present a representative time history of the LR-23 response to an encounter with the B727 wake at 2,743 meters (9,000 ft.) altitude during a simulated 6° landing approach flight path. Separation distance between the two aircraft was 2.7 nautical miles at the time of encounter. The initial encounter occurred at 1.2 seconds as indicated principally by large transient responses of the α and β

sensor vanes, plus rapid generation of pitch and roll angular accelerations with no change in the corresponding controls. Additional manifestations of the vortex flow on this run were an abrupt 20 knot increase in indicated airspeed coincident with an abrupt 0.1 g change in longitudinal acceleration. A second encounter occurred about 3.0 seconds later disturbing the airplane primarily in pitch. Recovery from these two encounters was achieved after the airplane had pitched down approximately 17° from its initial pitch attitude and rolled to a 90° left bank, using full opposite aileron control to return to wings level attitude. Protection from stall for the LR-23 is provided by a stick shaker and pusher system. Stick pusher actuation was initiated at 0.8 seconds and again at 3.8 seconds, contributing to the nose down pitch attitude change. A detailed analysis of the influence of these momentary stall conditions is contained in Appendix A.

A summary observation from all the encounters is that, in general, the LR-23 excursions were primarily about the roll and pitch axes, with minor dutch-roll disturbances.

Maximum Disturbance Summary.- Maximum responses of the LR-23 from deliberate encounters with the B727 wake are summarized on Figures 7a and 7b. They cover a separation range between the aircraft varying from 2.1 to 3.3 nautical miles. These data were obtained during flight along 3° and 6° descending flight paths from either 3,658 meters (12,000 ft.) or 1,524 meters (5,000 ft.) initial altitude levels. The B727 flew a steady descending flight path (either 3° or 6°) while the LR-23 probed the vortex wake of the B727. Therefore, the flight path of the probe aircraft varied about the nominal 3° or 6° descending flight path. Both aircraft (probe and generator) were in the landing configuration. Figures 8a and 8b present the same data as a function of vortex age rather than separation distance. This is done to facilitate analysis because vortex breakdown depends on its age rather than a separation distance; furthermore, separation distance varies with aircraft true airspeed.

The vortex wake encounters produced maximum roll angular accelerations of the LR-23 as high as 3.0 rad/sec^2. Angular accelerations in pitch and yaw reached maximums of about one-half and one-tenth the roll acceleration respectively. Peak-to-peak linear acceleration oscillations up to a maximum of about 0.3 g laterally were measured and peak-to-peak normal acceleration oscillations reached about 1.5 g. Maximum bank angles exceeded 45° in only one instance. Pitch attitude excursions, generally nose down, reached a maximum of 12°. The scatter in the data merely indicates that not all encounters result in large upsets or accelerations and the dynamics vary depending on entry angle, position, pilot control inputs, stability augmentation system inputs, and stick pusher inputs. One factor, developed in Appendix A, illustrates that a relationship exists between the severity of upset resulting from an encounter, and the conventional stall dynamics of the LR-23. It is shown that severity-of-encounter is linked with decreasing control power, as the angle of attack approaches stall values.

Any possible effect of altitude on the severity-of-encounter was obscured because at the time of these flight test measurements, atmospheric

turbulence, shown on Figure 9, varied from negligible to light at altitude, but approached heavy turbulence at the lower altitude. Presuming that increased turbulence would cause earlier attenuation of the wake (reference 6), less severe encounter excursions of the probing aircraft would be expected at lower altitudes, for similar separation distances.

Comparison of the 3° and 6° data, measured at high and low altitudes, indicates that there are no obvious differences in encounter dynamics due to the glide path angle of the generator aircraft.

LR-23 Roll Control Criteria for Separation Distance.- Reference 3 proposed a criterion for determining minimum safe separation behind larger aircraft using a rolling moment control ratio for the probe aircraft and the gross weight of the generating aircraft. The rolling moment control ratio is the measured vortex-induced roll acceleration divided by the maximum available roll acceleration control. When this ratio exceeds one, roll control is lost. The roll ratio data for the encounters by the LR-23 were calculated and are presented in figures 10 and 11 as a function of separation distance and vortex age respectively over the separation range covered. The B727 flaps were deflected to the landing configuration $\delta_f = 30°$.

To obtain the maximum roll acceleration induced by the vortex the measured values were adjusted for roll acceleration produced by any initial aileron deflection which may have existed at the time of encounter. Maximum roll control power was derived from data measured during a series of aileron pulses. An average value of $C_{l_{\delta_a}} = .00114$ per degree was obtained from the pulse maneuvers and this was used to determine $\dot{P}_{\delta_{a_{max}}}$ for each encounter.

Using maximum encounter roll acceleration equal to maximum control power as the criterion for minimum separation, the data presented in figure 10 suggest that 4 nautical miles would be required for this aircraft combination. However, the test data covered a very small range of separation distances, compared with previous flight tests using this criterion and any judgments should be tempered by the additional factors influencing minimum separation distance as enumerated in reference 3 and as discussed in the following pilots comments.

LR-23 Probe Pilot Comments.- Observations made by NASA and FAA pilots while flying the LR-23 probe airplane, and ground observations by the LR-23 pilot of low altitude over-flights by the generating aircraft, produced the following comments.

1. "Calm air and a 'flaps-up' configuration of the generating airplane presented the worst case to the trailing airplane. With the passage of time, even in calm air, wake vortices dissipate. The characteristic break-up occurs as a longitudinal gathering of the vortex, followed by a radial expansion appearing as a large doughnut, and within approximately five or so seconds after that, dissipation is complete.

[1]Radar controlled

From the pilot point of view, safe separation must be based on this worst case until other effects can be adequately measured and taken into account. The above described break-up and dissipation consistently happens between a minute, and a minute and a half, in the case of the B727. A separation of two minutes should therefore provide safety as well as an adequate margin. With a typical approach speed of 130 knots for the generating airplane, a separation distance of 4.5 nautical miles would assure vortex dissipation even in the worst case for the trailing airplane.

2. Generating airplane flap-deflection was observed very clearly to provide secondary vortices which tended to mingle with and speed the destruction of the primary wing tip vortices in proportion to the amount of flap deflection. Penetration of the trailing vortices produced significantly less disturbance at 30° or more flap deflection compared to the flaps-up configuration at equal vortex ages. Therefore, separation could be safely reduced somewhat (i.e., less than two minutes or 4.5 n.m.) if the generating B727 were known to have at least 30° of flaps extended. However, where decelerating approaches are made at lesser flap deflection until the last two or three miles prior to touchdown, the reduced separation could not be considered appropriate.

3. Generating-airplane thrust was observed to have a significant effect on vortex destruction. Encounters behind the B727 with 15° flaps extended, first with approach power during a 3° descent and then with climb power at the same speed and flap setting, showed a marked reduction in vortex strength for the high-thrust condition. Thus, safe separation during climbout could be somewhat less than during approach. This same observation was made while penetrating the wake of a C-5A in a CV-990 in similar tests conducted in 1970.

4. Atmospheric turbulence was observed (as is well known) to speed the break-up of the tip vortices significantly, leading to the conclusion that safe separation could also be reduced during periods of gusty wind or similar atmospheric instability.

5. No significant difference in aircraft upset and vortex wake dissipation characteristics could be determined while probing the wake vortex of the generator aircraft on either the 6° or 3° descending flight paths. Therefore, a separation distance which provides adequate margin when following another aircraft on a conventional approach should also be acceptable when following that aircraft on a two-segment approach."

Piper Twin Comanche Vortex Encounters

PA-30 Maximum Disturbance Summary.- Figures 12a and 12b present the maximum absolute excursions of the pertinent parameters for the PA-30 encounters with the B727 wake. Figures 13a and 13b present the same upset

information in terms of vortex age rather than separation distances. In general, the PA-30 excursions are similar in character to those of the LR-23. The attitude deviations of the PA-30 are larger, which would be expected as a result of its lower velocity and lighter wing loading. Deviations in yaw were on the order of seven times greater and pitch about two times greater for the PA-30. The PA-30 data cover a somewhat larger range of separation distances than the LR-23 data. No consistent differences can be observed for the encounter upsets resulting from the different flight paths.

PA-30 Roll Control Criteria for Separation Distance.- The ratio of the maximum vortex induced rolling accelerations to roll control power for the PA-30 flying at 100 KIAS, during several encounters are shown in Figures 14 and 15 plotted as functions of separation distance and vortex age respectively. The B727 was in the landing configuration (30° flaps, gear down) for all these encounters. The induced accelerations have been adjusted for control input in the same manner as the LR-23 data. Maximum available roll control power was determined by measuring the roll accelerations resulting from sharp aileron pulses and was found to be approximately $C_{l_{\delta_a}}$ = .00088 per degree. These data show the ratio of vortex induced roll acceleration to roll control power is still greater than one at separation distance in excess of 4 nautical miles.

PA-30 Probe Pilot Comments.- Observations made by a NASA pilot while flying the PA-30 Twin Comanche during deliberate wake vortex encounters at varying distances behind a Boeing 727-200 produced the following comments.

> "During all probes made by the PA-30, the B727 was in a landing configuration with 30° of flap and gear down. The vortex wake appeared to descend below the B727 about 76.2 meters (250 feet). All probes of the wake by the PA-30 were made from an in-trail position. Attempts were made to probe from above and below the wake. The majority of the probes of the wake were made from below the wake. Successful probes were made from between two and five nautical miles.
>
> To evaluate the upset of the PA-30 by the wake, I used the following criteria:
>
> 1. If the type of upset encountered could cause a break off of an ILS approach, it was considered severe.
>
> 2. If the bank angle exceeded 30° before the airplane roll could be controlled, this was considered a severe upset.
>
> 3. If normal accelerations excursions of ±1.0 g's were encountered, this was considered a severe upset.
>
> On the first two flights with the PA-30 I let the airplane respond to the wake by neutralizing controls. On the last two flights I tried to control the airplane at all times. During these last two flights, on

several occasions, full aileron and rudder control were used in attempts to control the airplane during upsets.

Severe upsets were occasionally encountered by the PA-30 at distances of up to four nautical miles behind the B727. However, most of the time only light to moderate turbulence was found in the vortex wake at distances greater than two miles behind the B727. It appeared as though there were patches of high energy wake behind the B727. If the PA-30 got into one of these, the upset was severe. If not, the upset was like flying in light to moderate atmospheric turbulence. It should be pointed out, however, that I never could be sure what part of the wake I encountered. When the PA-30 got a severe upset there was usually some very sharp normal acceleration changes followed by an uncontrollable rolling motion. Based on the results of these tests, I would not want to fly the PA-30 at separation distances closer than 4.5 nautical miles during approach to landing, behind a landing configured B727 type airplane."

Vortex Drift Characteristics

Figure 16a through 16f present the vertical position of the B727 vortex wake versus distance behind the aircraft for two conventional approaches (figures 16a and b), two two-segment approaches (figures 16c and d), and two take-off maneuvers (figures 16e and f). A review of these data shows that the vortices tend to settle to something of the order of 91.4 meters (300 feet) below the B727's flight path and then stop descending. Longer persistence of the smoke-marked vortex for the take-off configuration (15° flaps) allowed data to be taken for greater distances than during the landing approaches (30° flaps). It should not be concluded that the lack of vortex "track" indicates a lack of vortex existence. To the contrary, the PA-30 upsets shown in figure 14 verify that the vortex did exist behind the B727 to distances in excess of four nautical miles (note that the flagged symbols on figure 14 are encounters at low altitude that were performed on an actual approach).

Given then that the vortex tends to settle and that it could exist for distances in excess of four nautical miles behind the generating aircraft, the simplified geometric analysis presented in figure 17 can be performed. This analysis assumes a reasonable extrapolation of the wake settling data (for the vertical plane) presented in figure 16, and thereby indicates that the B727's vortex would be something of the order of 91.4 meters (300 feet) below its flight path at a separation distance of three miles. The vortex then superimposed on the approach geometries would indicate that an encounter by an aircraft on a conventional approach following an aircraft on a two-segment approach might occur somewhere prior to the "two-segment knee," at an altitude on the order of 243.8 meters (800 feet). Evaluating the possibilities of a wake encounter when both aircraft are flying a conventional approach it can be seen that if a lead aircraft is "right on glidepath" or slightly high and an aircraft following at three miles is low on the glidepath beam, an encounter could occur. However, these

encounters would likely occur at a higher altitude than the one predicted for the two-segment approach.

The question of the relative difference of the probability of encounter for the two types of approach profiles cannot be answered from this flight test. However, the data of this test should be of value for use in such a detailed analysis. The vortex location data for all the runs obtained during the tests (14) are presented in Appendix B. Figures B1a through B1n present the location as a function of distance behind the B727 generating aircraft. Figures B2a through B2n present the location data as a function of time after the B727 passage. Many other variables must be considered in a probability analysis including items such as statistical data on flight path control error, guidance system errors, wind shears, atmospheric turbulence, etc.

II. Effect of Generator Aircraft Flap Configuration

This section covers the effect of generator aircraft flap setting on the wake vortices. These effects are discussed in terms of (a) visual observations of the differences in the smoke-marked vortices, and (b) probe aircraft response as a function of flap setting.

Visual Observations

One significant observation of the program was that wing flap extension on the B727 aircraft had a pronounced effect on the characteristics and persistence of the trailing vortex system. With no flap extension ("clean configuration") the vortex, as visualized by the smoke, was small in diameter, approximately 0.61 meters (2 feet), and retained a well defined structure to a distance of approximately eight nautical miles behind the aircraft in smooth air at 3,658 meters (12,000 feet) altitude. This corresponded to a vortex age of approximately 120 seconds. Probes of this clean configuration vortex system led to the qualitative assessment that these vortices produced large upsets of the probing aircraft (LR-23 and F-104) at separation distances of six to seven nautical miles. Figure 18 presents a photograph of the "clean configuration" B727 vortex.

Figures 19a and 19b present a photograph of the B727 with the flaps extended to the landing configuration (30°). In this configuration an interaction of the flap vortices with the wing-tip vortices creates a vortex system that was much larger in diameter than that of the vortex system associated with the clean configuration. This interaction appears to occur within a few span lengths behind the wing. One effect of this interaction was that it tended to diffuse the vortex-marking smoke. With the smokers operating with peak-performance, probe pilots could discern vortex-marking smoke at approximately three to four nautical miles behind the landing configured B727.

Figures 20 through 22 show the effect of aircraft flap configuration on vortex persistence. These photos were taken during low altitude

fly-overs in smooth morning air. Figures 20a through 20o present photographs taken at five second time intervals of the B727's vortex with the clean wing. A review of the figures shows that vortex bursting starts to occur at 55 seconds of age, and that complete vortex breakdown has occurred by 70 seconds.

Figures 21a through 21p present the same information for the take-off configuration (15° flaps) of the B727. The mode of breakdown appears to be viscous decay occurring at 75 seconds. Data for this configuration illustrate the possible wake encounter hazard for a small aircraft during climbout after take-off.

Figures 22a through 22h present the landing configuration persistence. It is interesting to note that the vortex system 10 seconds behind the aircraft has begun to take on a "ragged" appearance as compared to the previous configurations. However, at later times the vortex appears to regain a smooth appearance until at 40 seconds, the vortex became invisible to the photographer. This disappearance of the 30° flap configuration vortex before any onset of breakdown is obviously a result of the smoke becoming so diffuse that it can no longer mark the vortex. The diffusion is caused by the effect shown in figure 19 wherein the smoke entrained in the tip vortex appears to wrap around the flap vortex, thereby diffusing the smoke.

The fact that the landing configuration vortex smoke was diffusing prior to vortex breakdown created operational problems throughout the flight test. Lack of vortex visibility made the vortex encounters for this configuration difficult to achieve, limited the vortex drift measurements and eliminated a visual measurement of vortex persistence.

Aircraft Response Data

Figures 23a and 23b present a summary of maximum response of the Lear Jet to encounter with the B727 wake for two flap configurations during level flight tests near the nominal 3,658 meter (12,000 feet) altitude. Shown are comparisons between the wake generated from the landing-flaps configuration versus the clean-wing configuration, in terms of the Lear Jet response. The severity-of-encounter behind the clean configuration was roughly equivalent to the landing flaps data at over twice the separation distance. Figures 24a and 24b present the same data versus vortex age. The upset response data indicate that the vortex wake for the clean configuration persisted for a longer time by a factor of 2.5 to 3.0, considering the difference in B727 speeds in the two configurations. In addition, these comparisons illustrate the effect of the vortex characteristics shown in figures 20 and 22 in terms of the upsets induced by the vortex.

III. Comparison With Previous Data

A comparison of the landing-configured Boeing 727 wake vortex data obtained from these tests was made with data from previous tests as reported

in reference 3. As discussed earlier, the criteria used for this comparison was the measure of the ratio of roll disturbance to roll control capability. The distances where this ratio becomes one are plotted in figure 25 for various average gross weights. The pilot opinions of minimum separation distances are also plotted. Perhaps the most significant aspect of the pilot comments from the subject test is that pilots of both aircraft agree that 4.5 nautical miles would be the minimum separation distance that they would deem satisfactory for an operational encounter of the landing-configured B727's vortex. This agrees with the roll control criteria data of 4.5 nautical miles for the PA-30 and 4 nautical miles for the LR-23.

Figure 25 presents a relatively complete set of data for the determination of minimum separation distances for various generating and encountering aircraft combination. In general, the figure shows good correlation of the B727 results with those of other aircraft. The figure then would lead to the conclusion that the gross weight of the vortex generating aircraft is a dominant factor affecting separation distance.

CONCLUSIONS

A. Based on a limited number of deliberate penetrations of the B727 landing configuration (30° flaps) wake vortex, there were no readily apparent differences in the upsets resulting from two-segment and conventional approach paths.

B. The vortices from the B727 tend to settle to approximately 300 feet below the flight path of the aircraft and then stop descending.

C. NASA and FAA pilot opinion and roll acceleration data indicate that 4.5 nautical miles would be a minimum separation distance at which roll control could be maintained during parallel encounters of the B727's landing configuration vortex wake by small aircraft. This minimum separation distance is generally in scale with results determined from previous tests of other aircraft using the same roll control criteria.

D. Based on an analysis of the LR-23 data, it appears that stall aerodynamics can contribute significantly to the severity of upset resulting from an encounter.

E. B727 flap configuration has a definite effect on the vortex shed by the aircraft. The clean wing results in a concentrated, well-defined vortex core. As the flaps are lowered the vortex tends to become more diffuse and creates less of an upset on an encountering aircraft.

REFERENCES

1. Denery, D. G., White, K. C., and Drinkwater III, F. J.: "A Resume of the Status and Benefits of the Two-Segment Approach and Its Applicability to the Jet Transport Fleet." AIAA 6th Aircraft Design, Flight Test, and Operations Meeting, Los Angeles, California, August 14, 1974.

2. Schwind, G. K., Morrison, J. A., Nylen, W. A., and Anderson, E. B.: "Operational Flight Evaluation of the Two-Segment Approach for Use in Airline Service." United Air Lines, January 1974.

3. Andrews, William H., Robinson, Glenn H., Larson, Richard R.: "Exploratory Investigation of Aircraft Response to the Wing Vortex Wake Generated by Jet Transport Aircraft." NASA TN D-6655, March 1972.

4. Soderman, Paul T., and Aiken, Thomas N.: "Full-Scale Wind-Tunnel Tests of a Small Unpowered Aircraft with A T-Tail." NASA TN D-6573, November 1971.

5. MacGready, Paul B., Jr.: "Standardization of Gustiness Values from Aircraft." Journal of Applied Meteorology, Vol 3, No. 4, August 1964, pp. 439-449.

6. Tombach, Ivar: "Observations of Atmospheric Effects on Vortex Wake Behavior." Journal of Aircraft, Vol. 10, No. 11, November 1973, pp. 641-647.

TABLE I - TEST AIRCRAFT CHARACTERISTICS

	B 727-200	LR-23	PA-30
TEST WEIGHT, Kg (lbs)	68,038 (150,000)	5,443 (12,000)	1,587 (3,500)
WING SPAN, m (ft)	32.9 (108.0)	10.4 (34.1)	10.9 (36.0)
WING AREA, m^2 (ft^2)	157.9 (1,700)	21.5 (231.8)	16.5 (178.0)
TEST WING LOADING, Kg/m^2 (lbs/ft^2)	431 (88.2)	253 (51.8)	96 (19.7)
TEST FLAP SETTINGS			
TAKE-OFF, deg	15	20	15
LANDING, deg	30	40	27
NOMINAL TEST SPEEDS			
APPROACH, KIAS	145	150	90
CLIMB, KIAS	150	150-170	90
STALL, KIAS (LANDING CONFIGURATION)	110	90-100	61

TABLE II - FLIGHT-TEST INVESTIGATION OF WAKE TURBULENCE BEHIND B727

DATE: OCT. 31, 1973

TEST OBJECTIVES	AIRCRAFT STATUS									TM*	RADAR	LAKEBED	NOISE	ECHO 2
	FLT NO	TEST TIME	B 727	F-104	LEARJET	PA-30	C-402	T-28	GULFSTREAM					
A. TAKEOFF RWY. 04 FOR NOISE MEASUREMENTS	1	0615	GEN.†				MET. MEAS.				X	X	X	
B. TWO-SEGMENT APPROACH VORTEX MAPPING (2)			LNDG.				↓				X	X	X	
C. FLYOVERS (6) (TO, CLN, LDG, TO, CLN, LDG)											X			
D. CONVENTIONAL APPROACH VORTEX MAPPING (2)			LNDG.				↓				X	X	X	
		0745												
IN-TRAIL PROBES (727 LANDING CONFIG) 12,000'	2	1045	GEN.				MET.	PHOTO						
A. F-104 PROBES (2 RUNS)**			↓	PROBE	PROVIDE SEPARATION DISTANCE		MEAS. ↓	CHASE ↓		X	X			
B. LEAR PROBES (3 RUNS)					PROBE						X			
		1200												
IN-TRAIL PROBES (727 CLN & LNDG. CONFIG) 12,000'	3	1430	GEN.				MET.	PHOTO						
A. F-104 PROBES			CLN	PROBE	SEPARATION DISTANCE		MEAS. ↓	CHASE ↓		X	X			
B. LEAR PROBES			CLN		PROBE						X			
C. PA-30 PROBES (6)			LNDG.			PROBE				X	X			
		1600												

*T.M. = TELEMETERED DATA
RADAR = RADAR TRACKING
LAKEBED = VORTEX MAPPING MEASUREMENTS
NOISE MEAS. = NOISE MEASUREMENTS
ECHO 2 = GROUND BASED PHOTOGRAPHY

**EACH RUN IS SEVEN MINUTES WITH SEVERAL PROBES

†GEN. = WAKE VORTEX GENERATOR

TABLE II - FLIGHT-TEST INVESTIGATION OF WAKE TURBULENCE BEHIND B727 - Continued

DATE: NOV. 1, 1973

TEST OBJECTIVES	AIRCRAFT STATUS									TM*	RADAR	LAKEBED	NOISE	ECHO 2
	FLT NO	TEST TIME	B 727	F-104	LEARJET	PA-30	C-402	T-28	GULFSTREAM					
APPROACH VORTEX MAPPING & NOISE MEAS.	4	0615	GEN.				MET. MEAS.		PHOTO CHASE					
A. TAKEOFF 04 FOR NOISE MEAS. (2)			T.O.				↓		↓		X	X	X	
B. TWO-SEGMENT APPROACHES (2)			LNDG.								X	X	X	
C. CONVENTIONAL APPROACHES (2)			LNDG.								X	X	X	
		0745												
TWO-SEG. APPROACH PROBES AT ALTITUDE 12,000'	5	1300	GEN. (LNDG)				MET. MEAS.		PHOTO CHASE					
A. F-104 PROBE (1 RUN)			↓	PROBE	PROVIDE SEPARATION DISTANCE		↓		↓	X	X			X
B. LEAR PROBES (3 RUNS)					PROBE						X			X
C. PA-30 PROBES (3 RUNS)						PROBE				X	X			X
		1430												

*T.M. = TELEMETERED DATA
RADAR = RADAR TRACKING
LAKEBED = VORTEX MAPPING MEASUREMENTS
NOISE MEAS. = NOISE MEASUREMENT
ECHO 2 = GROUND BASED PHOTOGRAPHY

TABLE II - FLIGHT-TEST INVESTIGATION OF WAKE TURBULENCE BEHIND B727 - Continued

DATE: NOV. 2, 1973

TEST OBJECTIVES	AIRCRAFT STATUS									TM*	RADAR	LAKEBED	NOISE	ECHO 2
	FLT NO	TEST TIME	B 727	F-104	LEARJET	PA-30	C-402	T-28	GULFSTREAM					
SMOKE OBSERVATION & IN-TRAIL PROBES LEVEL FLT, 12,000' 727 ALL CONFIGS.	6	1030	GEN.				MET. MEAS.		PHOTO CHASE					
A. SMOKE OBSERVATIONS				OBSERVE	OBSERVE						X			X
B. LEAR PROBES IN-TRAIL		1215			PROBE						X			X
CROSS-TRACK PROBES – LEVEL FLT, 12,000' 727 ALL CONFIGS.	7	1430	GEN.				MET. MEAS.		SEPARATION DISTANCE & PHOTO					
CROSS-TRACK PROBES		1600		PROBE						X	X			X

*T.M. = TELEMETERED DATA
RADAR = RADAR TRACKING
LAKEBED = VORTEX MAPPING MEASUREMENTS
NOISE MEAS. = NOISE MEASUREMENT
ECHO 2 = GROUND BASED PHOTOGRAPHY

TABLE II - FLIGHT-TEST INVESTIGATION OF WAKE TURBULENCE BEHIND B727 - Continued

DATE: NOV. 3, 1973

TEST OBJECTIVE	FLT NO	TEST TIME	AIRCRAFT STATUS							TM*	RADAR	LAKEBED	NOISE	ECHO 2
			B 727	F-104	LEARJET	PA-30	C-402	T-28	GULFSTREAM					
CROSS-TRACK PROBES LEVEL FLT, 12,000', 727 ALL CONFIGS.	8	1030	GEN. (IMPROVE SMOKER ON LEFT)				MET. MEAS.		PHOTO CHASE					
RUN FLAPS GEAR														
1 UP UP OBSERVE ONLY			↓				↓		↓					
2 UP UP PROBE					PROBE									X
3 15° DN "					↓									X
4 15° UP "														X
5 25° DN "														X
6 25° UP "														X
7 30° DN "														X
8 30° DN "														X
9 30° UP "														X
		1200												
CROSS-TRACK AND IN-TRAIL PROBES DESCENTS & CLIMBS, 12,000'	9	1430	GEN. (FURTHER IMPROVE LEFT SMOKER)				MET. MEAS.		PHOTO CHASE					
A. 3° DESCENT & CLIMB (2)					PROBE									X
B. LEVEL FLIGHT (2)			↓		↓		↓		↓					X
C. 3° DESCENT (1)														X
D. SMOKE OBSERVATIONS														
		1600												

*T.M. = TELEMETERED DATA
RADAR = RADAR TRACKING
LAKEBED = VORTEX MAPPING MEASUREMENTS
NOISE MEAS. = NOISE MEASUREMENT
ECHO 2 = GROUND BASED PHOTOGRAPHY

TABLE II - FLIGHT-TEST INVESTIGATION OF WAKE TURBULENCE BEHIND B727 - Concluded

DATE: NOV. 5, 1973

TEST OBJECTIVE	FLT NO	TEST TIME	AIRCRAFT STATUS							TM*	RADAR	LAKEBED	NOISE	ECHO 2
			B 727	F-104	LEARJET	PA-30	C-402	T-28	GULFSTREAM					
TAKEOFF WITH CLIMBING TURNS (2)	10	0700	GEN.				MET.		PHOTO					
A. CLEAN CONFIG			(T.O.) &				MEAS.		CHASE		X	X	X	
B. T.O. CONFIG			(LNDG)								X	X	X	
IN-TRAIL PROBES AT ALTITUDE						PROBE								
A. 3° DESCENT										X	X		X	X
B. TRANSITION										X	X		X	X
C. 6° DESCENT										X	X		X	X
PHOTOS OF CLEAN CONFIG VORTEX		0815	(CLEAN)								X		X	X
TAKEOFF WITH CLIMBING TURN	11	1100	GEN.				MET.		PHOTO		X	X	X	X
TWO-SEGMENT APPROACH "DEMONSTRATION FLT"			(T.O.)			PROBE	MEAS.		CHASE					
A. TWO-SEGMENT APPROACH			(LNDG)							X	X	X	X	X
B. CONVENTIONAL APPROACH			(LNDG)							X	X	X	X	X
PHOTOS OF VORTEX AT VARIOUS FLAP SETTINGS		1230	(VARIOUS)								X			
TAKEOFF WITH CLIMBING TURN	12	1400	GEN.				MET.		PHOTO		X	X	X	X
			(T.O.)				MEAS.		CHASE					
IN-TRAIL PROBE OF TWO-SEG. APR. AT 12,000'			(LNDG)		PROBE						X			
TWO-SEGMENT APPROACH "DEMONSTRATION FLT"														
A. TWO-SEGMENT APPROACH			(LNDG)								X	X	X	X
B. CONVENTIONAL APPROACH			(LNDG)								X	X	X	X
CROSS-TRACK PROBES AT 12,000'														
A. LEVEL FLT., CLEAN		1530	(CLEAN)											

*T.M. = TELEMETERED DATA
RADAR = RADAR TRACKING
LAKEBED = VORTEX MAPPING MEASUREMENTS
NOISE MEAS. = NOISE MEASUREMENTS
ECHO 2 = GROUND BASED PHOTOGRAPHY

TABLE III - SEPARATION DISTANCES AT WHICH UPSET RESPONSE DATA WERE OBTAINED
B727 CONFIGURATION: LANDING FLAPS (30°)

PROBE AIRCRAFT	SEPARATION DISTANCES, Km, (n. mi.)				
	HIGH ALTITUDE			LOW ALTITUDE[2]	
	LEVEL	THREE DEGREE	TWO SEGMENT	THREE DEGREE	TWO SEGMENT
LEARJET LR-23	2.96 – 6.48[1] (1.6 – 3.5)	4.26 – 6.11 (2.3 – 3.3)	3.89 – 5.18 (2.1 – 2.8)	5.18 – 5.56 (2.8 – 3.0)	5.37 – 5.93 (2.9 – 3.2)
PIPER PA-30	4.63 – 5.55 (2.5 – 3.0)	6.57 – 8.06 (3.55 – 4.35)	6.94 – 7.04 (3.75 – 3.80)	6.17 – 7.63 (3.33 – 4.12)	NO UPSET DATA OBTAINED

[1]ADDITIONAL LR-23 DATA WAS OBTAINED BEHIND THE B 727 CLEAN CONFIGURATION AT DISTANCES OF 5.6 TO 7.5 n. mi.

[2]ONLY ONE PASS WAS MADE FOR EACH OF THE TWO TYPES OF APPROACHES FOR THE LOW ALTITUDE FLIGHTS

Figure 1.- Wake vortex generating aircraft.

Figure 2.- Vortex marking smoke generators mounted on the generating aircraft wing tip.

Figure 3.- Wake vortex probe aircraft; Lear Jet model 23.

Figure 4.- Wake vortex probe aircraft; Piper Twin Comanche.

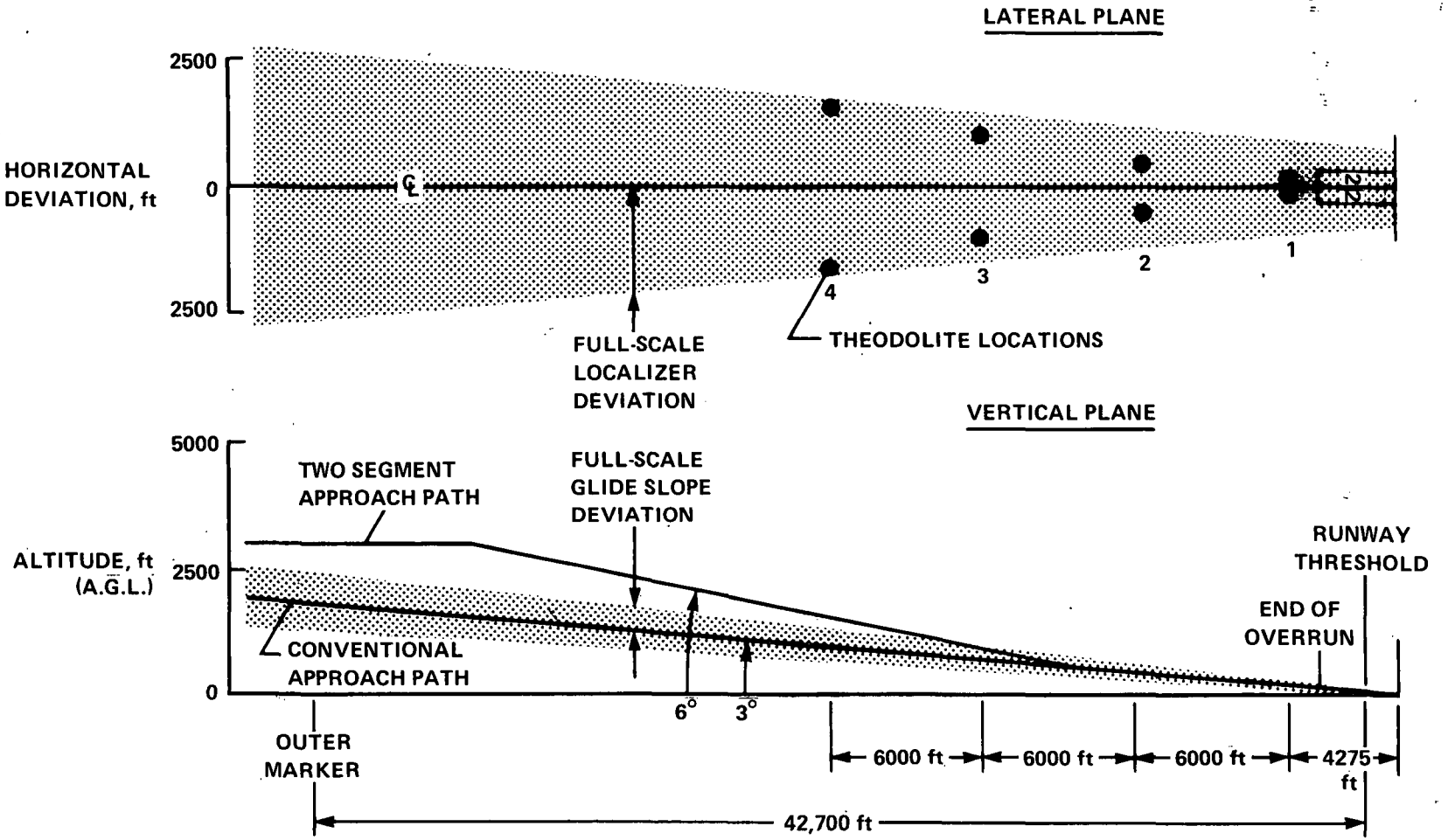

Figure 5.- Landing approach geometry; conventional and two-segment.

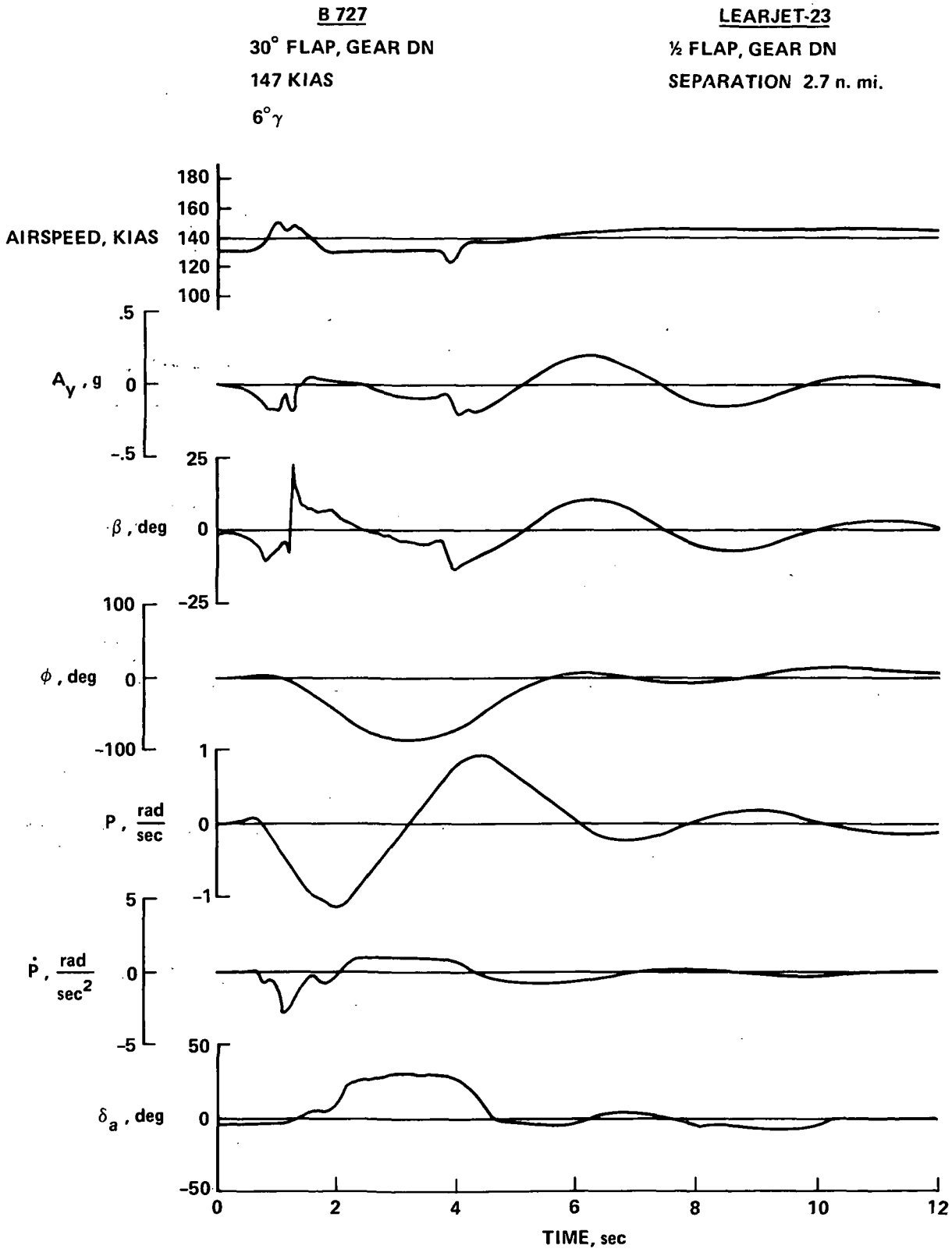

(a) Lateral-Directional

Figure 6.- Time histories of excursions experienced by the Lear Jet flying in the wake of the Boeing 727

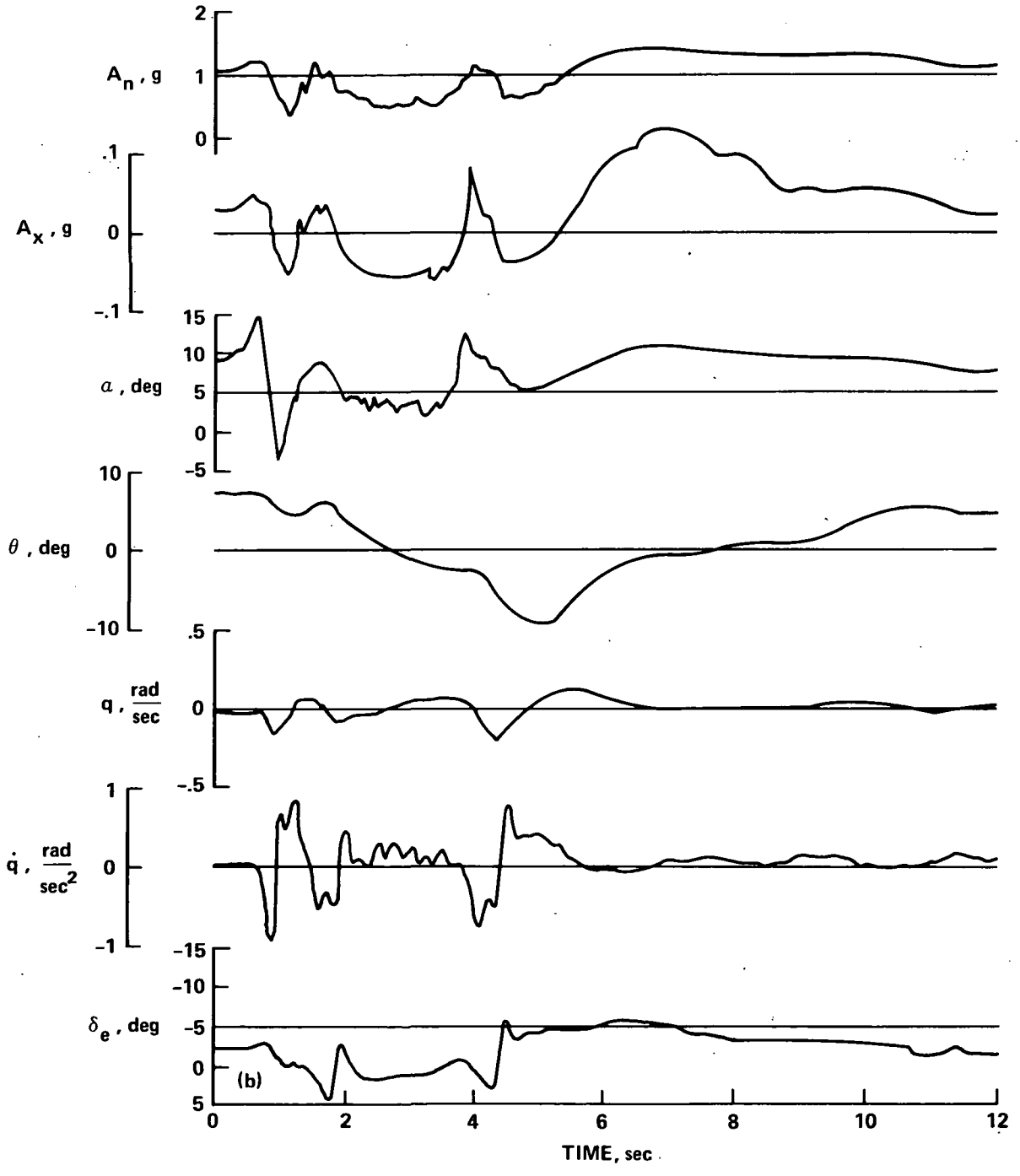

(b) Longitudinal

Figure 6.- Concluded.

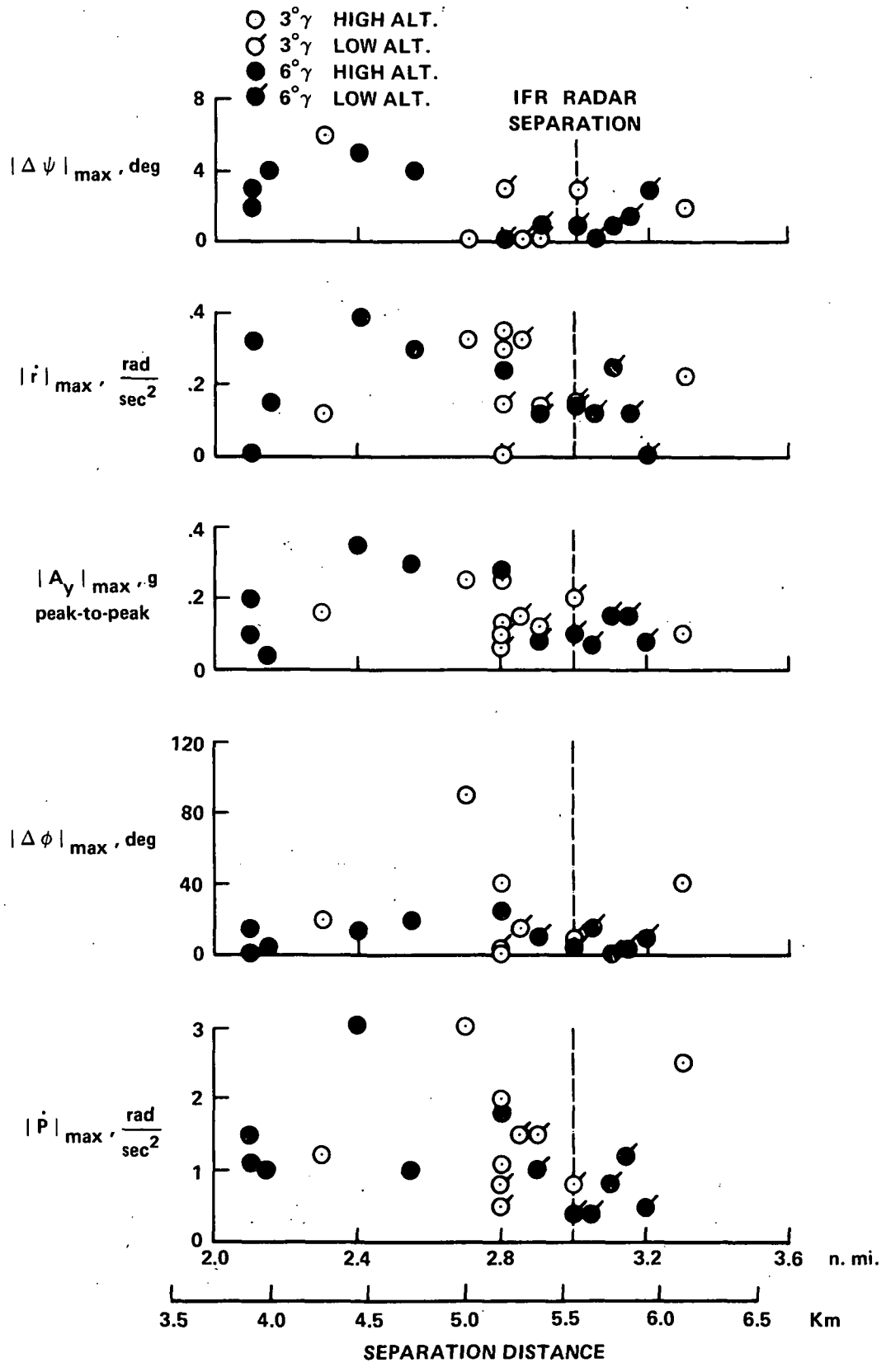

(a) Lateral-directional

Figure 7.- Maximum excursions experienced by Lear Jet versus separation distance.

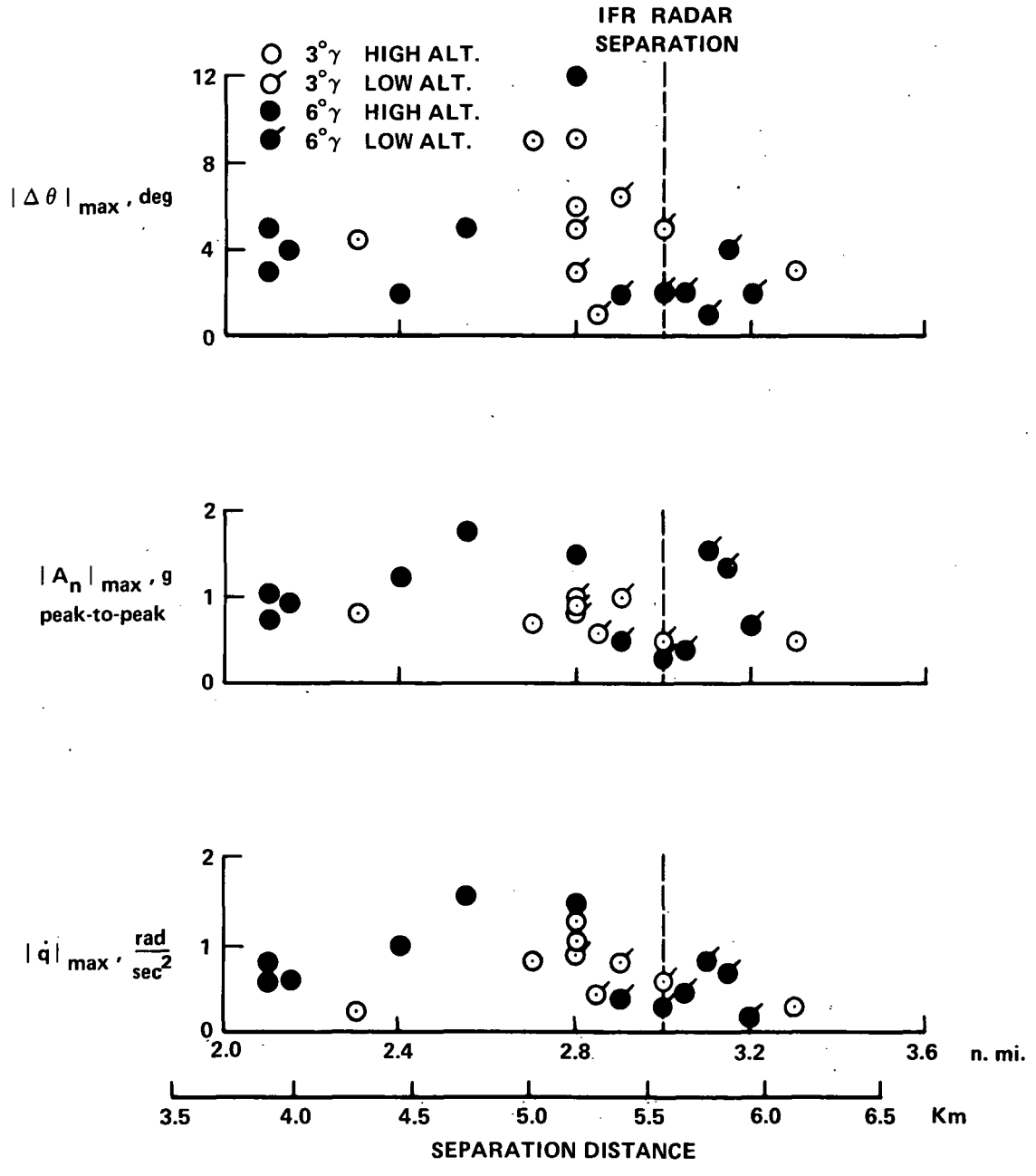

(b) Longitudinal

Figure 7.- Concluded.

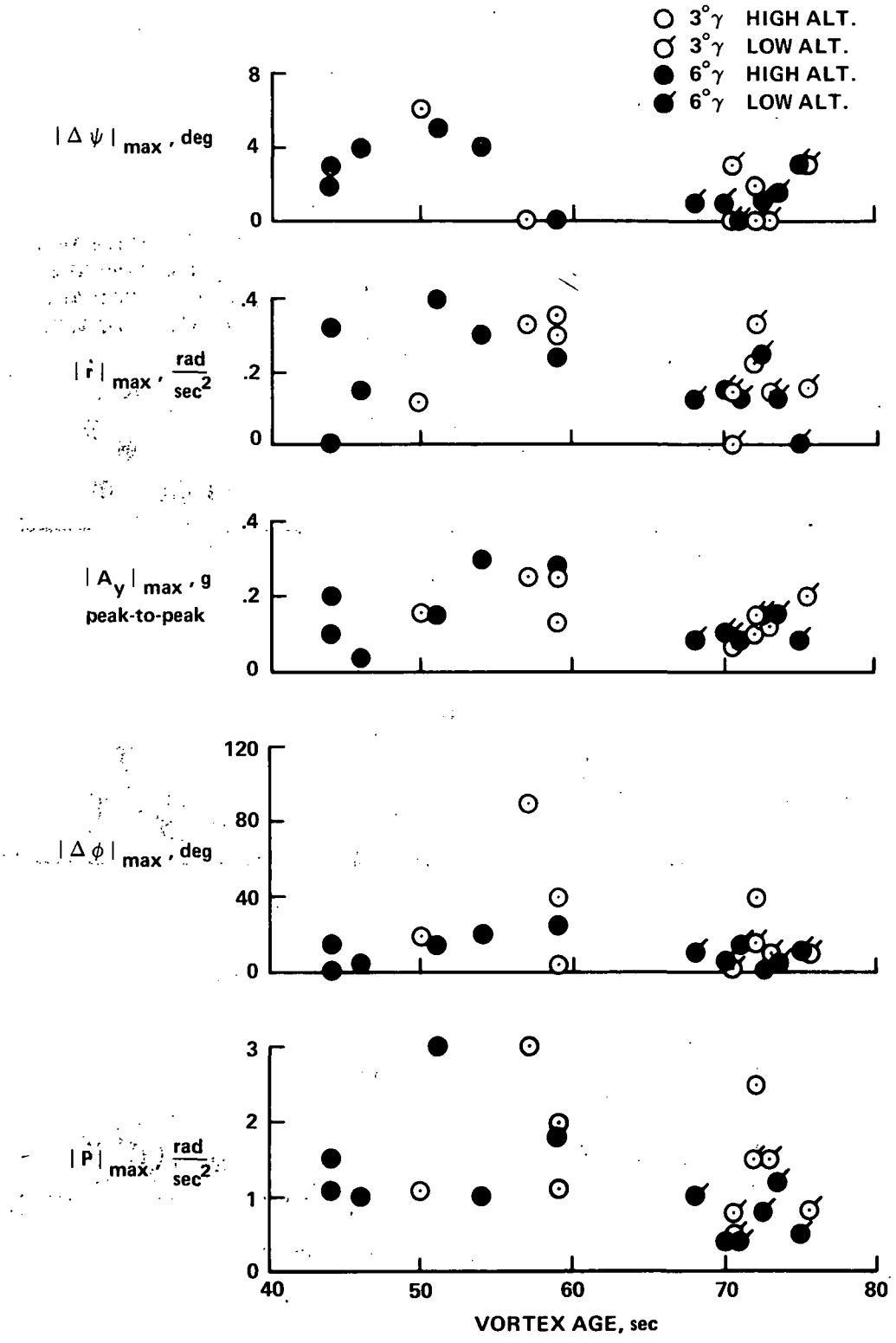

(a) Lateral-directional

Figure 8.- Maximum excursions experienced by Lear Jet versus vortex age.

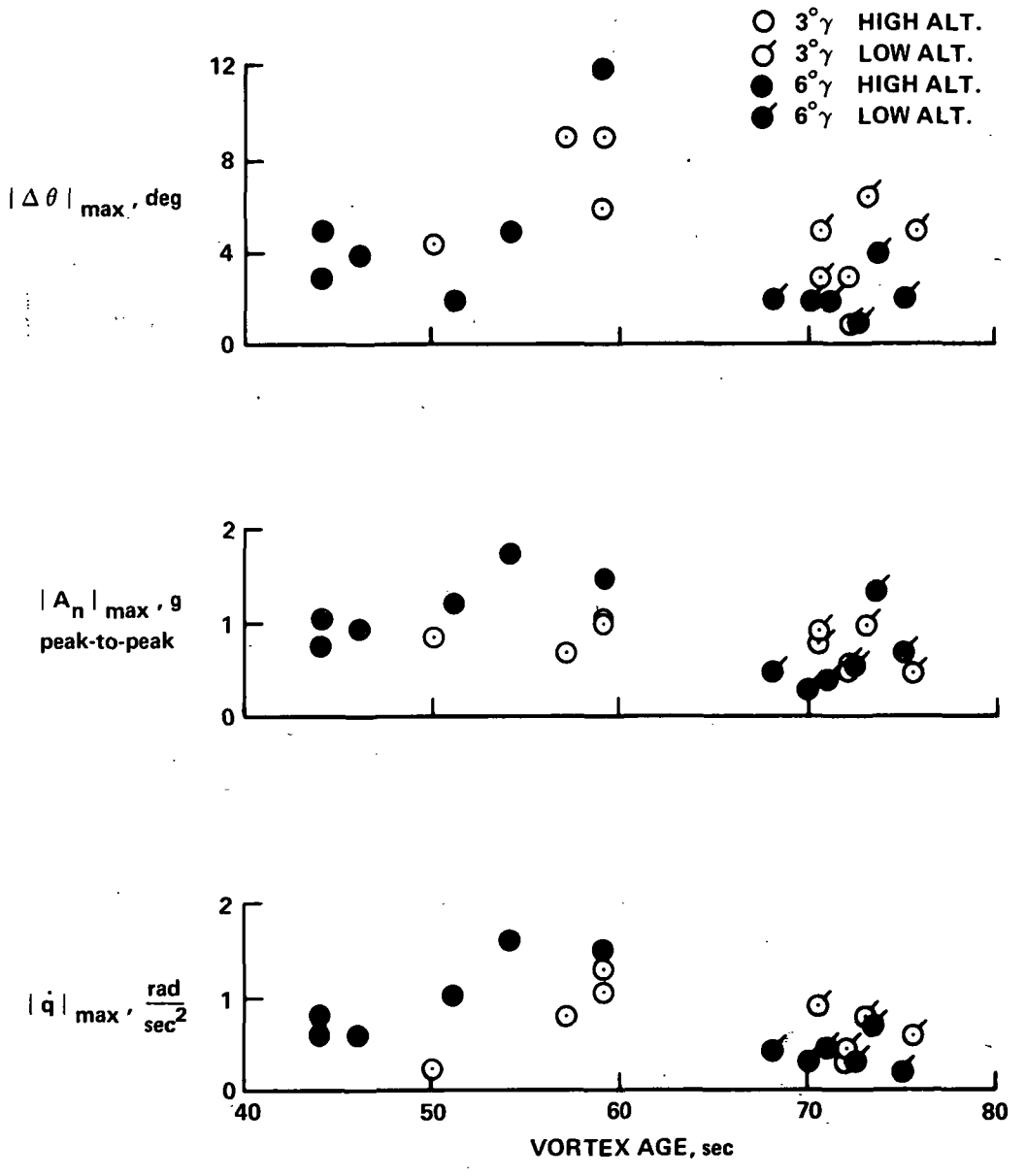

(b) Longitudinal

Figure 8.- Concluded.

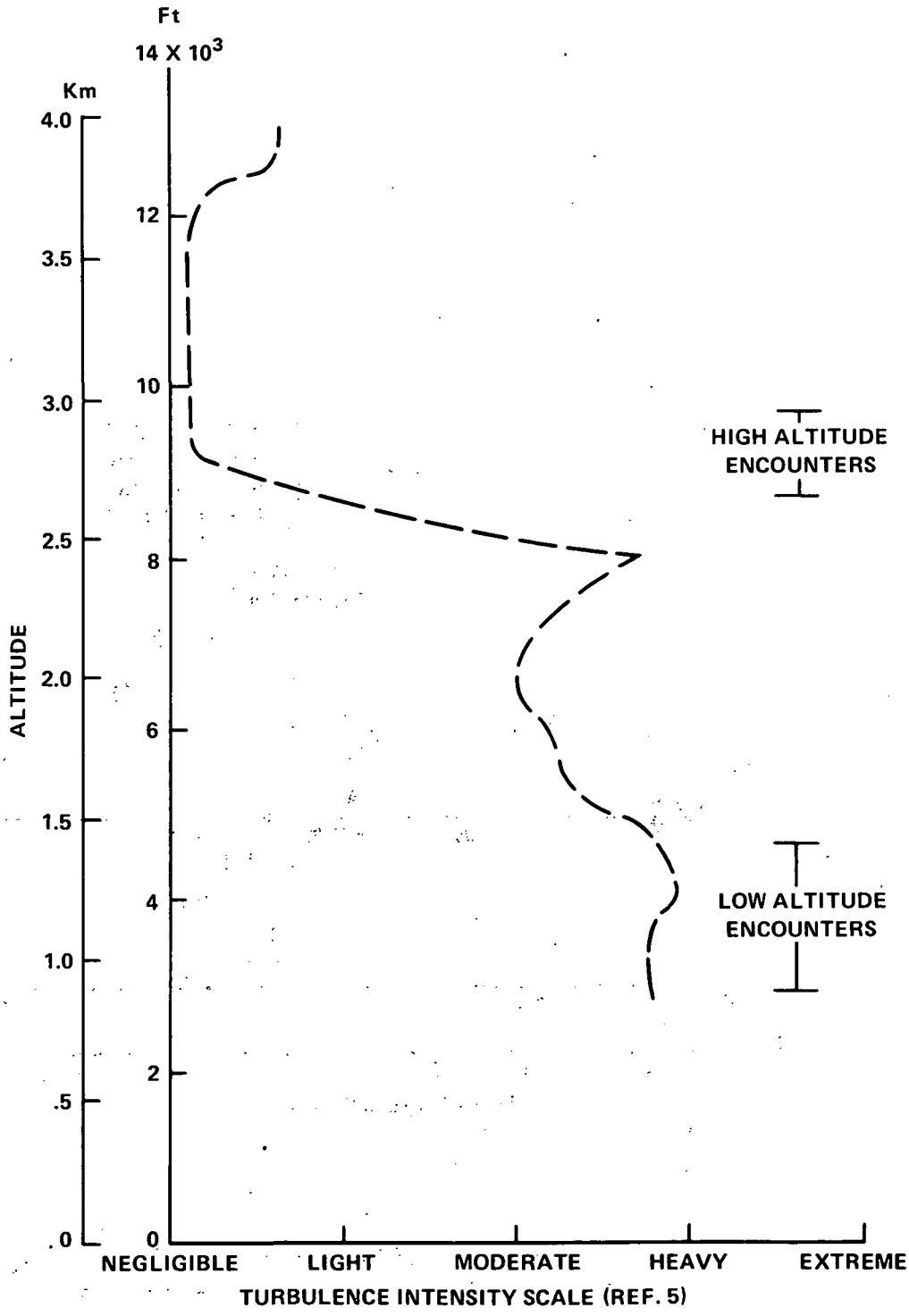

Figure 9.- Effect of altitude on turbulence environment for Lear Jet encounters during landing approaches.

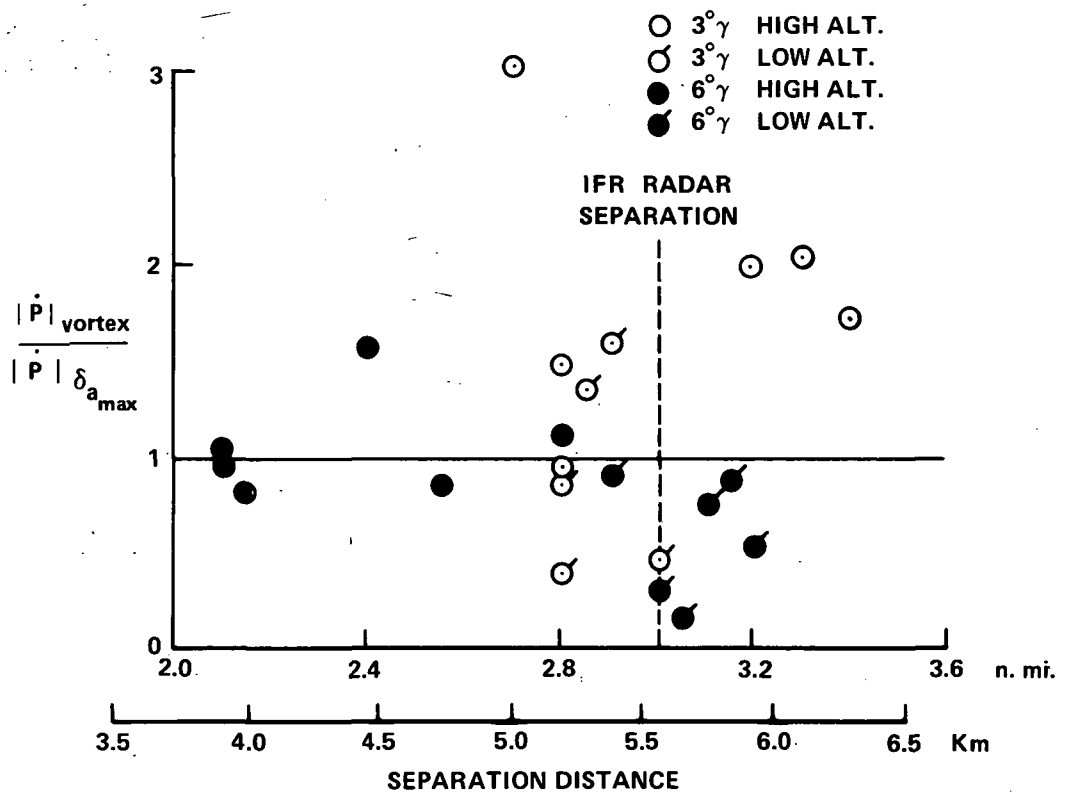

Figure 10.- Ratio of the vortex induced roll acceleration to maximum roll control power for the Lear Jet versus separation distance.

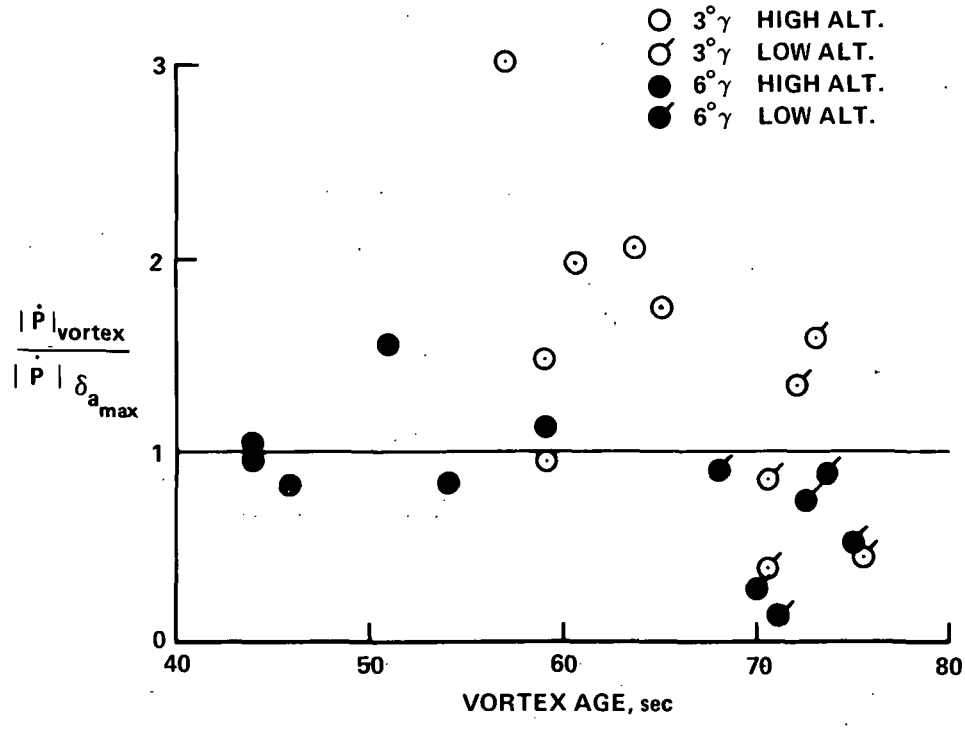

Figure 11.- Ratio of the vortex induced roll acceleration to maximum roll control power for the Lear Jet versus vortex age.

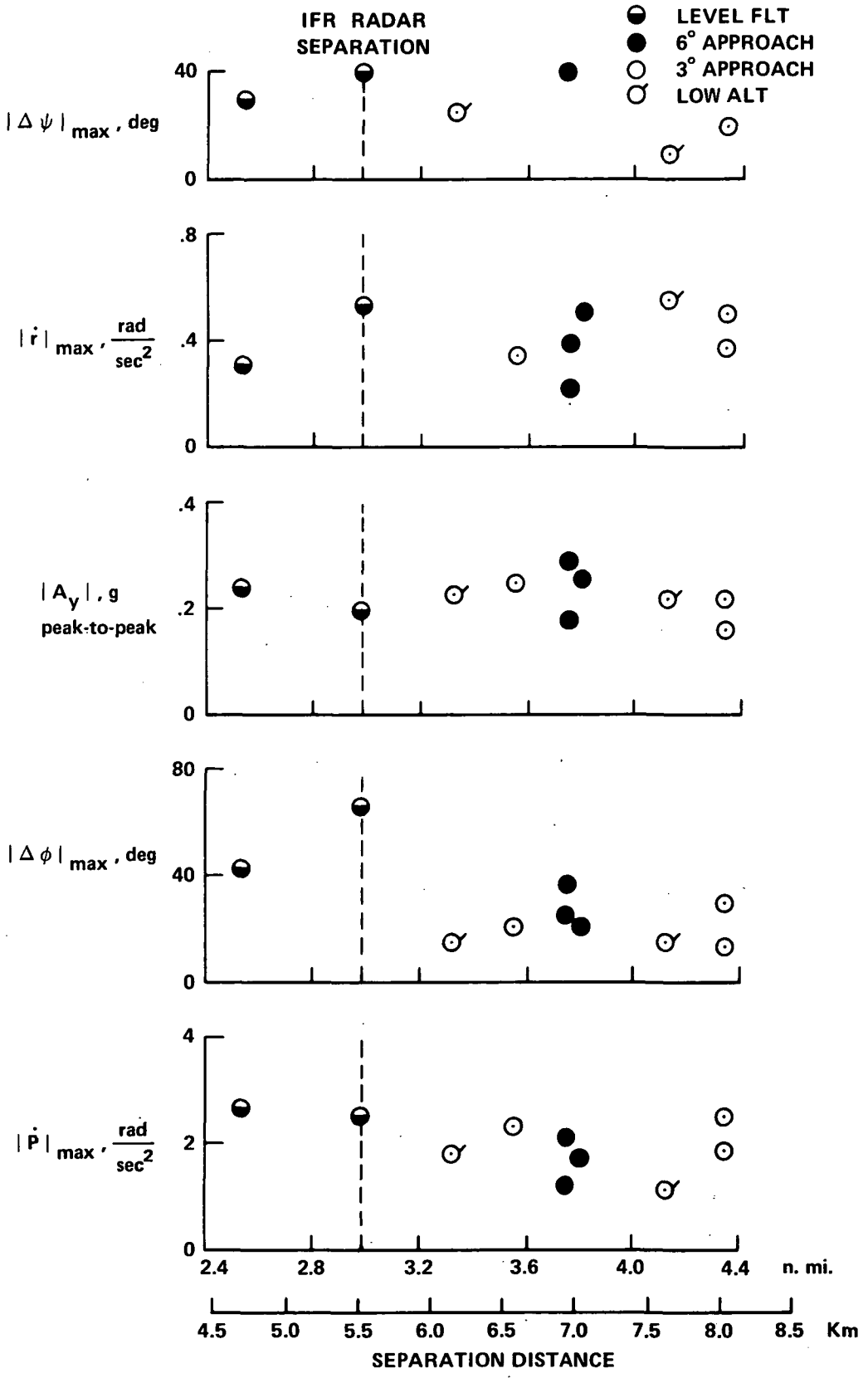

(a) Lateral-directional

Figure 12.- Maximum excursions experienced by PA-30 versus separation distance.

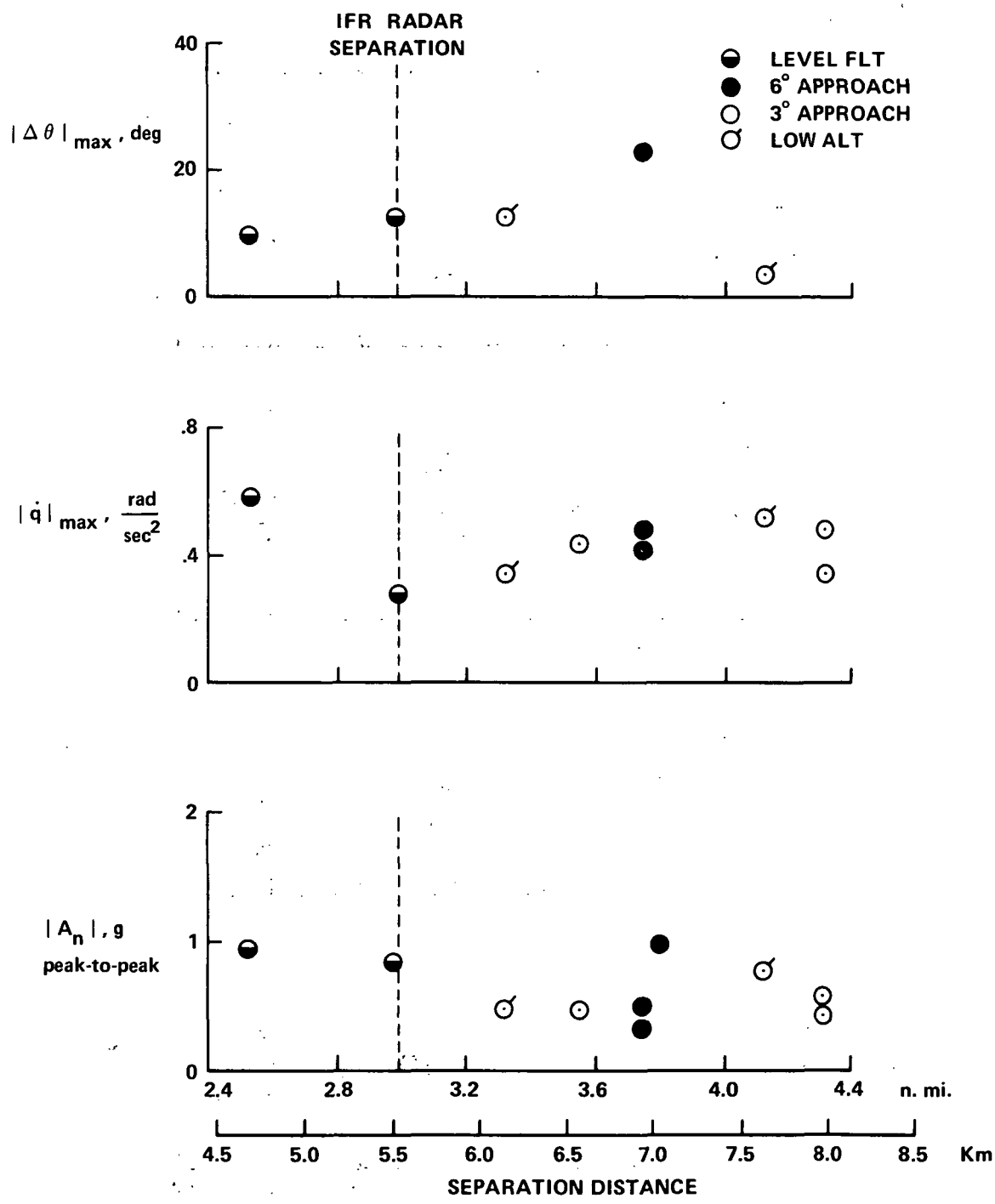

(b) Longitudinal

Figure 12.- Concluded.

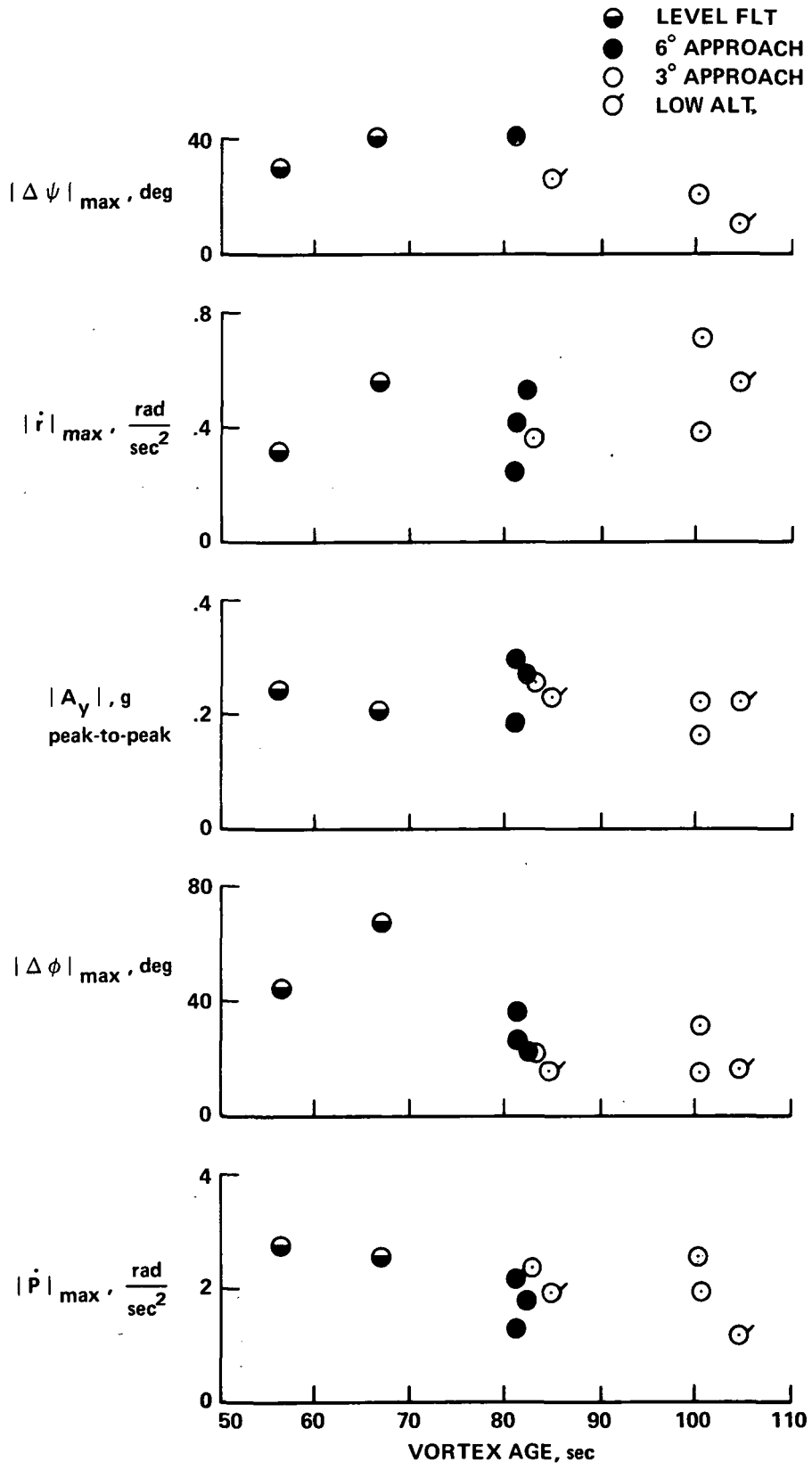

(a) Lateral-directional

Figure 13.- Maximum excursions experienced by PA-30 versus vortex age

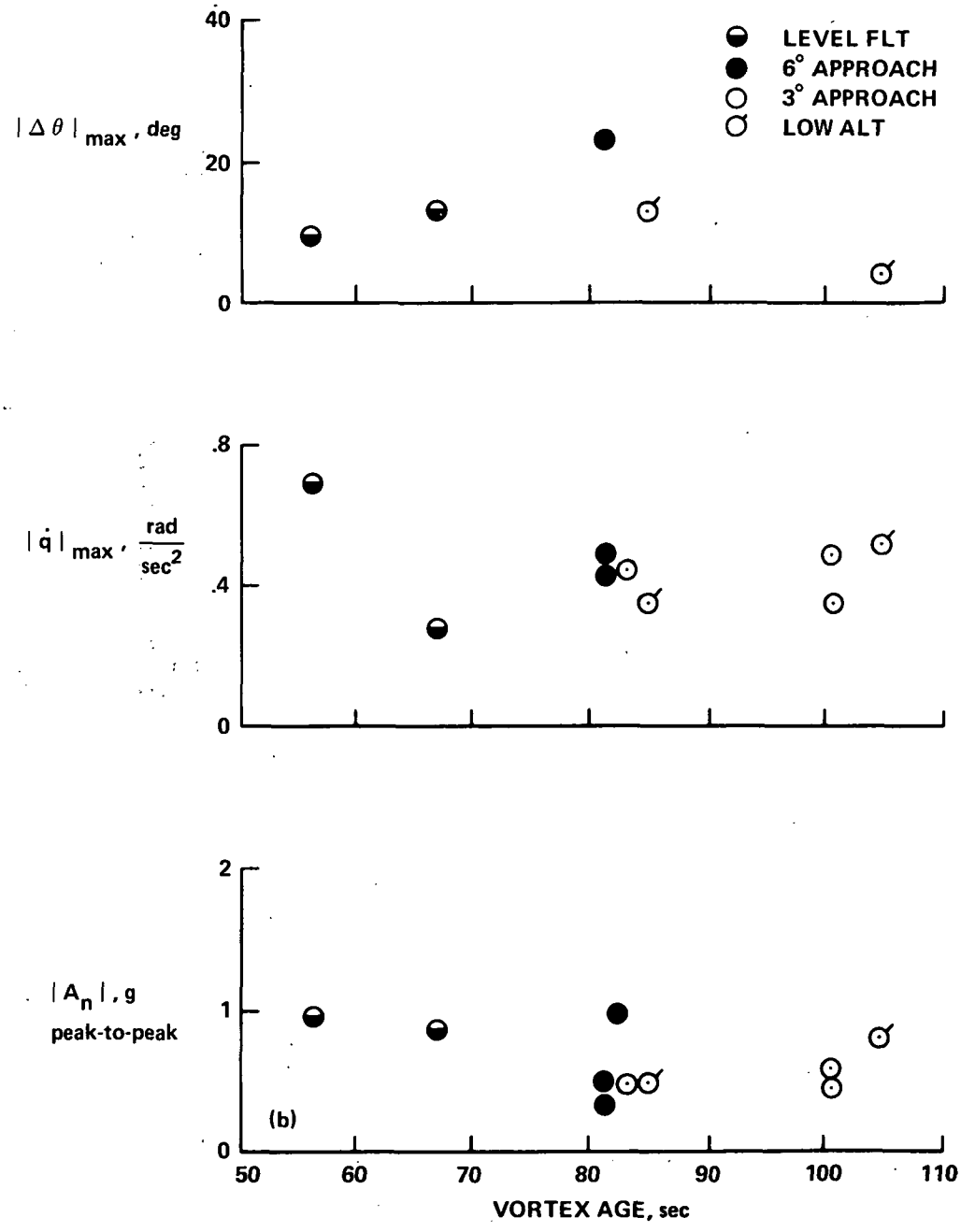

(b) Longitudinal

Figure 13.- Concluded

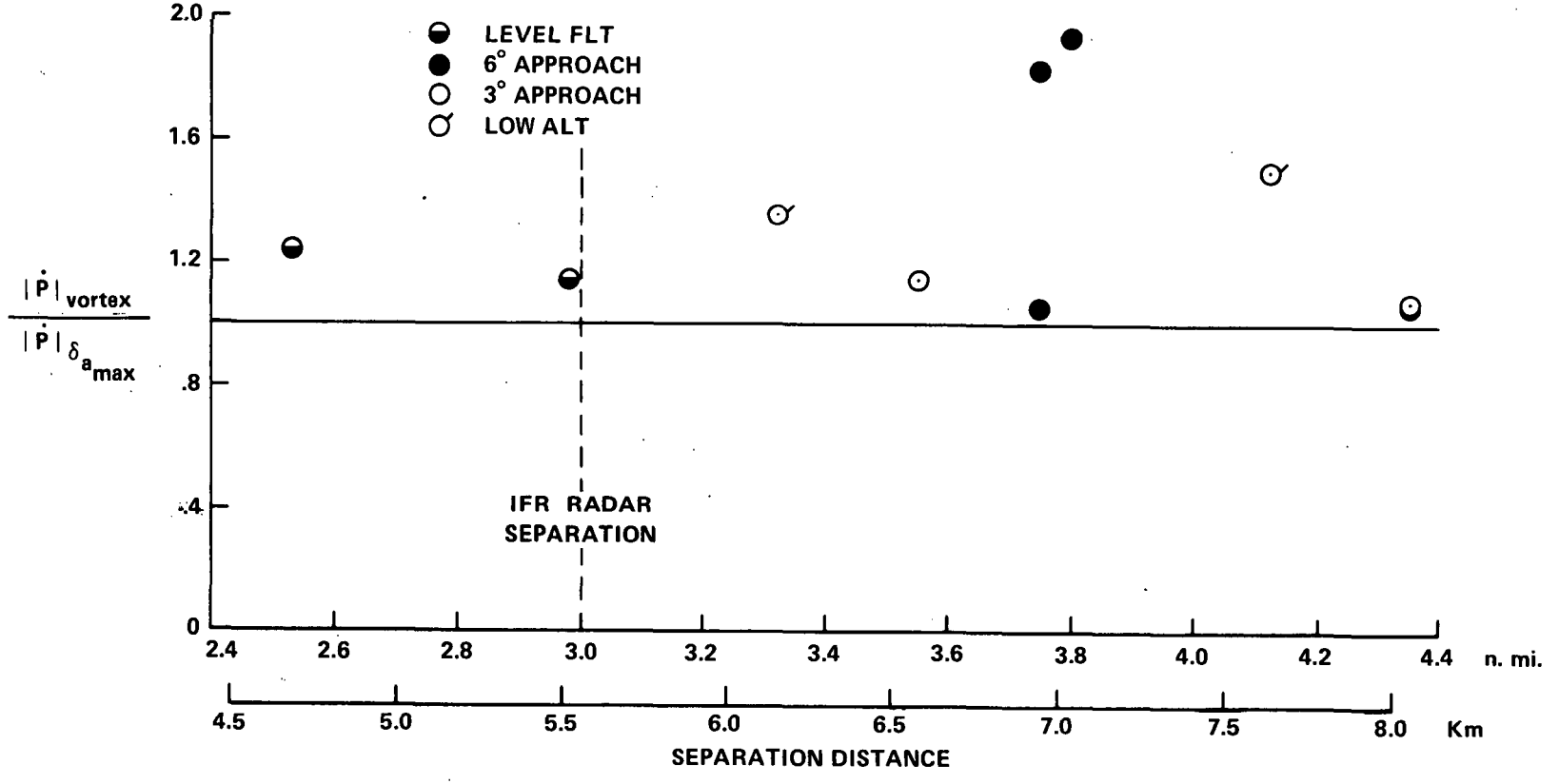

Figure 14.- Ratio of vortex induced roll acceleration to maximum roll control power for the PA-30 versus separation distance.

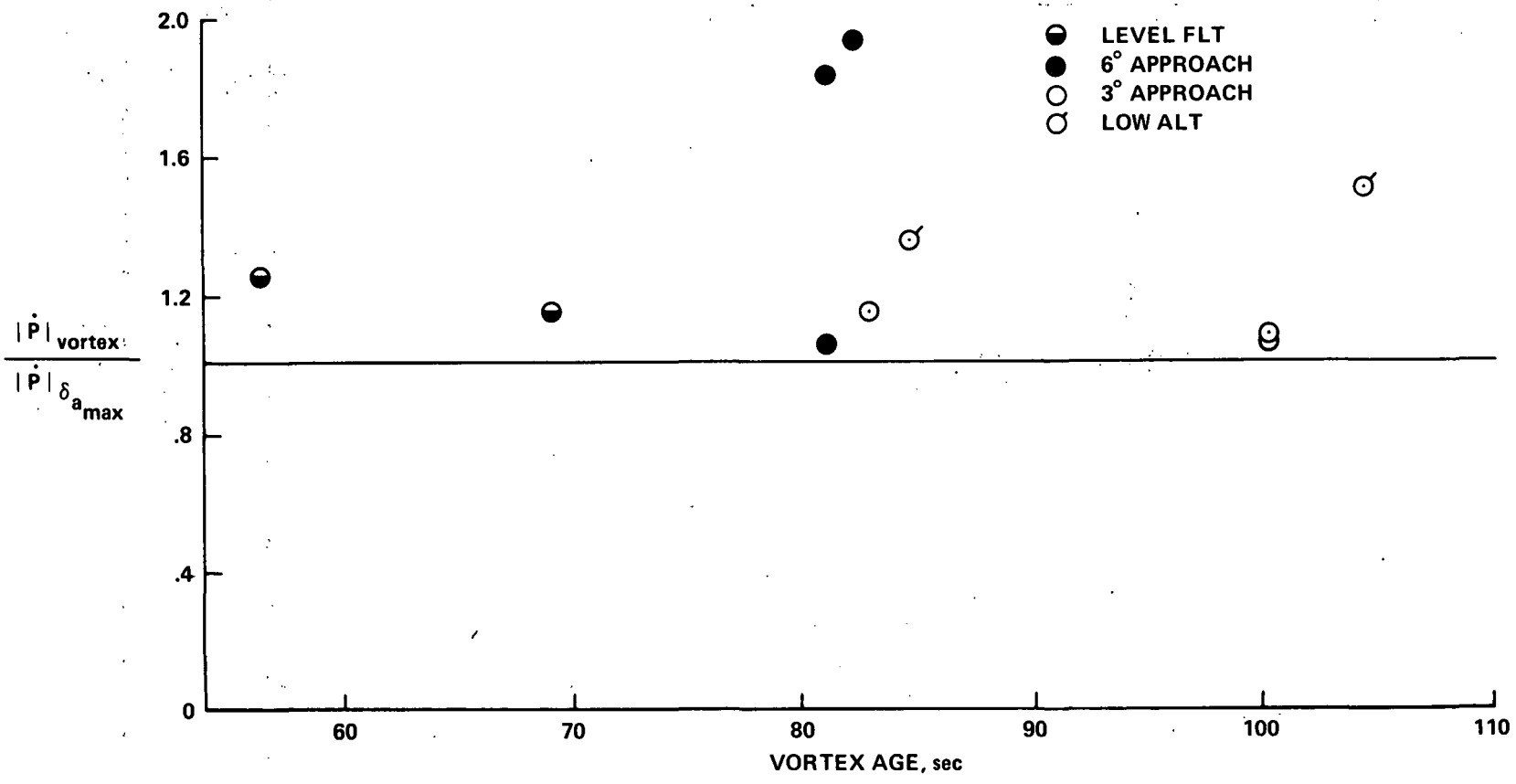

Figure 15.- Ratio of vortex induced roll acceleration to maximum roll control power for the PA-30 versus vortex age.

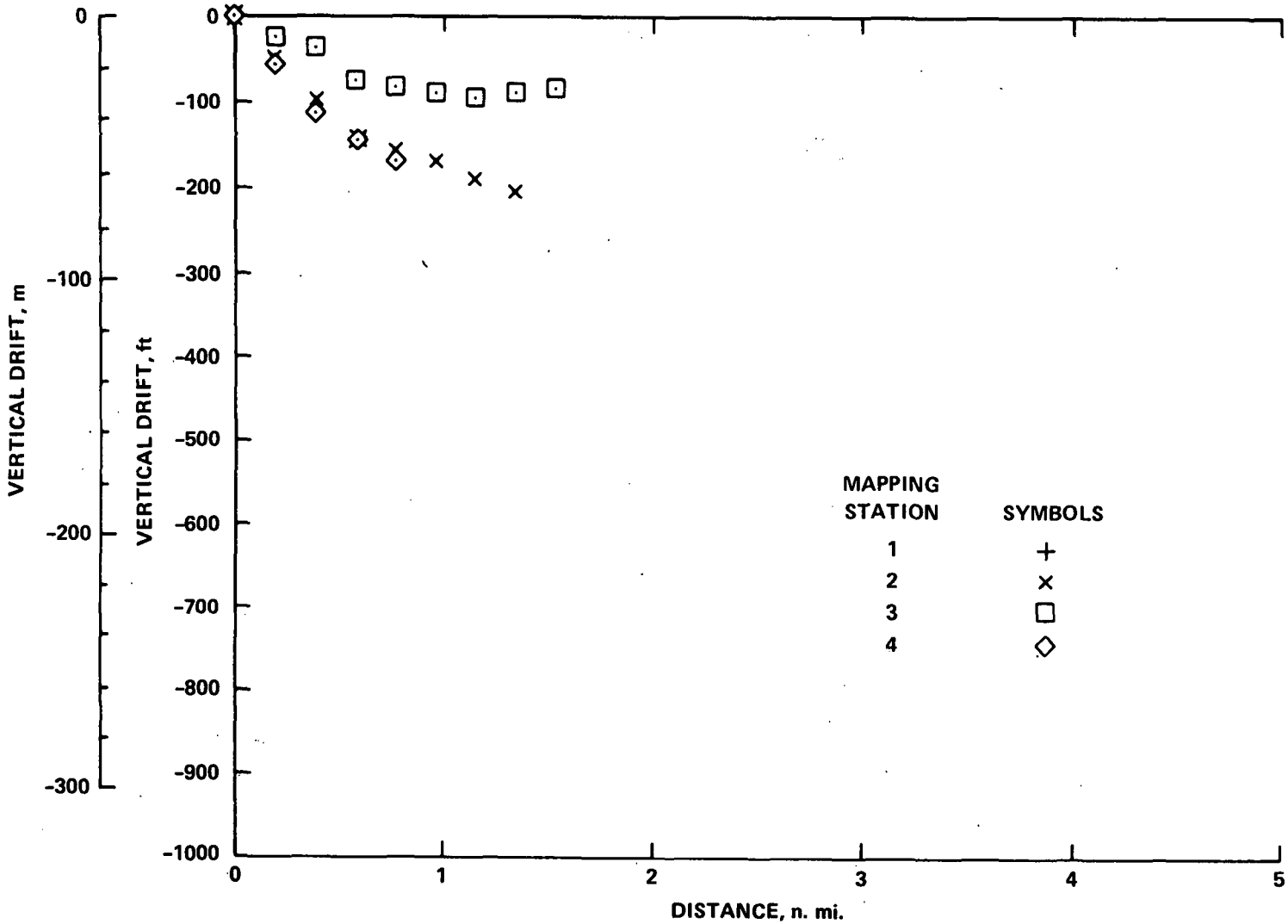

(a) Conventional approach; approach configuration, 132 knots

Figure 16.- Trailed wake vortex position behind a Boeing 727 aircraft.

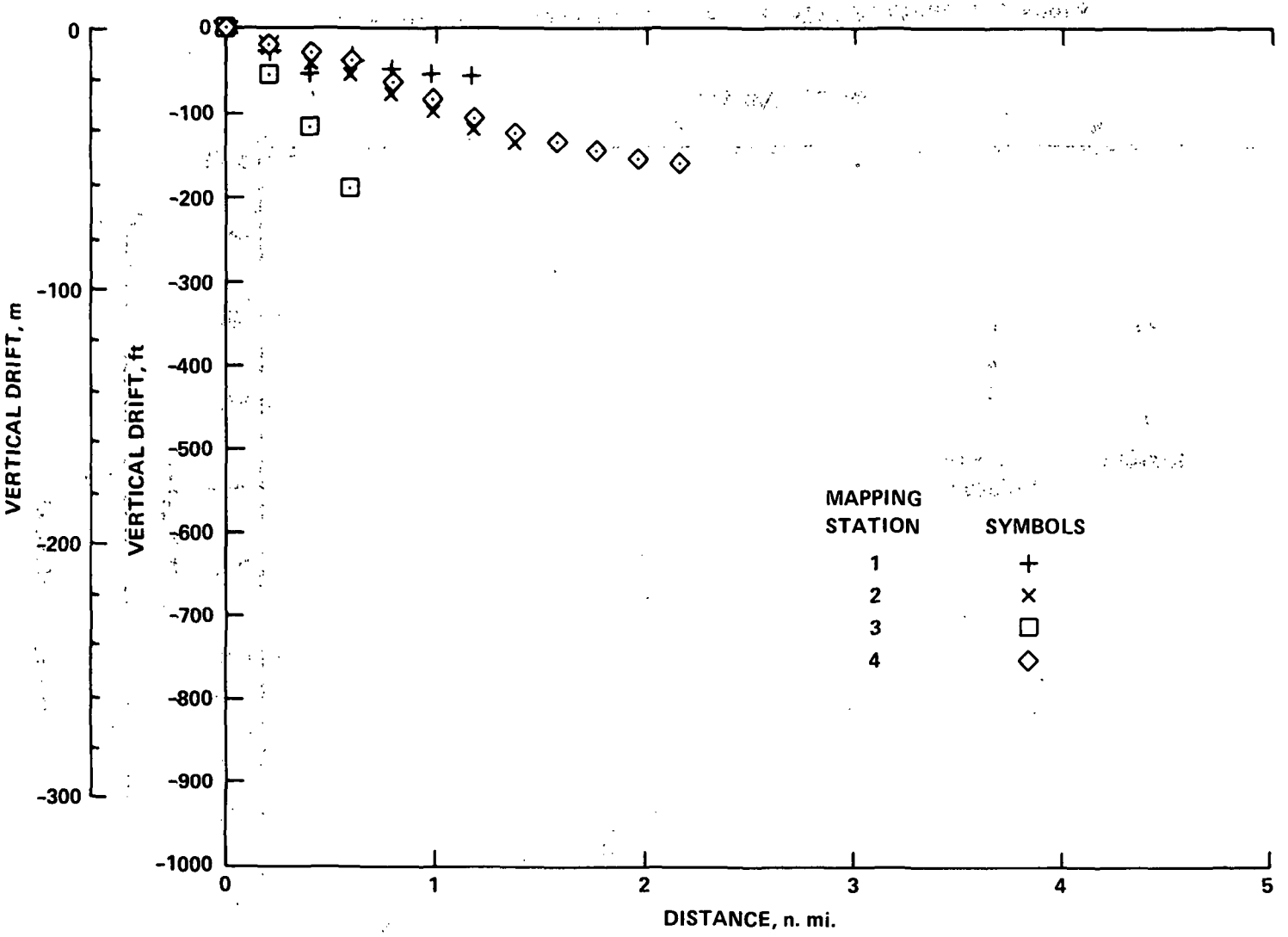

(b) Conventional approach; approach configuration, 135 knots

Figure 16.- Continued.

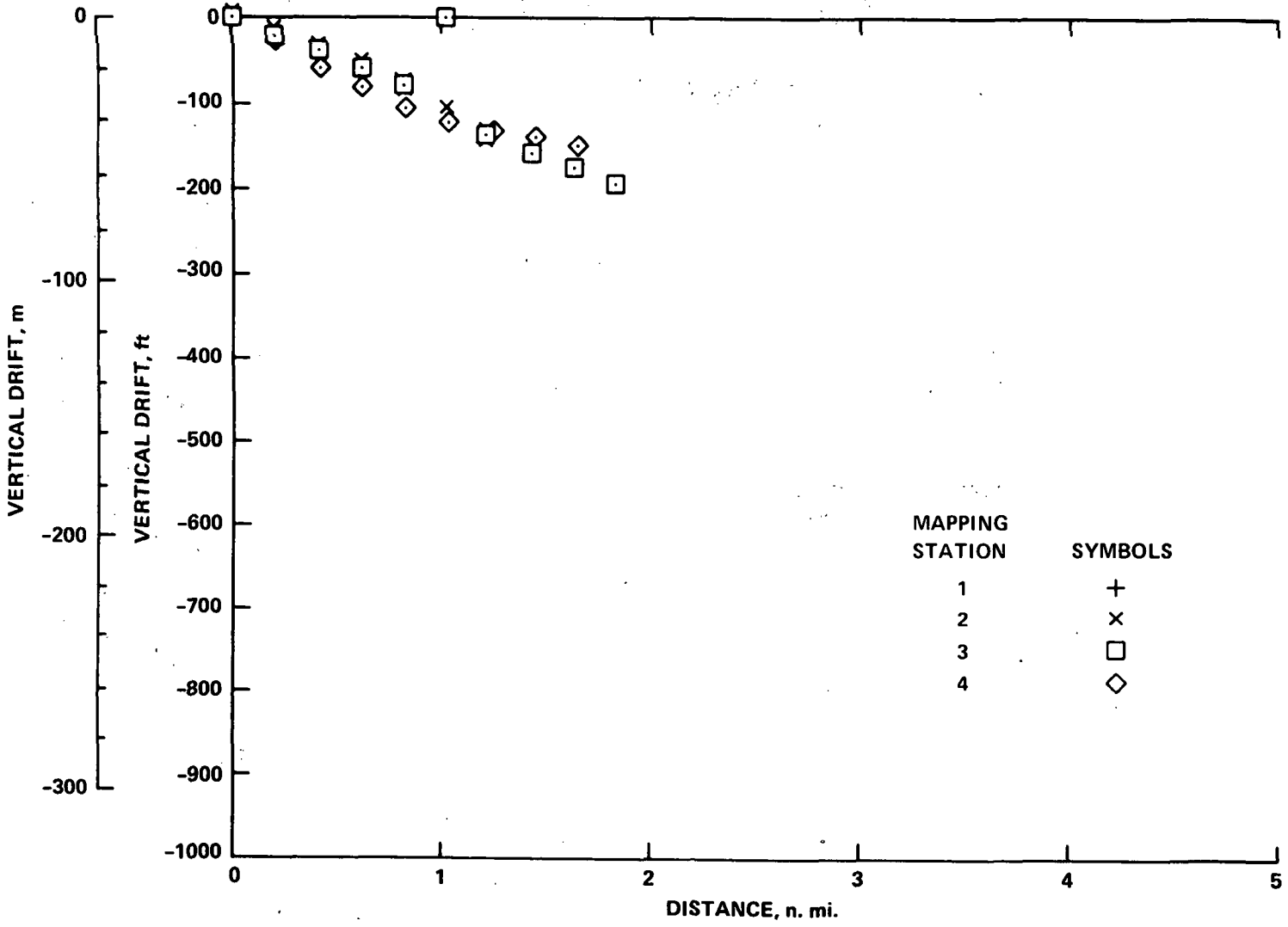

(c) Two-segment approach; approach configuration, 135 knots

Figure 16.- Continued.

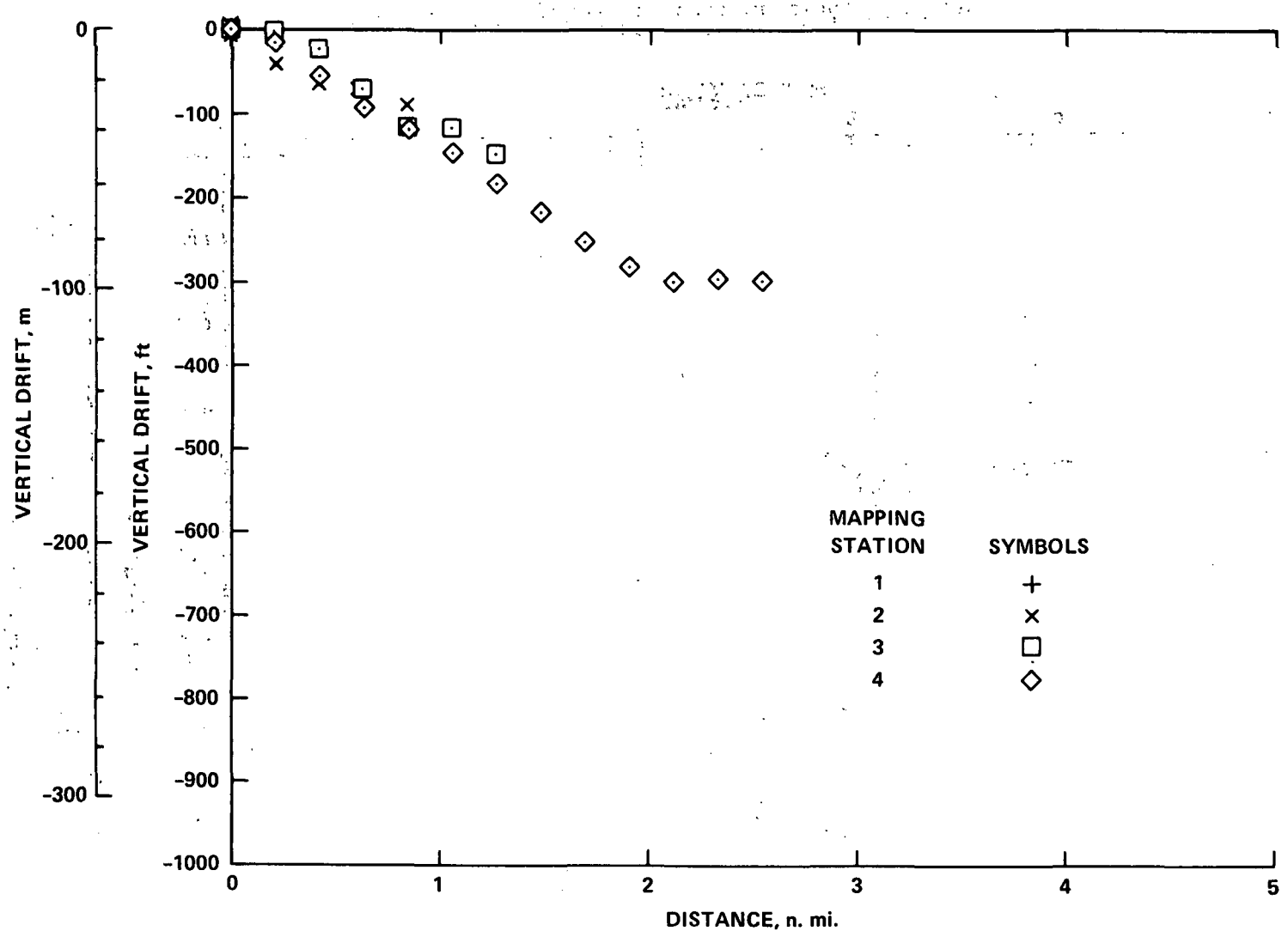

(d) Two-segment approach; approach configuration, 145 knots

Figure 16.- Continued.

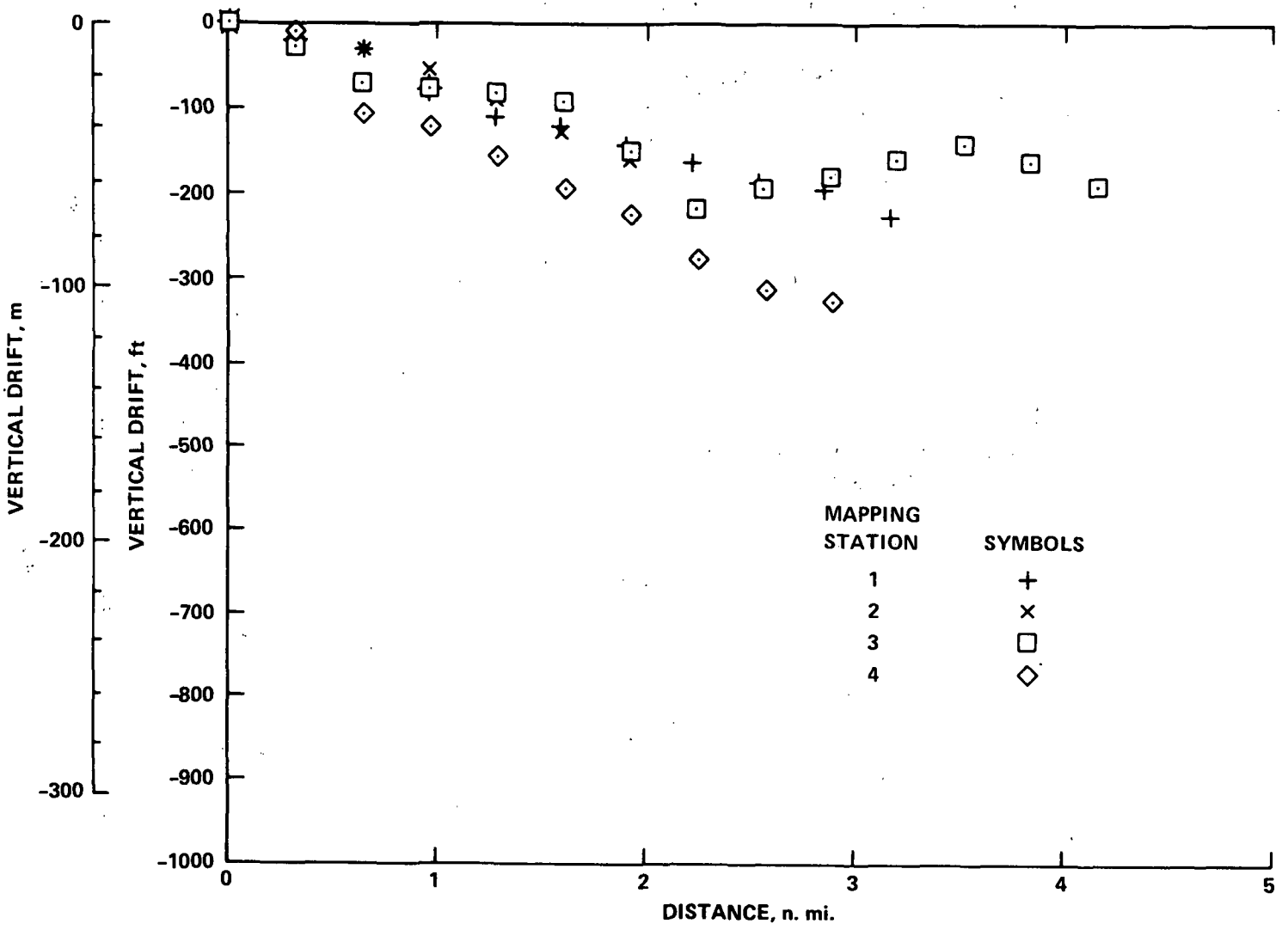

(e) Take-off; take-off configuration, 220 knots

Figure 16.- Continued.

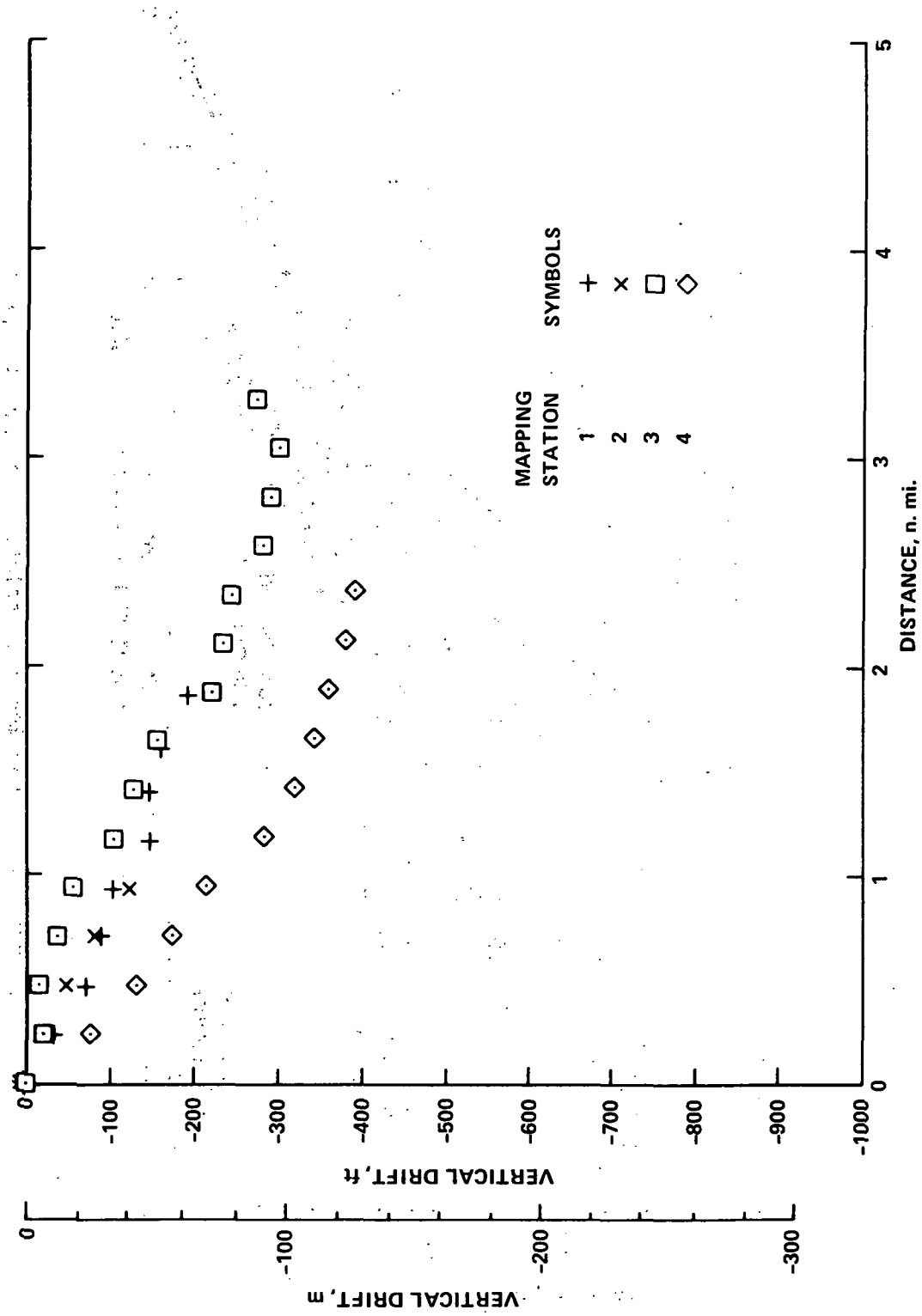

(f) Take-off; take off configuration, 160 knots

Figure 16.- Concluded.

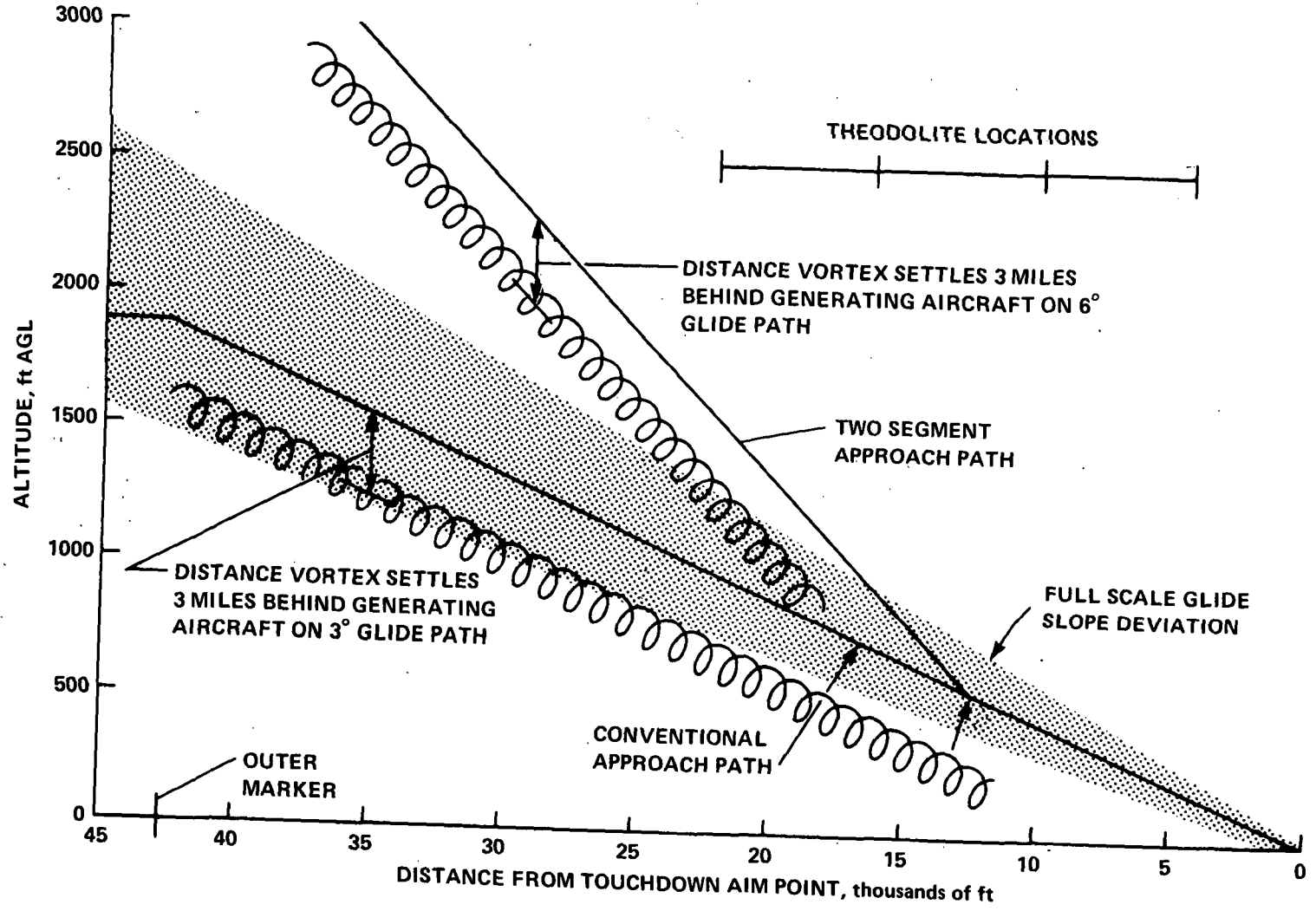

Figure 17.- Vortex location relative to approach path.

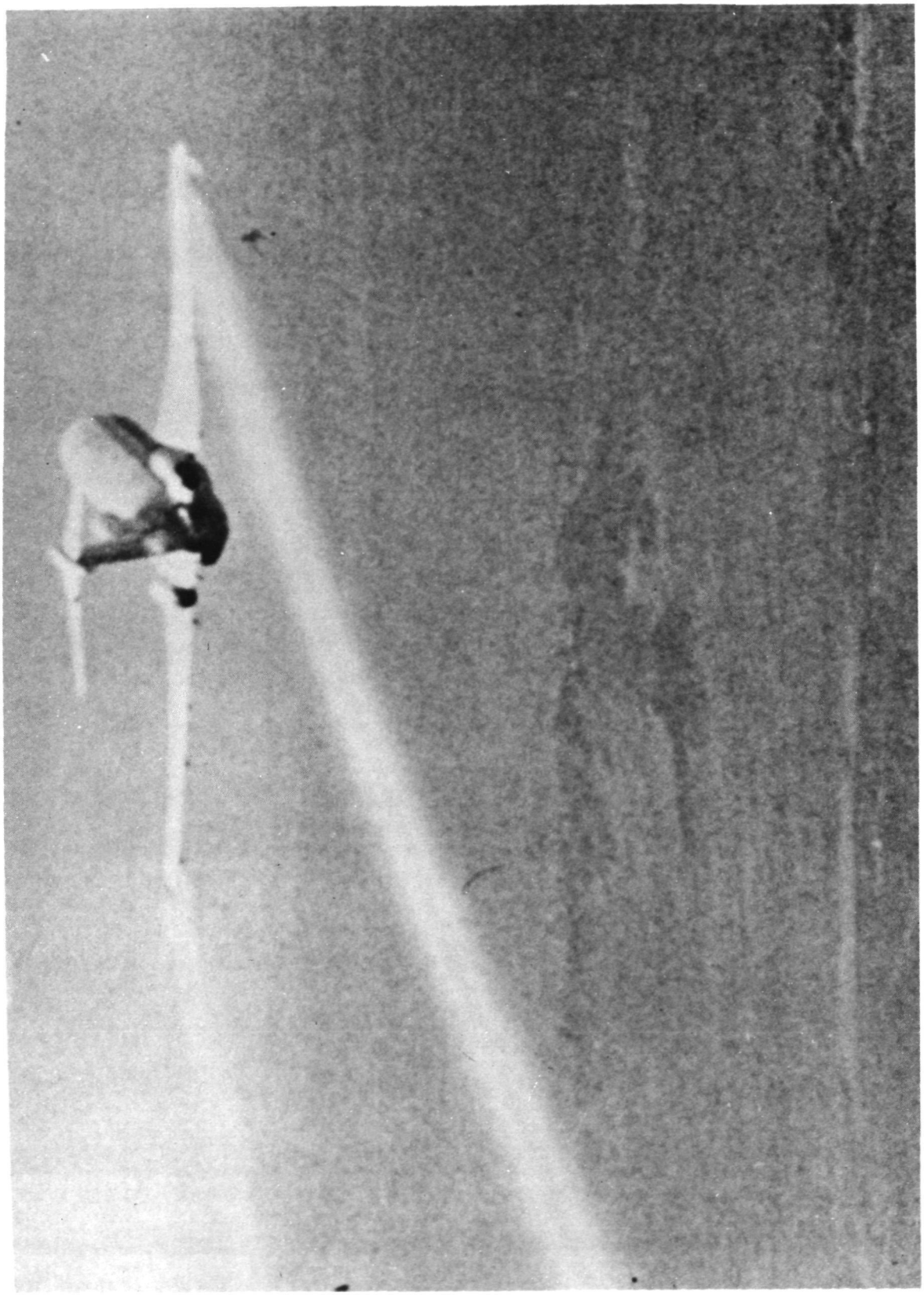

Figure 18.- Boeing 727 clean configuration vortex

(a) Front view

Figure 19.- Boeing 727 landing configuration vortex.

(b) Rear view
Figure 19.- Concluded

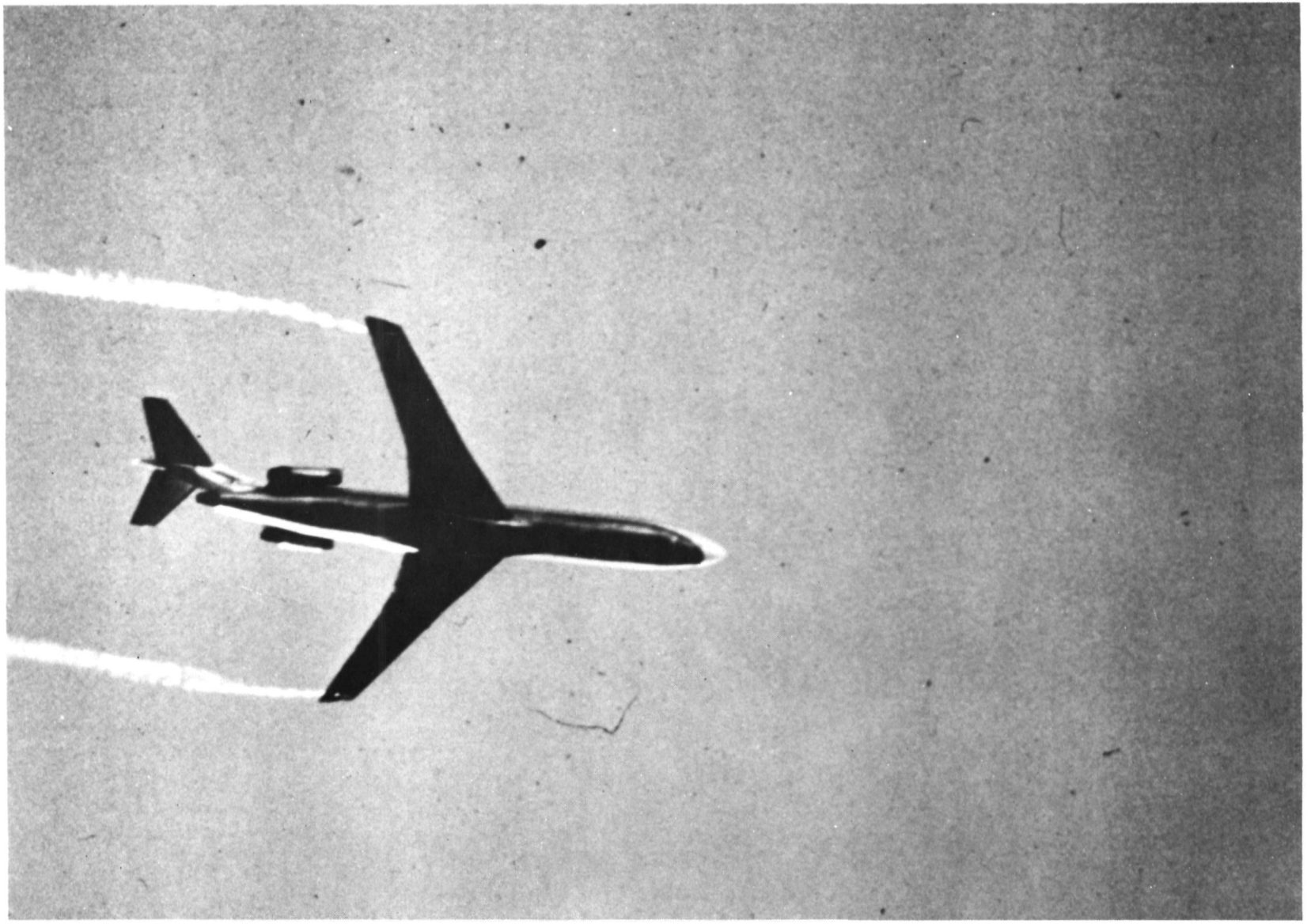

(a) Time = 0 seconds

Figure 20.- B727 wake vortex (clean configuration: weight = 334,000 kg (151,500 lbs.)

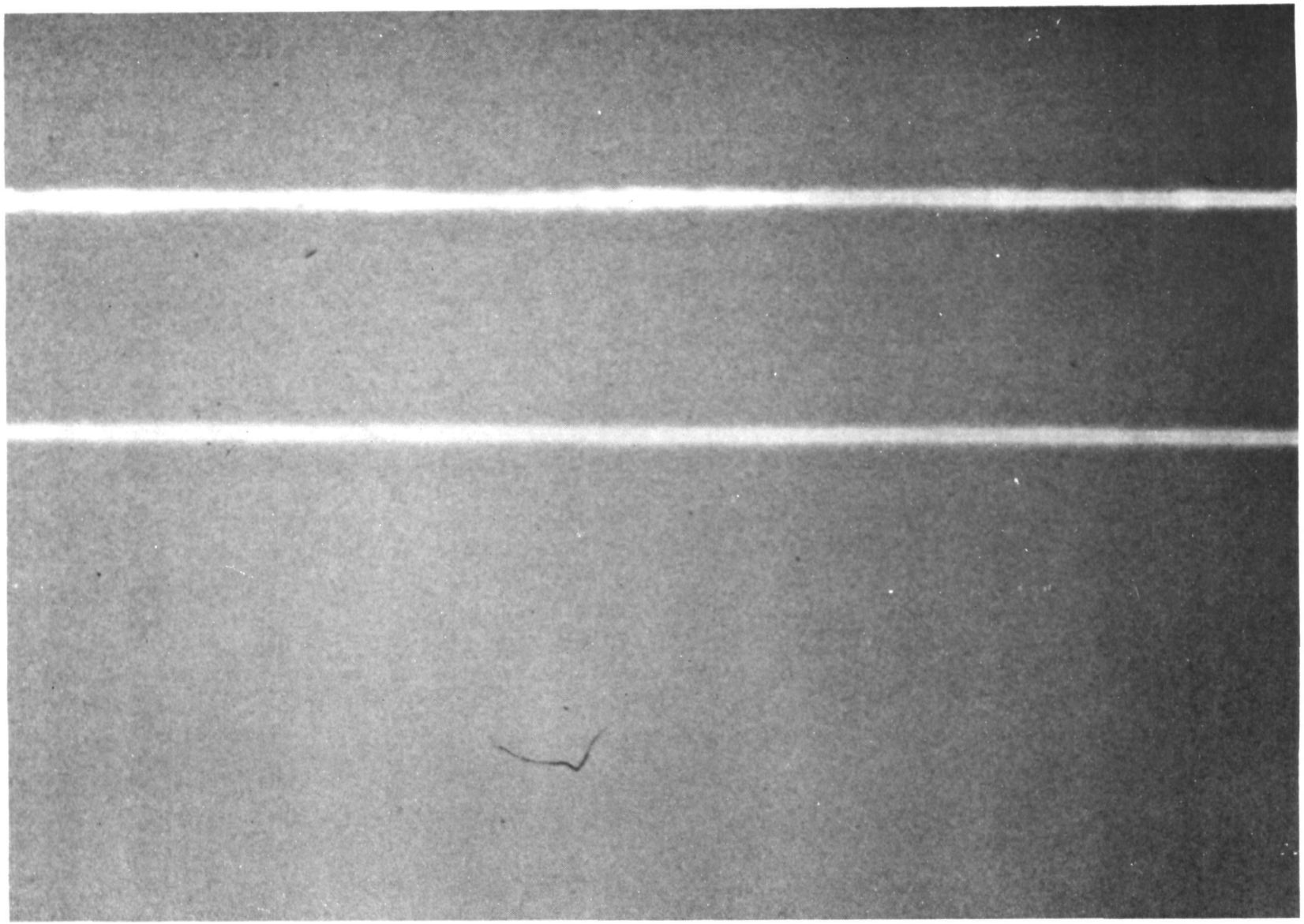

(b) Time = 5 seconds

Figure 20.- Continued.

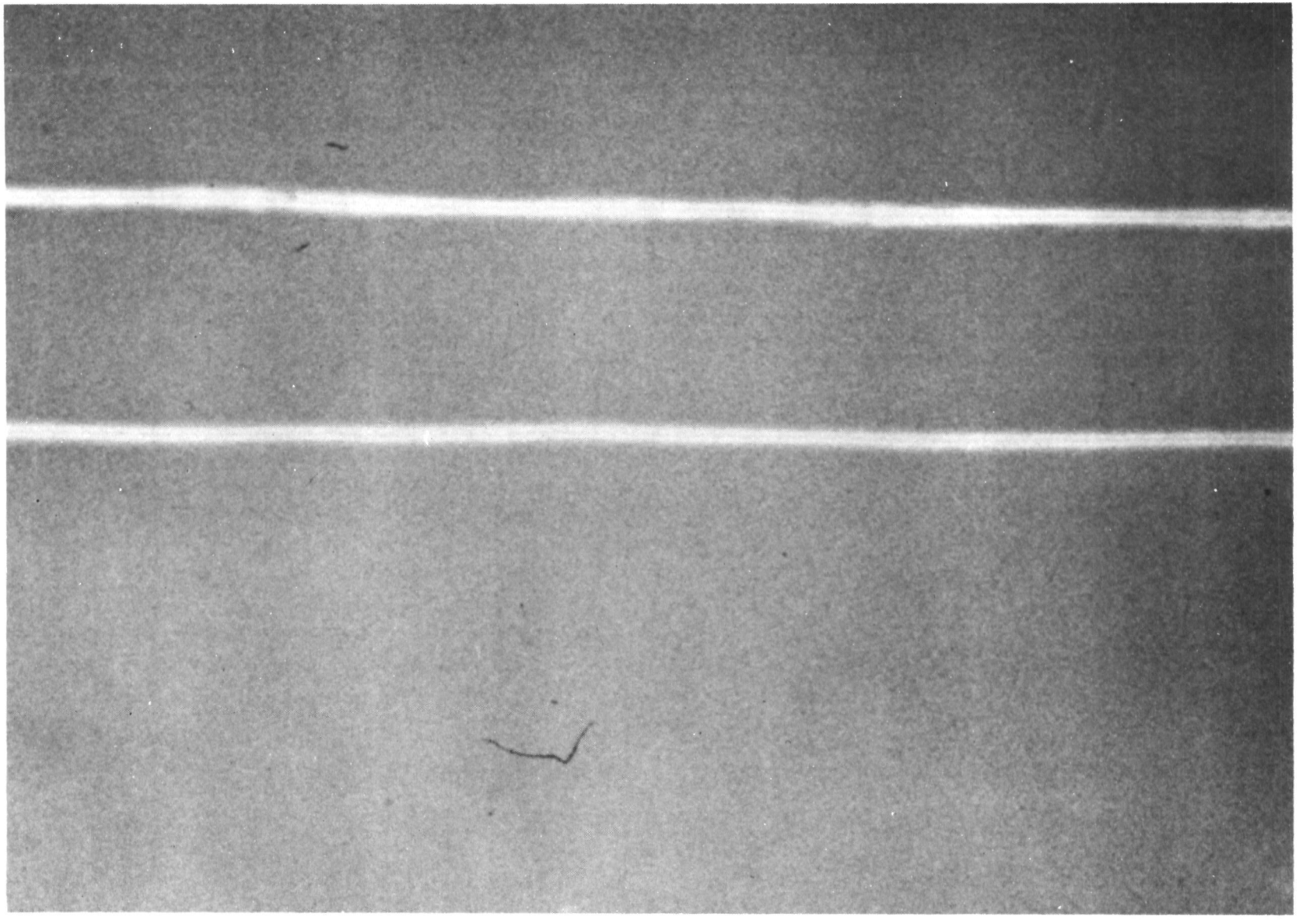

(c) Time = 10 seconds

Figure 20.- Continued.

(d) Time = 15 seconds

Figure 20.- Continued.

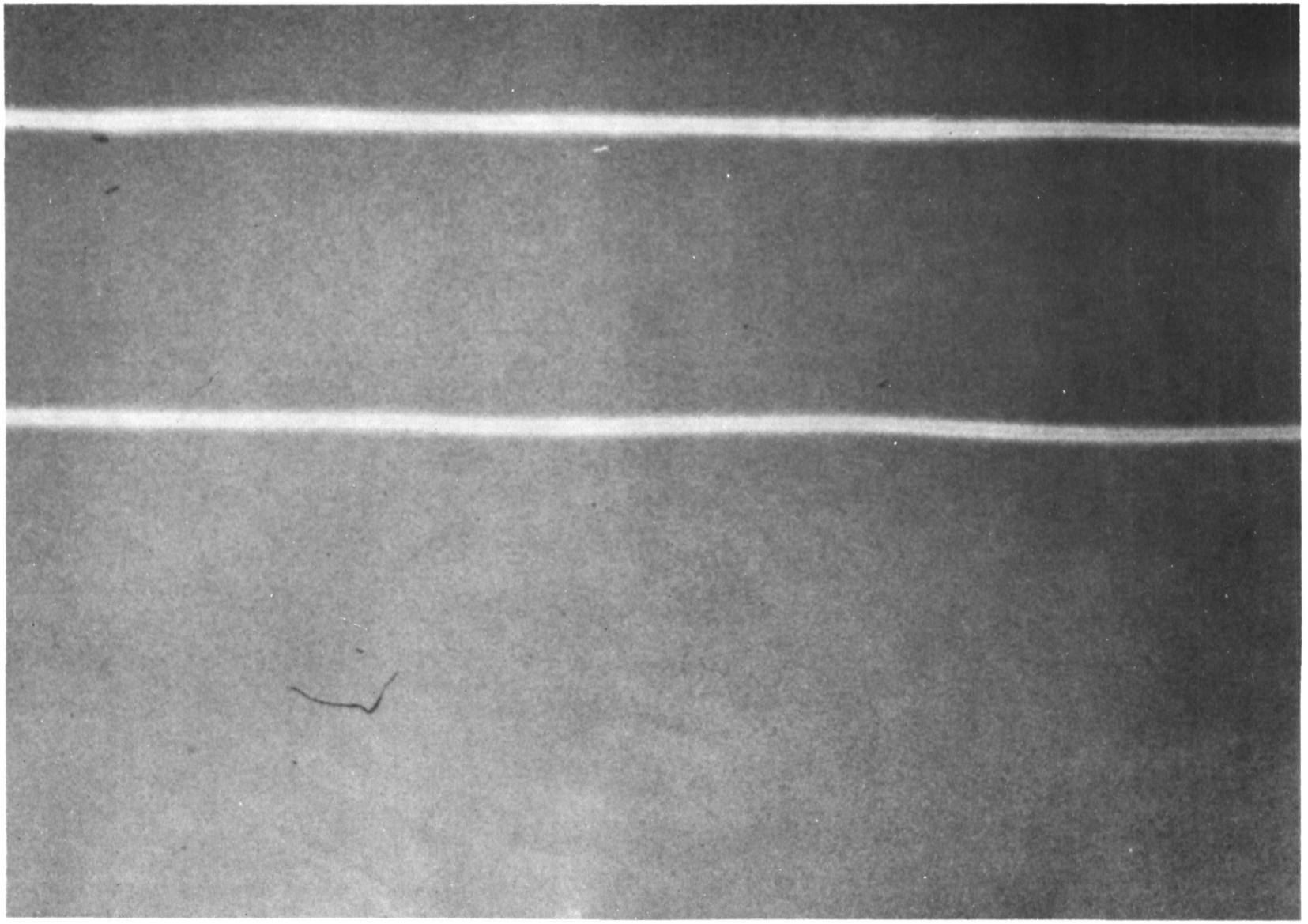

(e) Time = 20 seconds

Figure 20.- Continued.

(f) Time = 25 seconds

Figure 20.- Continued.

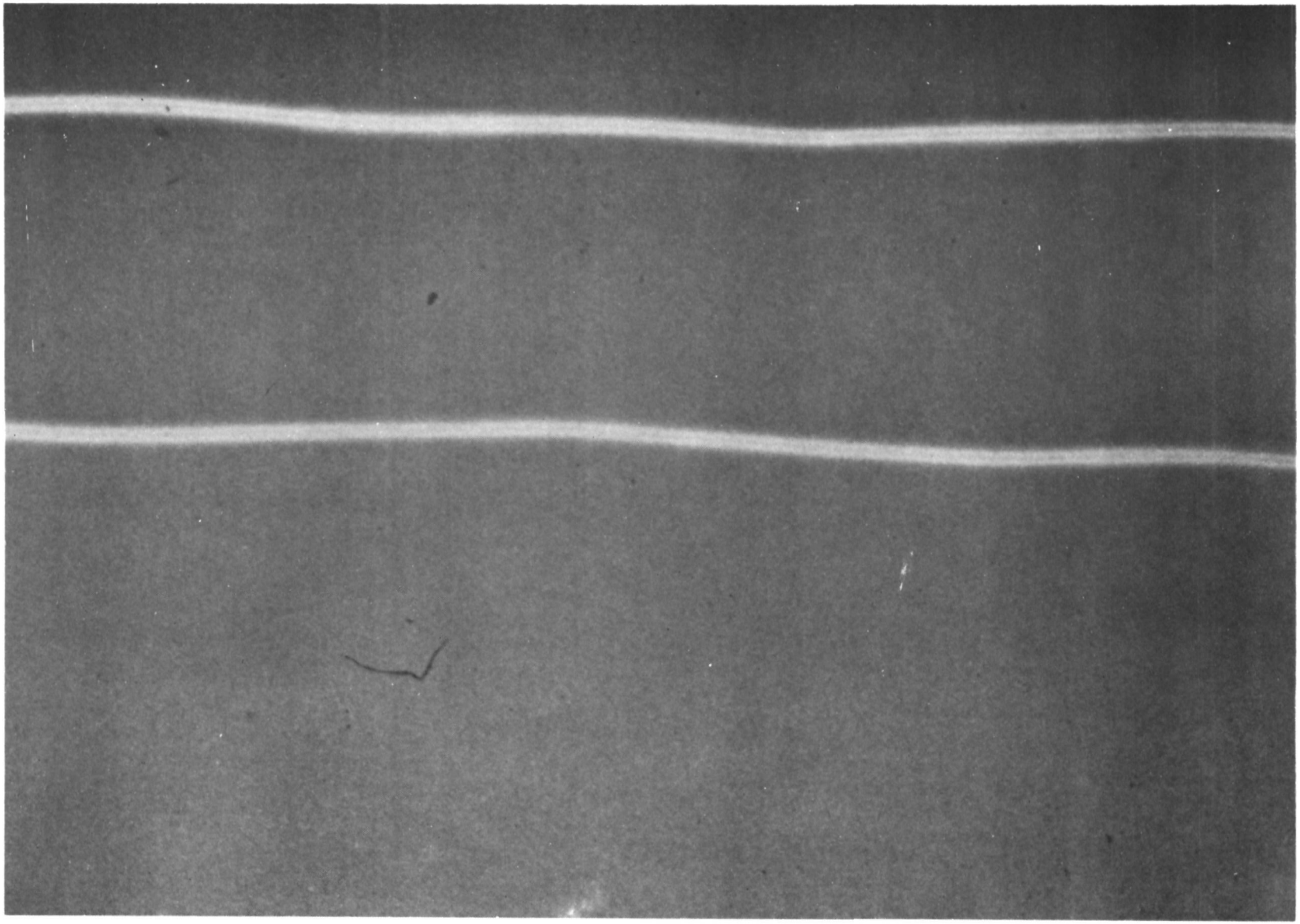

(g) Time = 30 seconds

Figure 20.- Continued.

(h) Time = 35 seconds

Figure 20.- Continued.

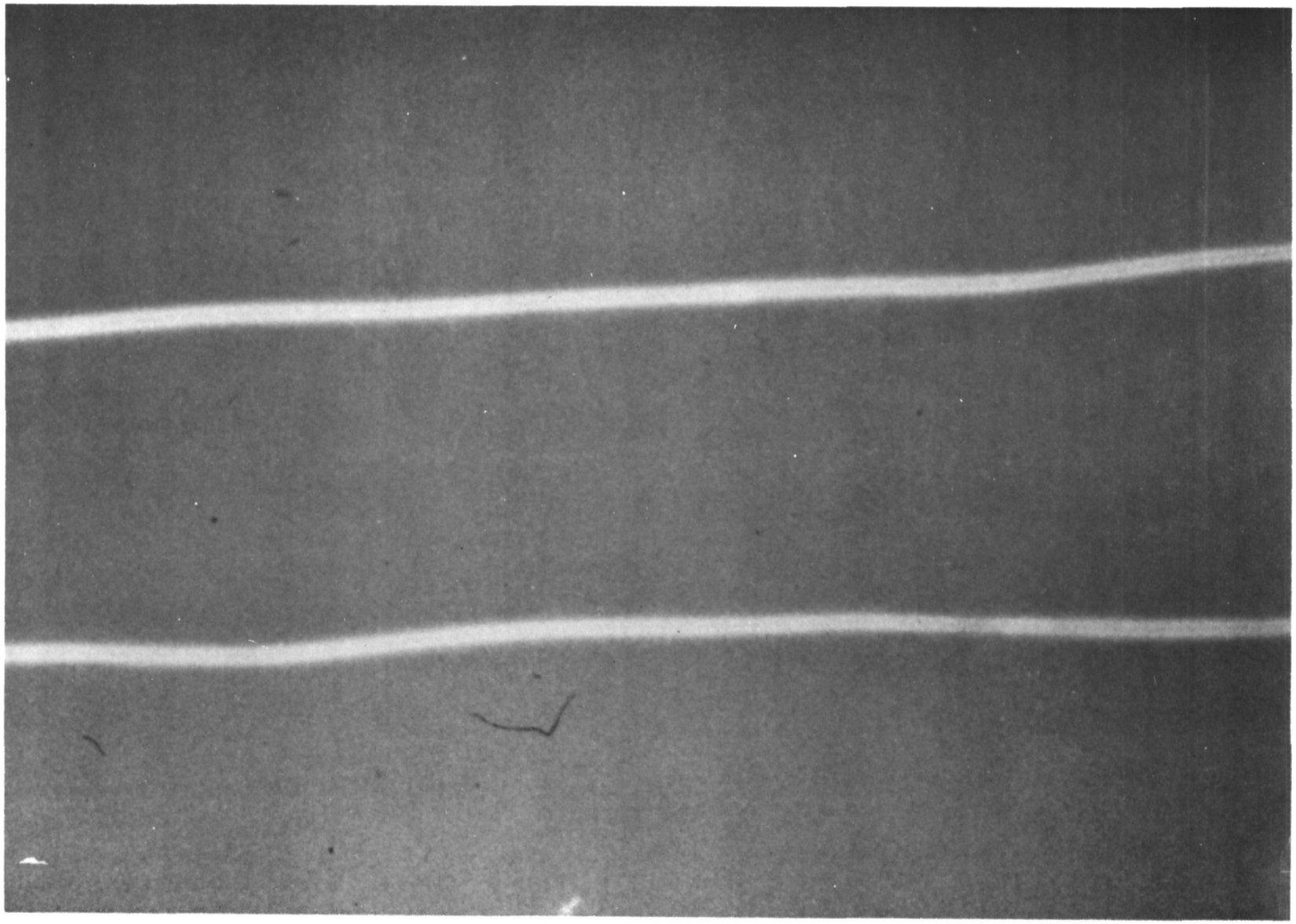

(i) Time = 40 seconds

Figure 20.- Continued.

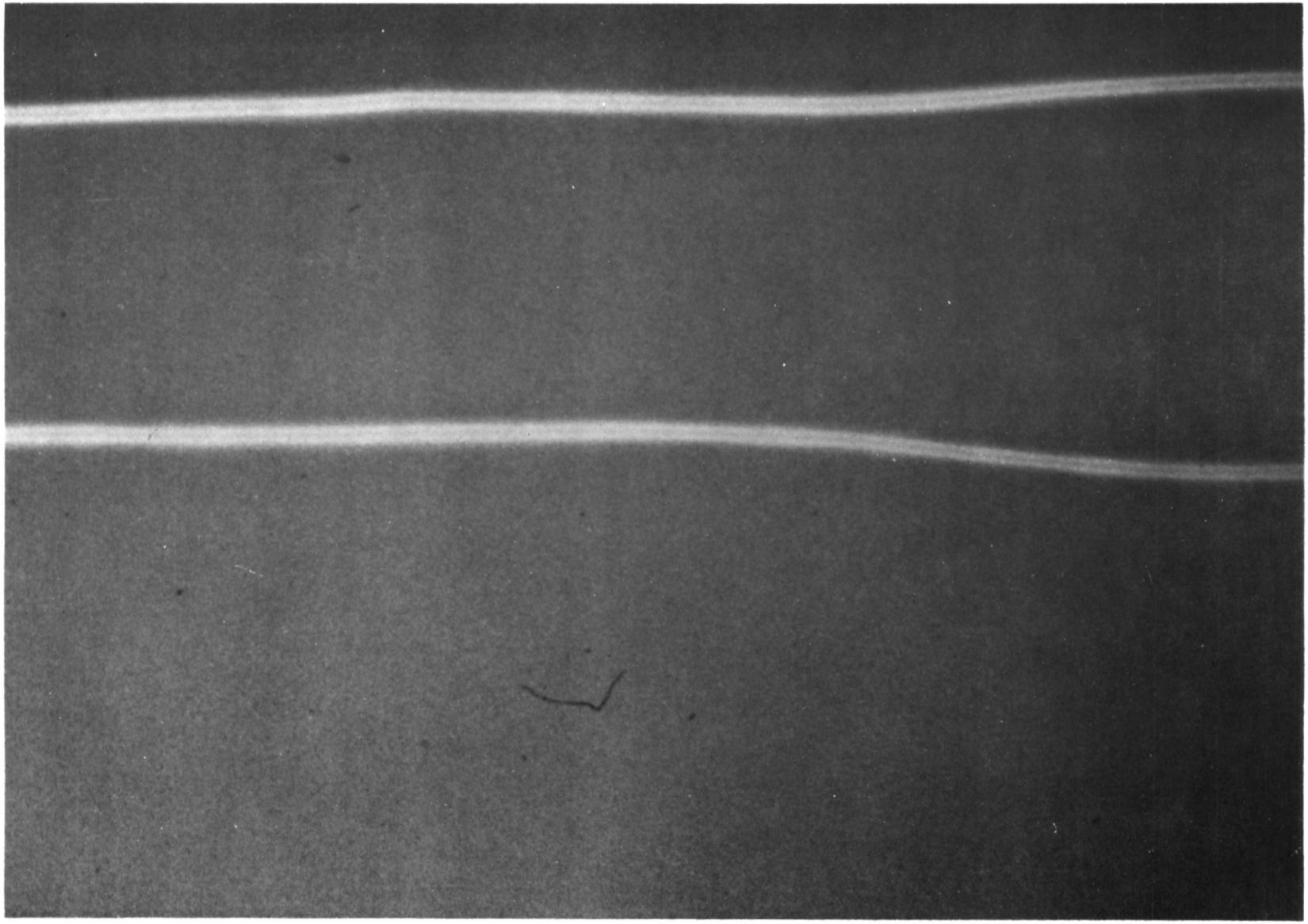

(j) Time = 45 seconds

Figure 20.- Continued.

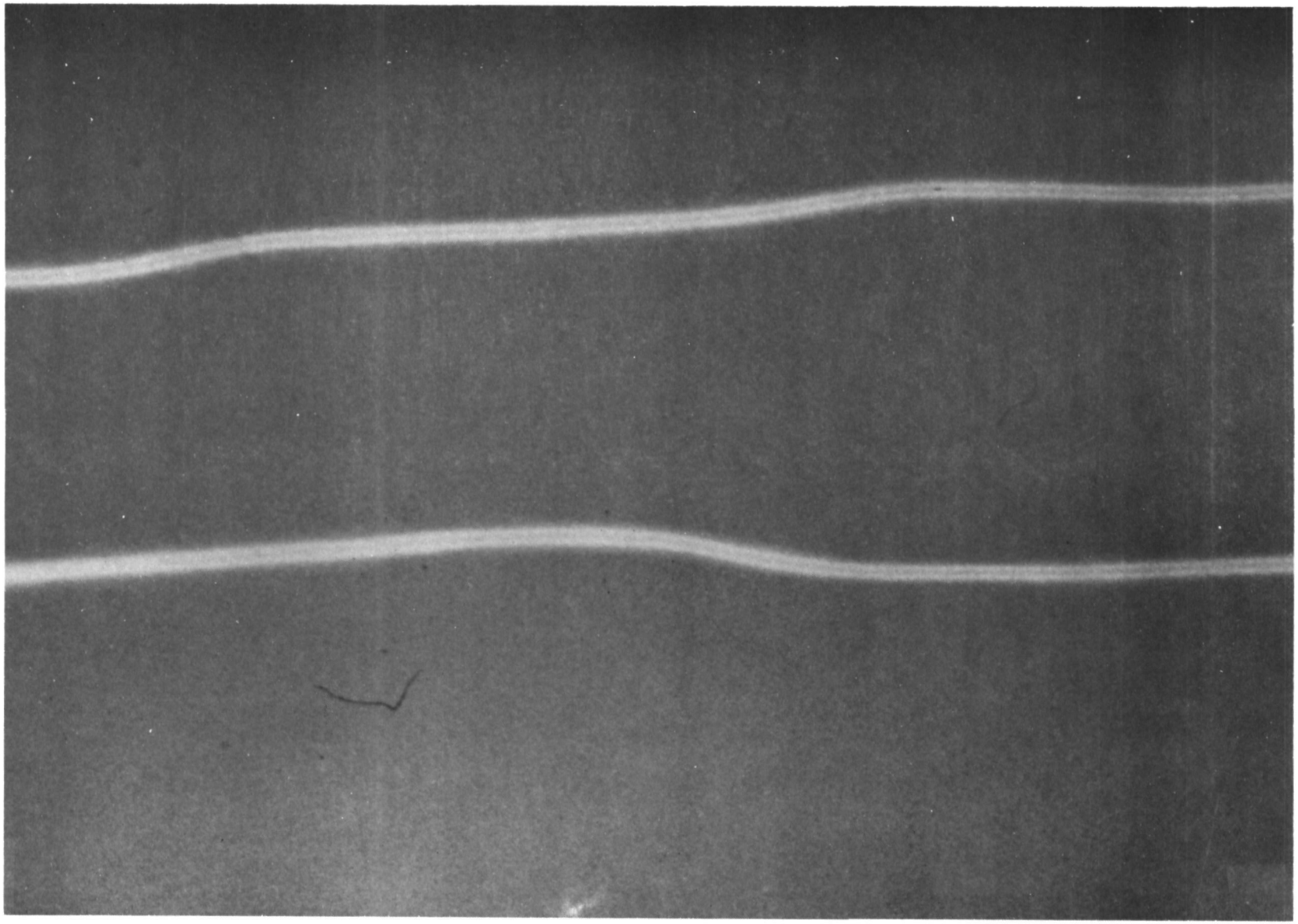

(k) Time = 50 seconds

Figure 20.- Continued.

(1) Time = 55 seconds

Figure 20.- Continued.

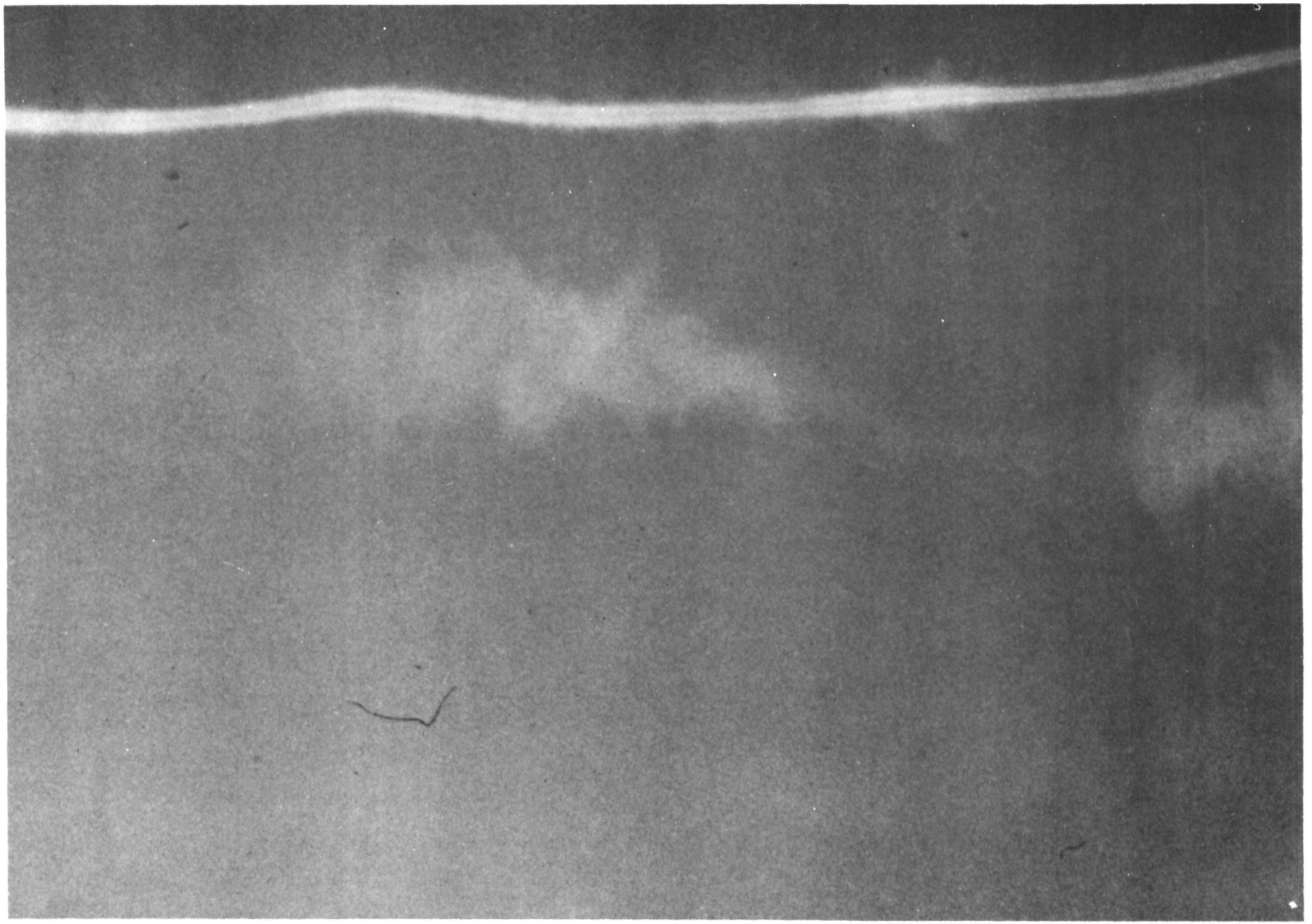

(m) Time = 60 seconds

Figure 20.- Continued.

(n) Time = 65 seconds

Figure 20.- Continued.

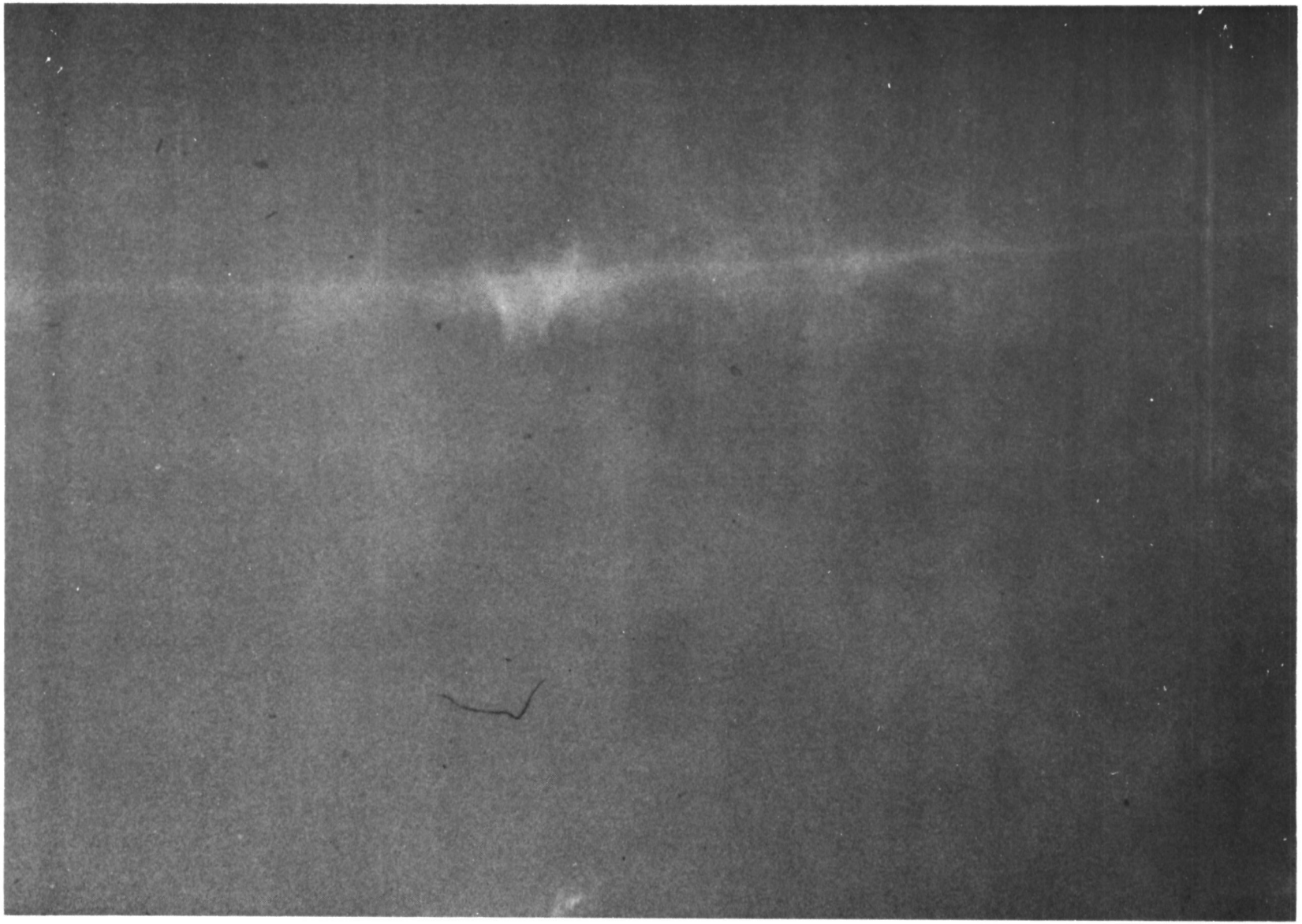

(o) Time = 70 seconds

Figure 20.- Concluded.

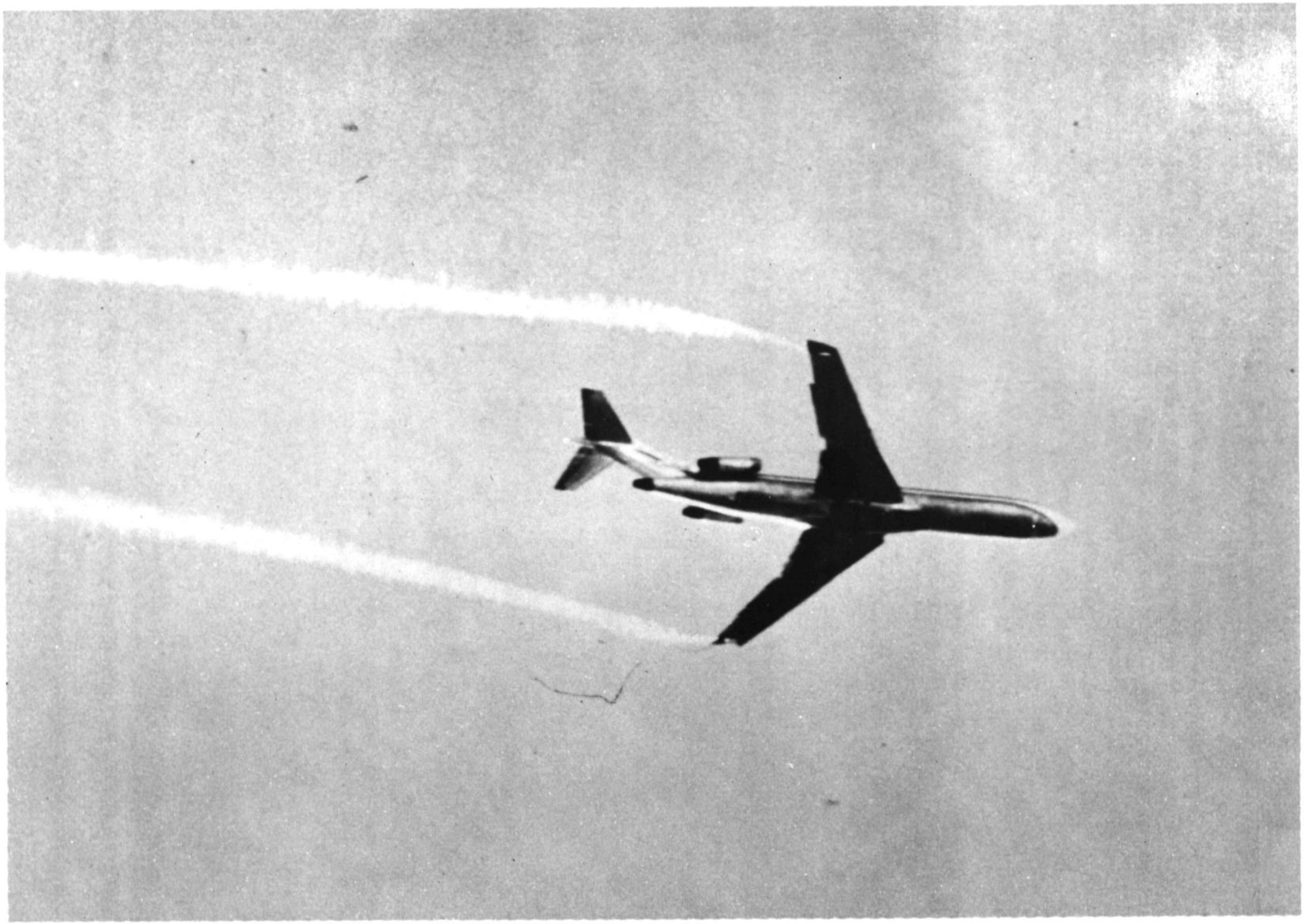

(a) Time = 0 seconds

Figure 21.- B727 wake vortex (takeoff configuration: weight = 329,000 kg (149,000 lbs.)

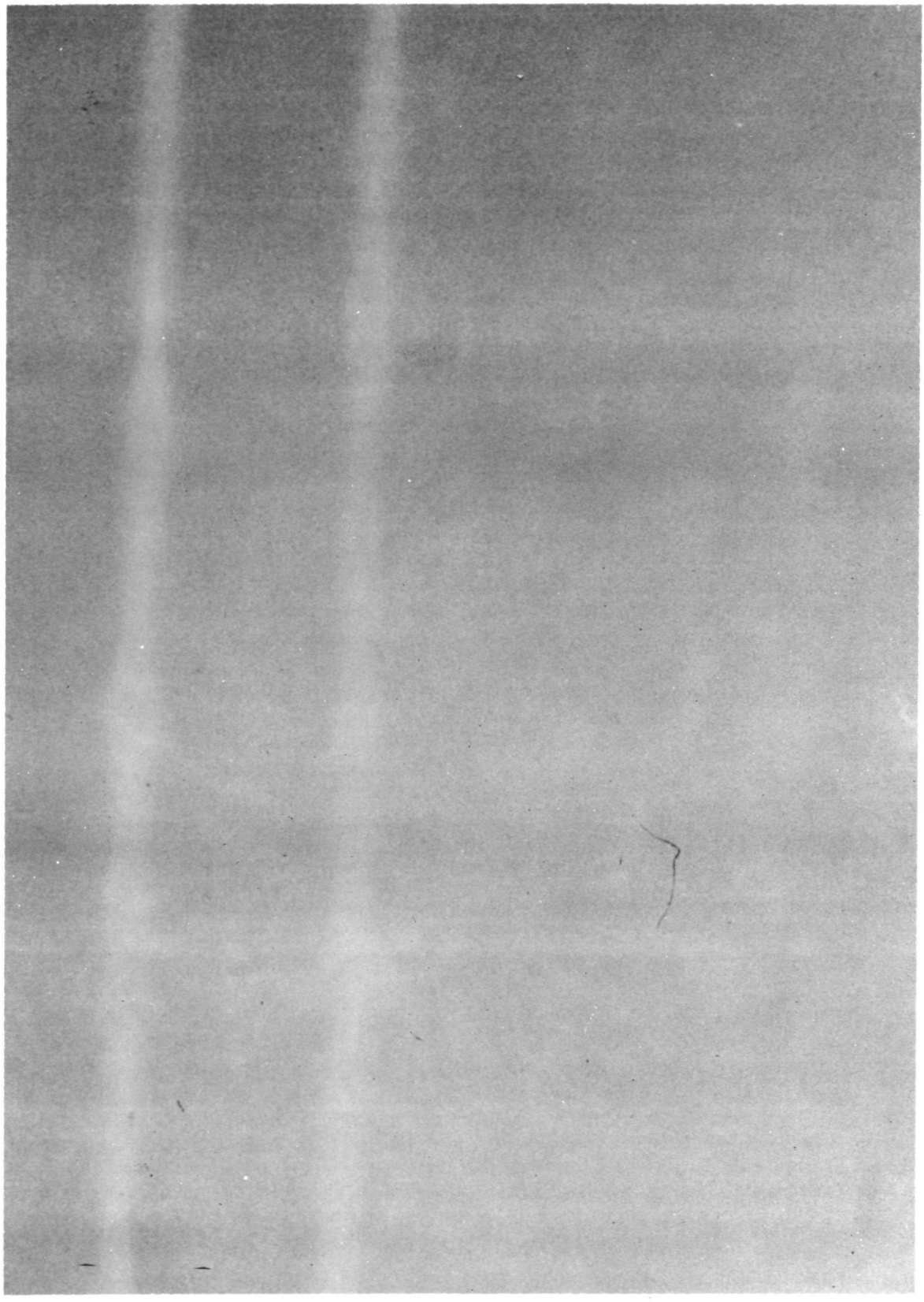

(b) Time = 5 seconds

Figure 21.- Continued.

(c) Time = 10 seconds

Figure 21.- Continued.

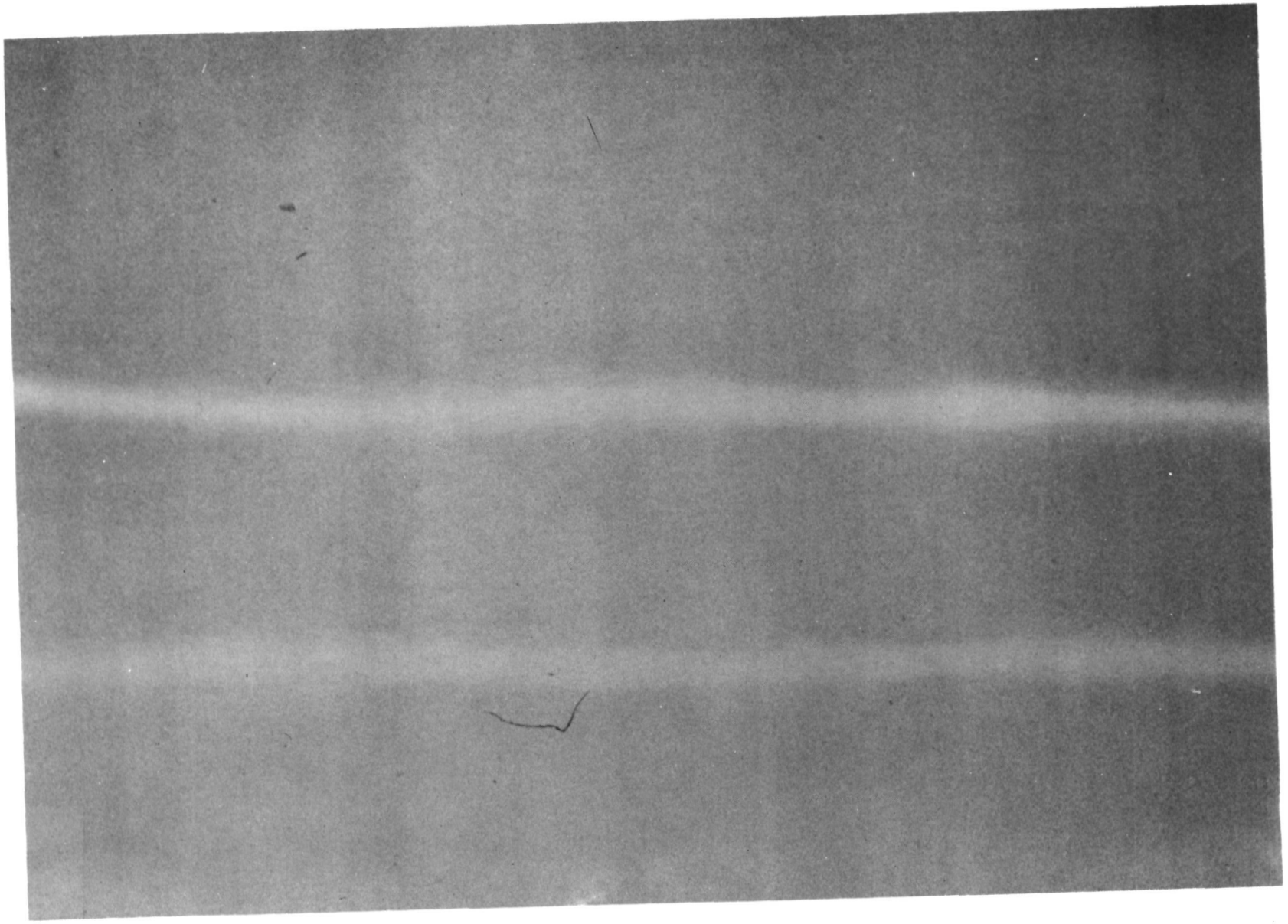

(d) Time = 15 seconds

Figure 21.- Continued.

(e) Time = 20 seconds

Figure 21.- Continued.

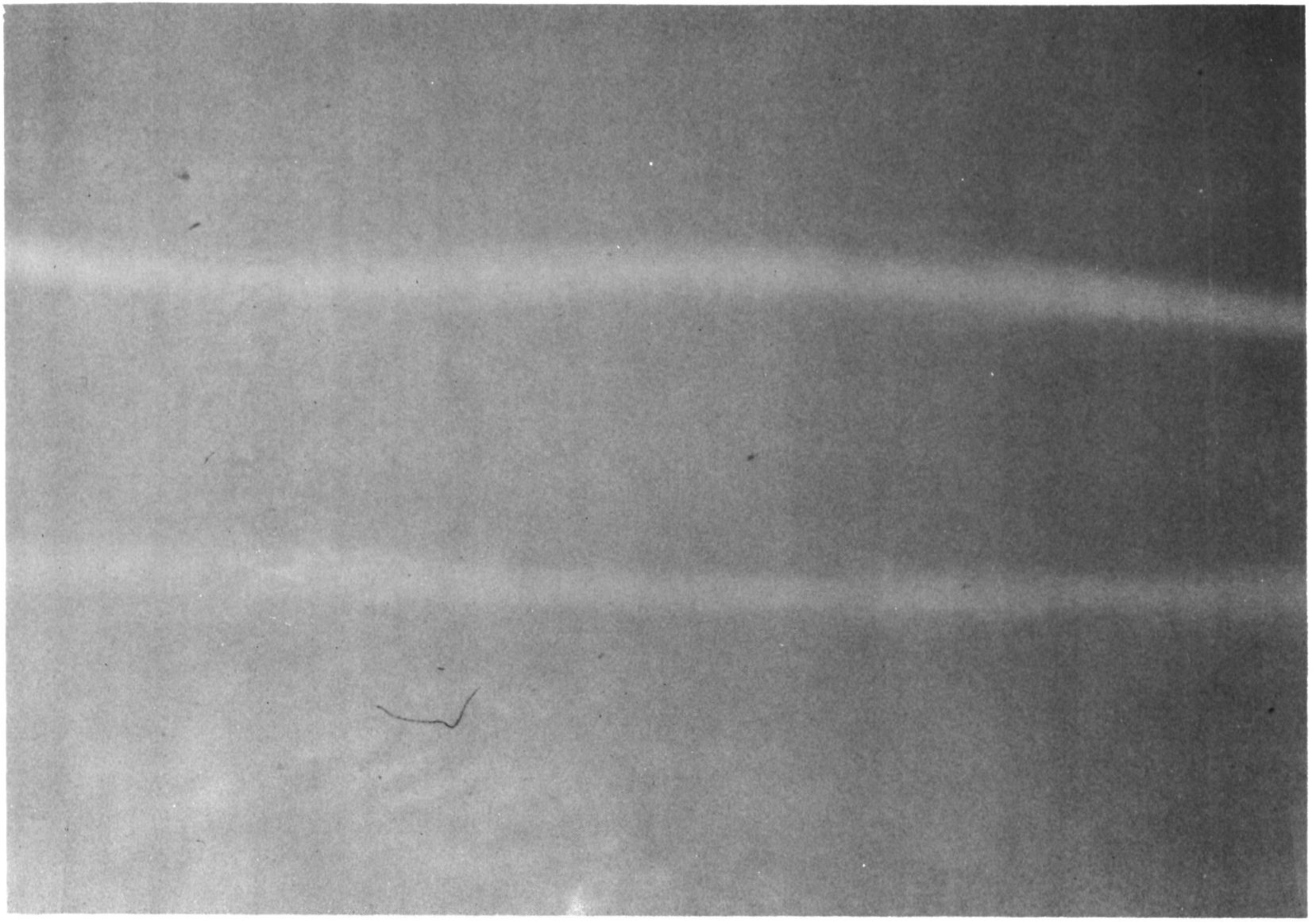

(f) Time = 25 seconds

Figure 21.- Continued.

(g) Time = 30 seconds

Figure 21.- Continued.

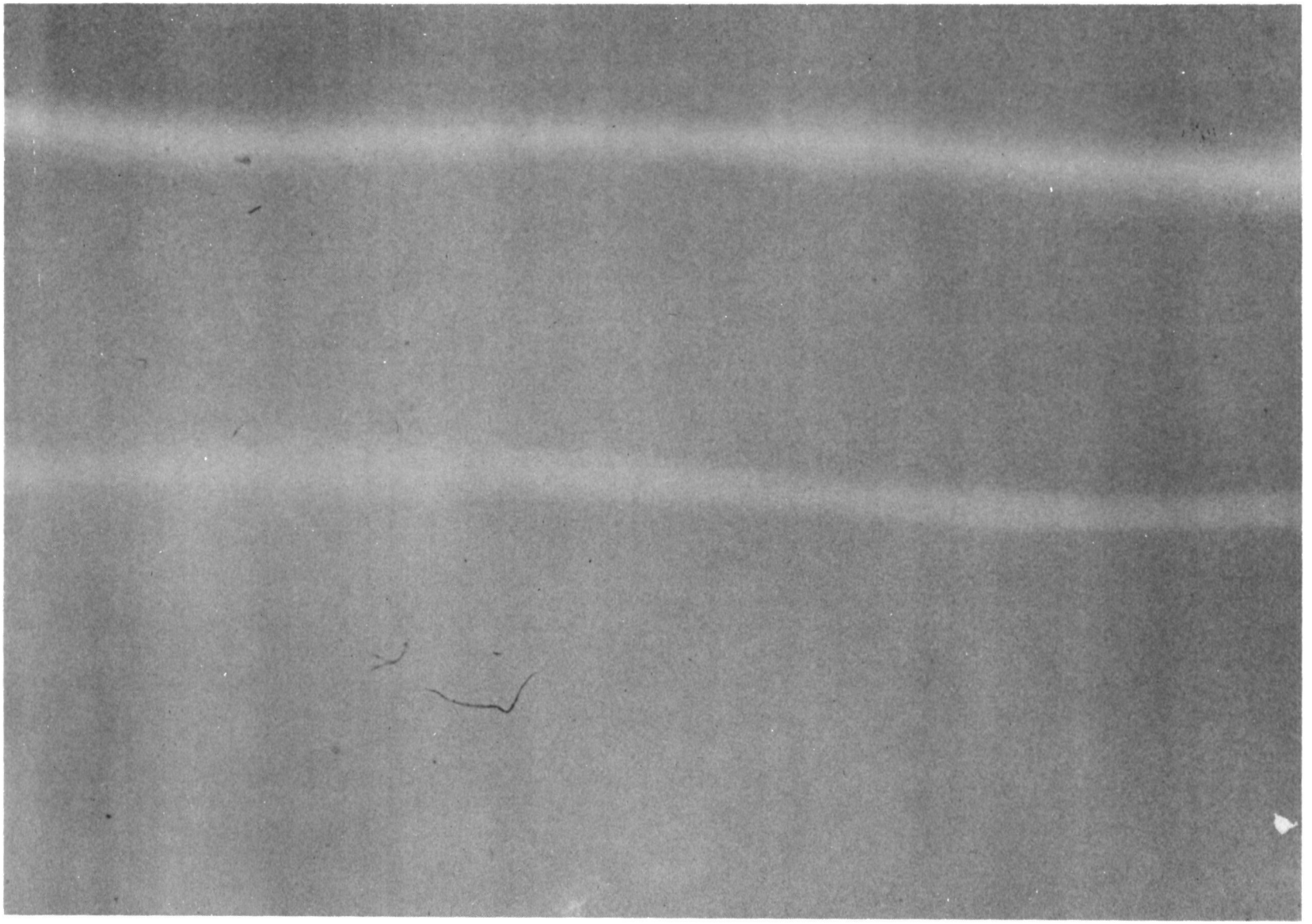

(h) Time = 35 seconds

Figure 21.- Continued.

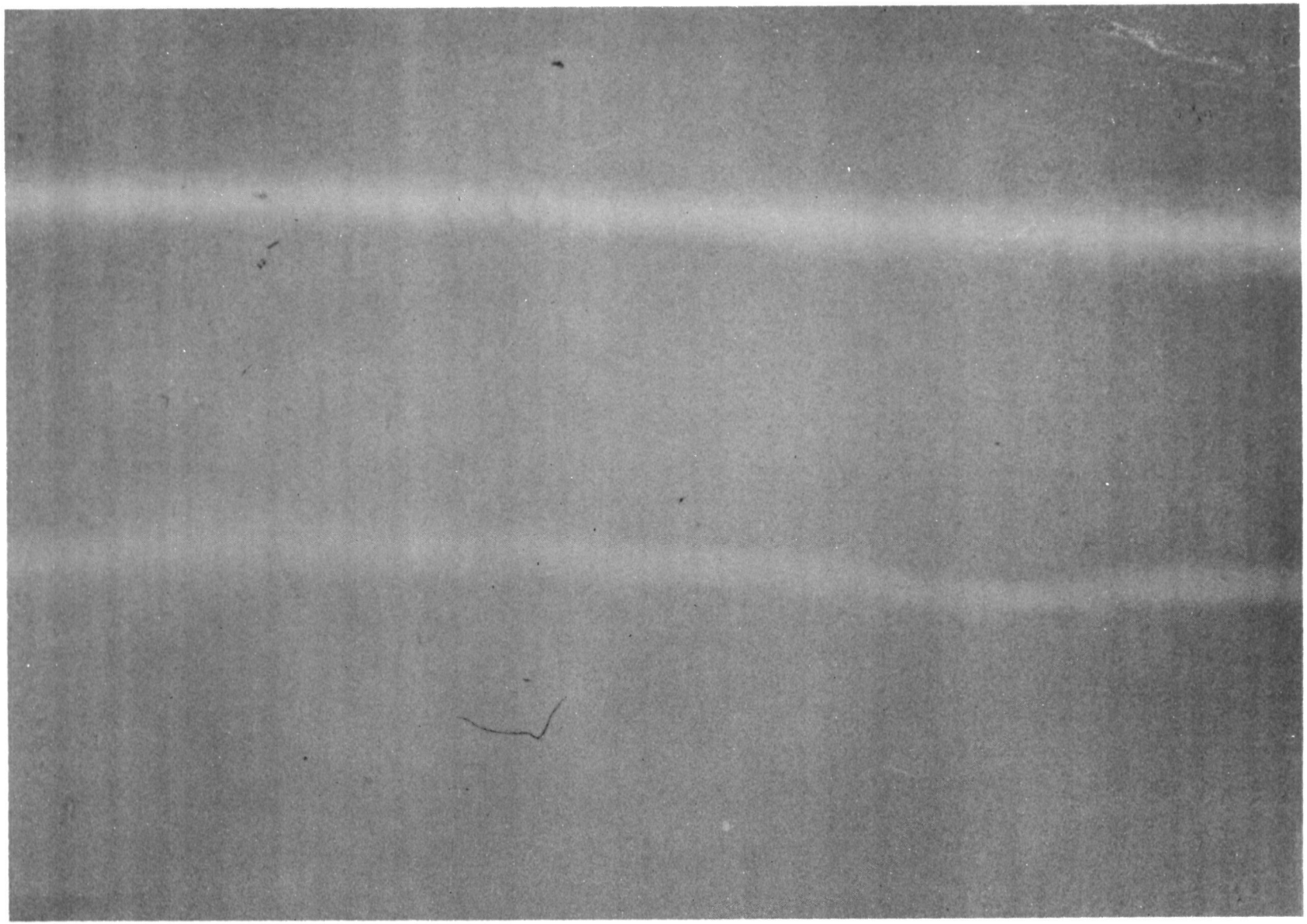

(i) Time = 40 seconds

Figure 21.- Continued.

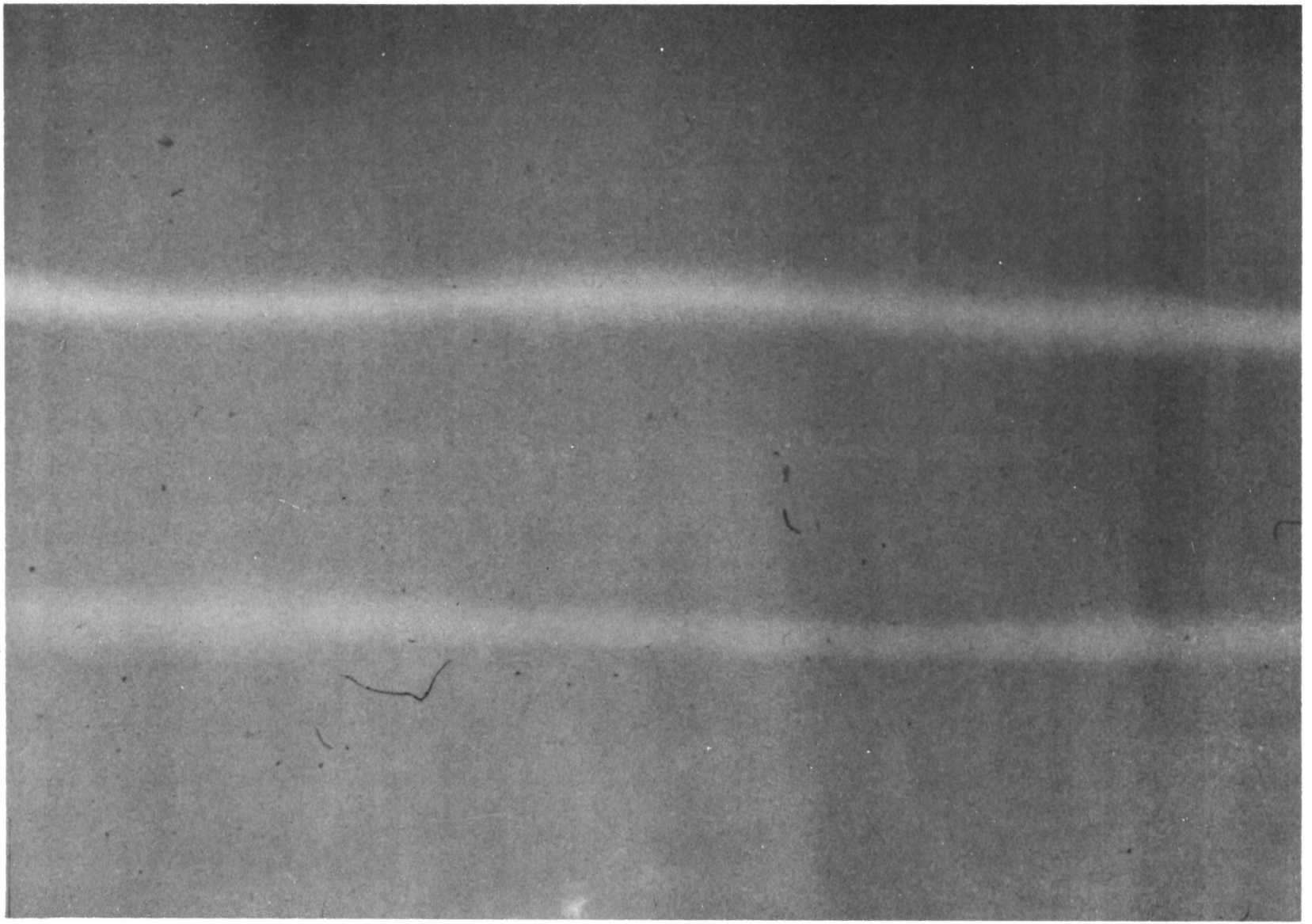

(j) Time = 45 seconds

Figure 21.- Continued.

(k) Time = 50 seconds

Figure 21.- Continued.

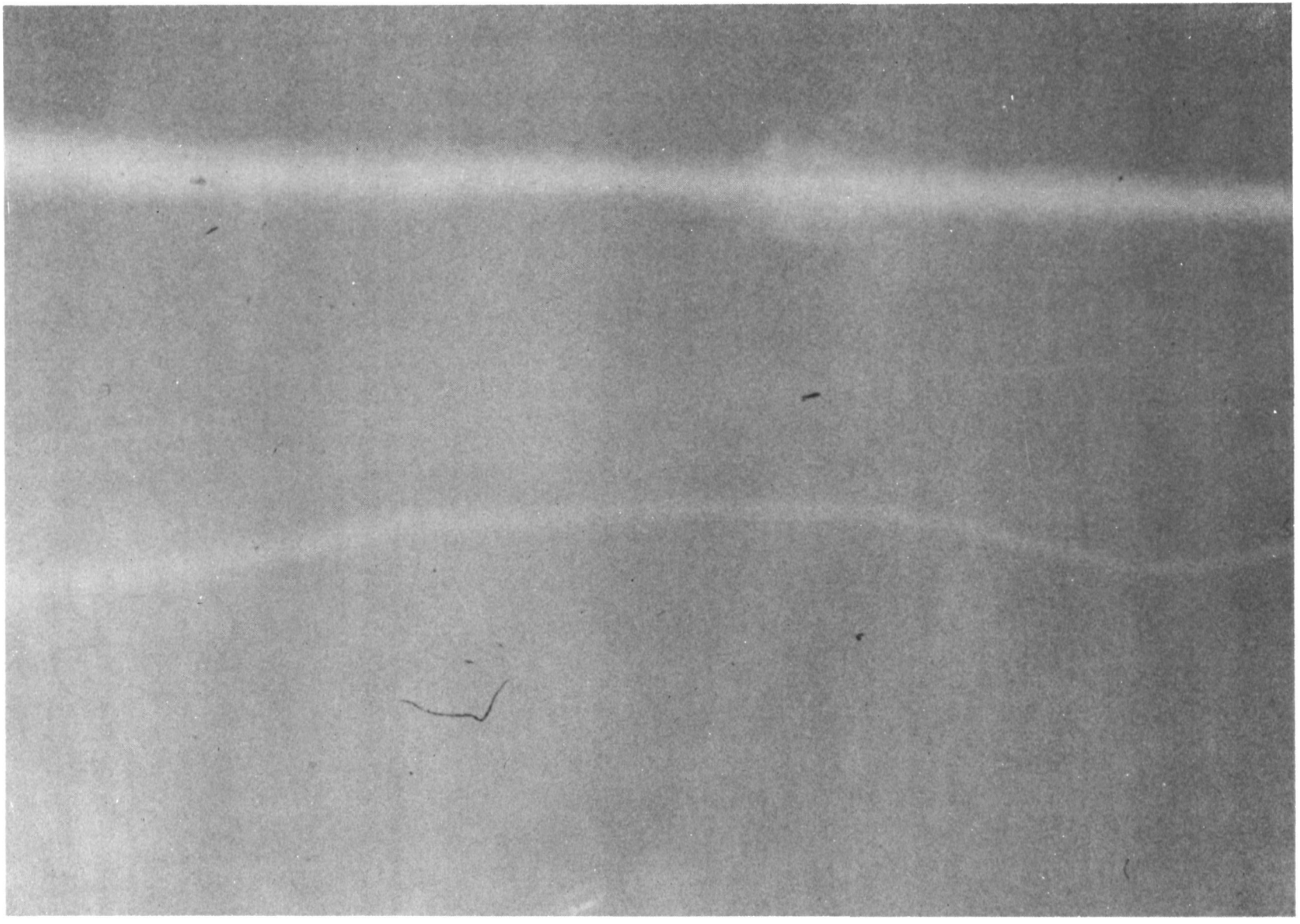

(1) Time = 55 seconds

Figure 21.- Continued.

(m) Time = 60 seconds

Figure 21.- Continued.

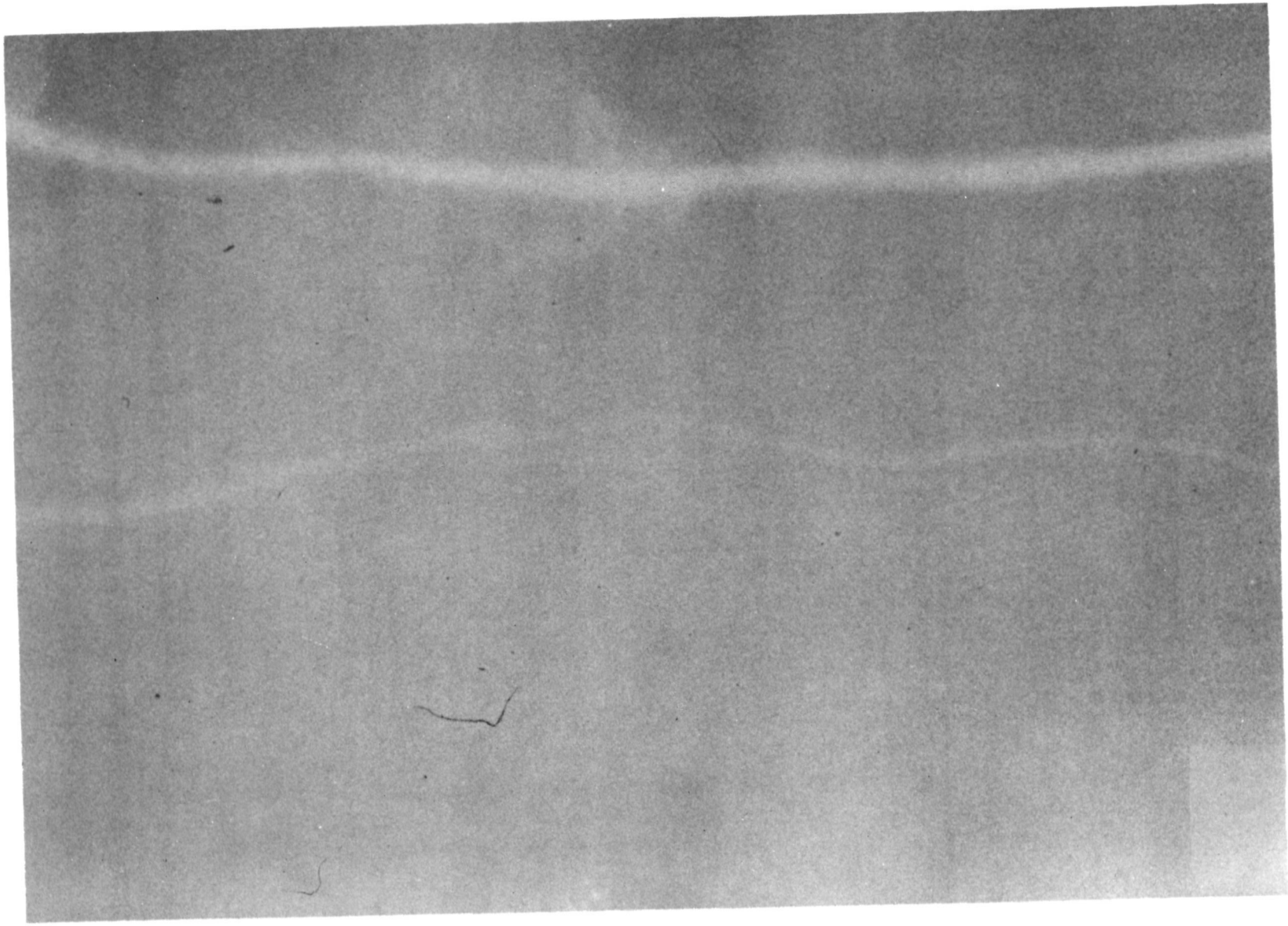

(n) Time = 65 seconds

Figure 21.- Continued.

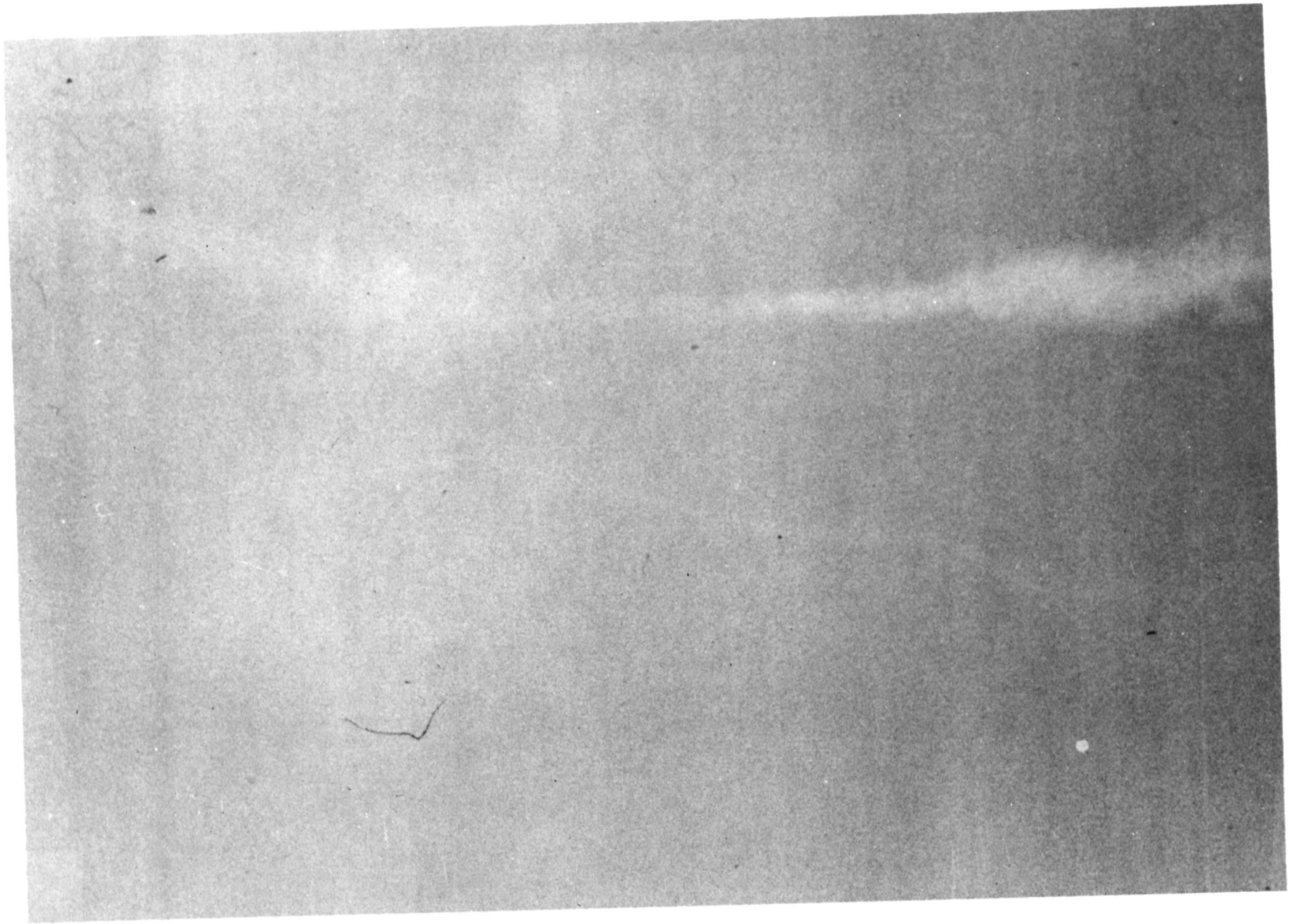

(o) Time = 70 seconds

Figure 21.- Continued.

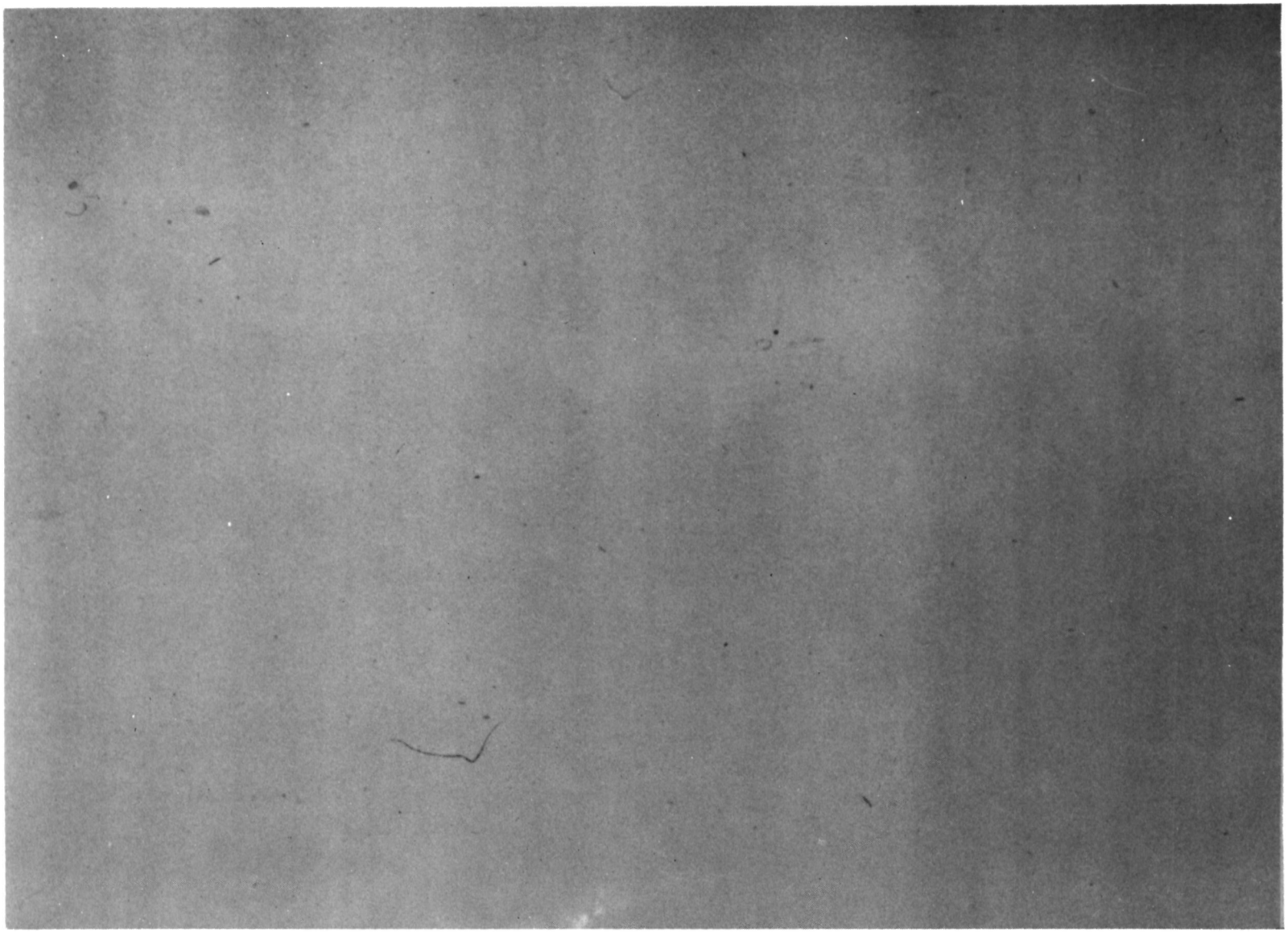

(p) Time = 75 seconds

Figure 21.- Concluded.

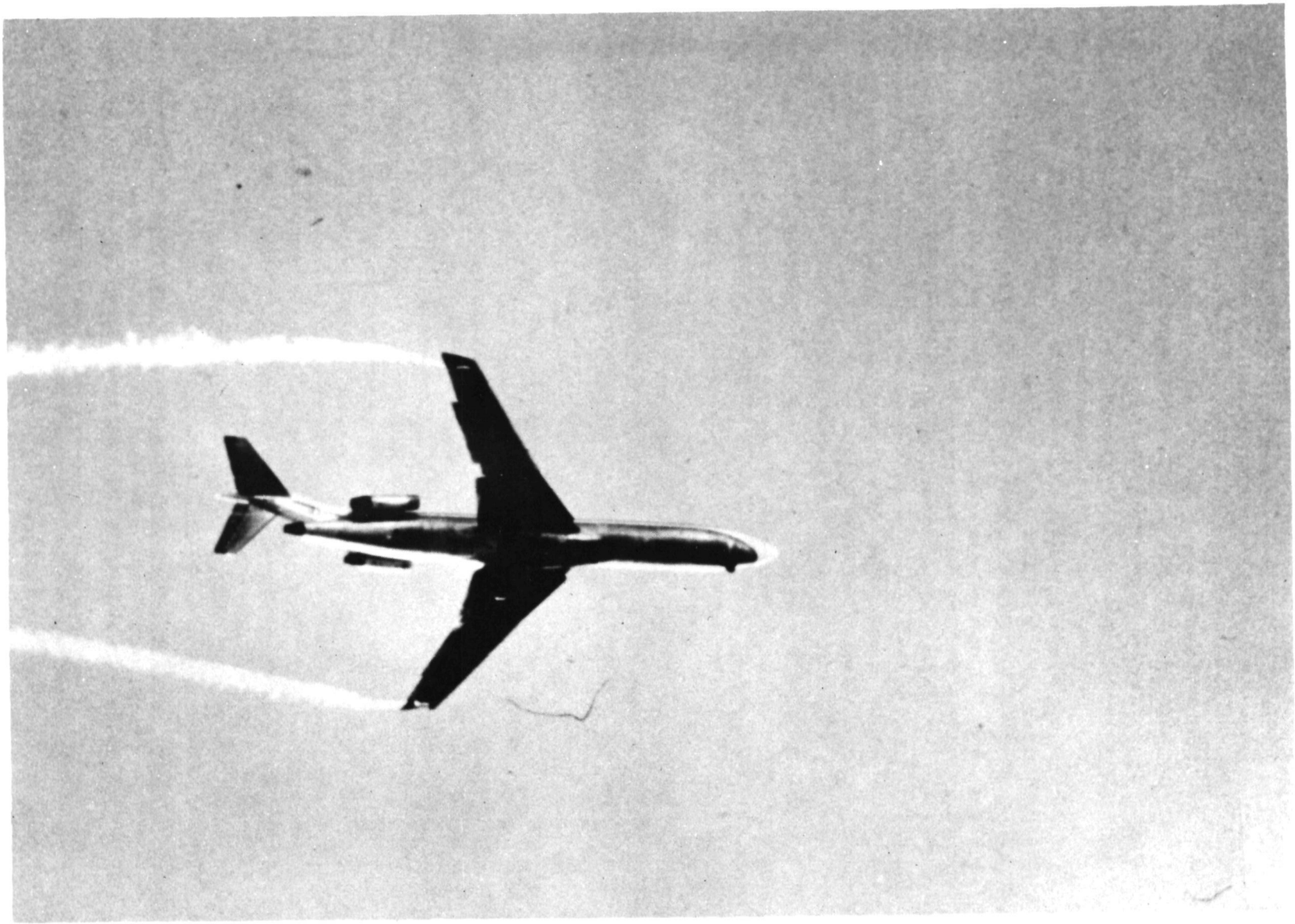

(a) Time = 0 seconds

Figure 22.- B727 wake vortex (landing configuration: weight = 330,500 kg (150,000 lbs.)).

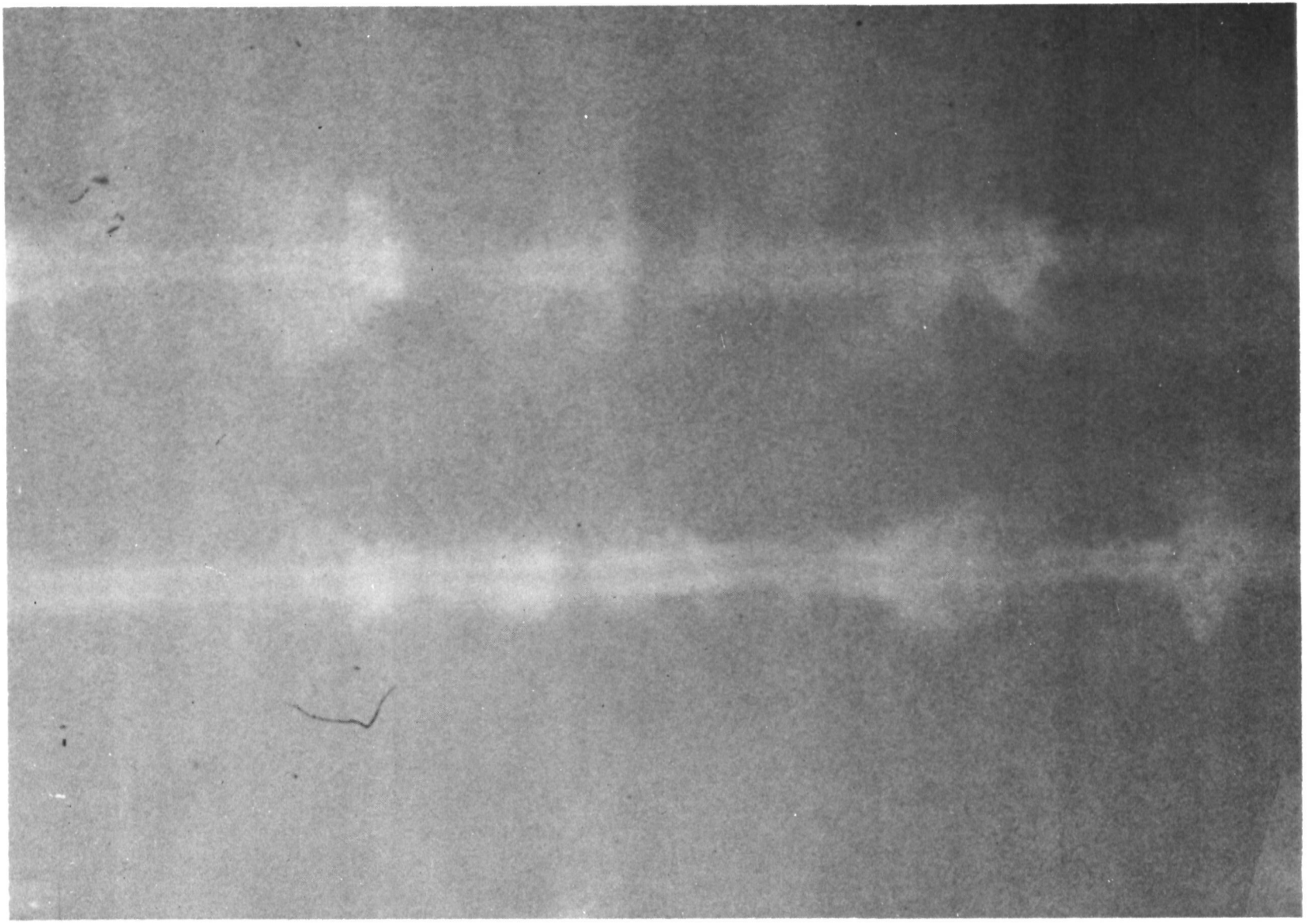

(b) Time = 10 Seconds

Figure 22.- Continued.

(c) Time = 15 seconds

Figure 22.- Continued.

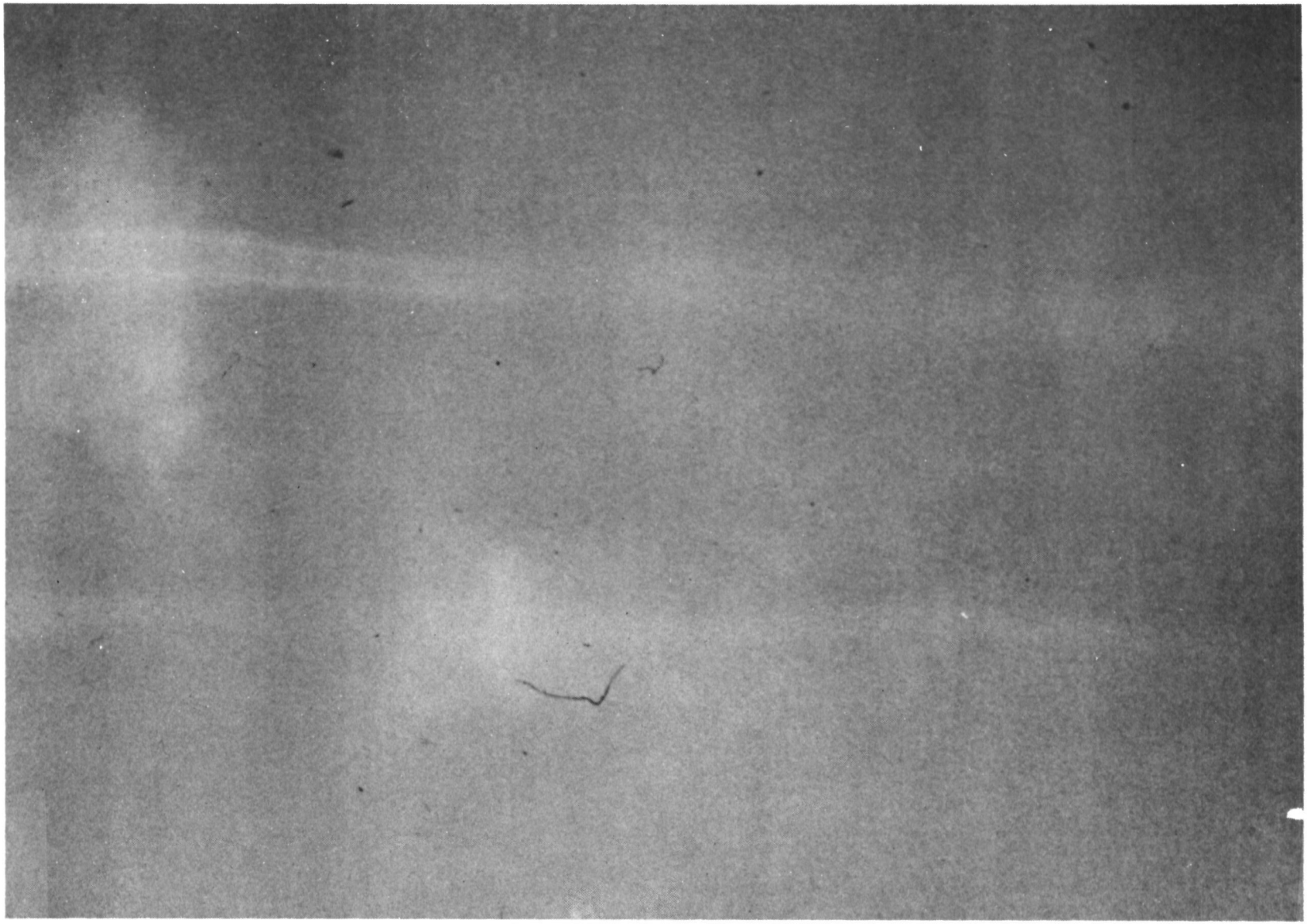

(d) Time = 20 seconds

Figure 22.- Continued.

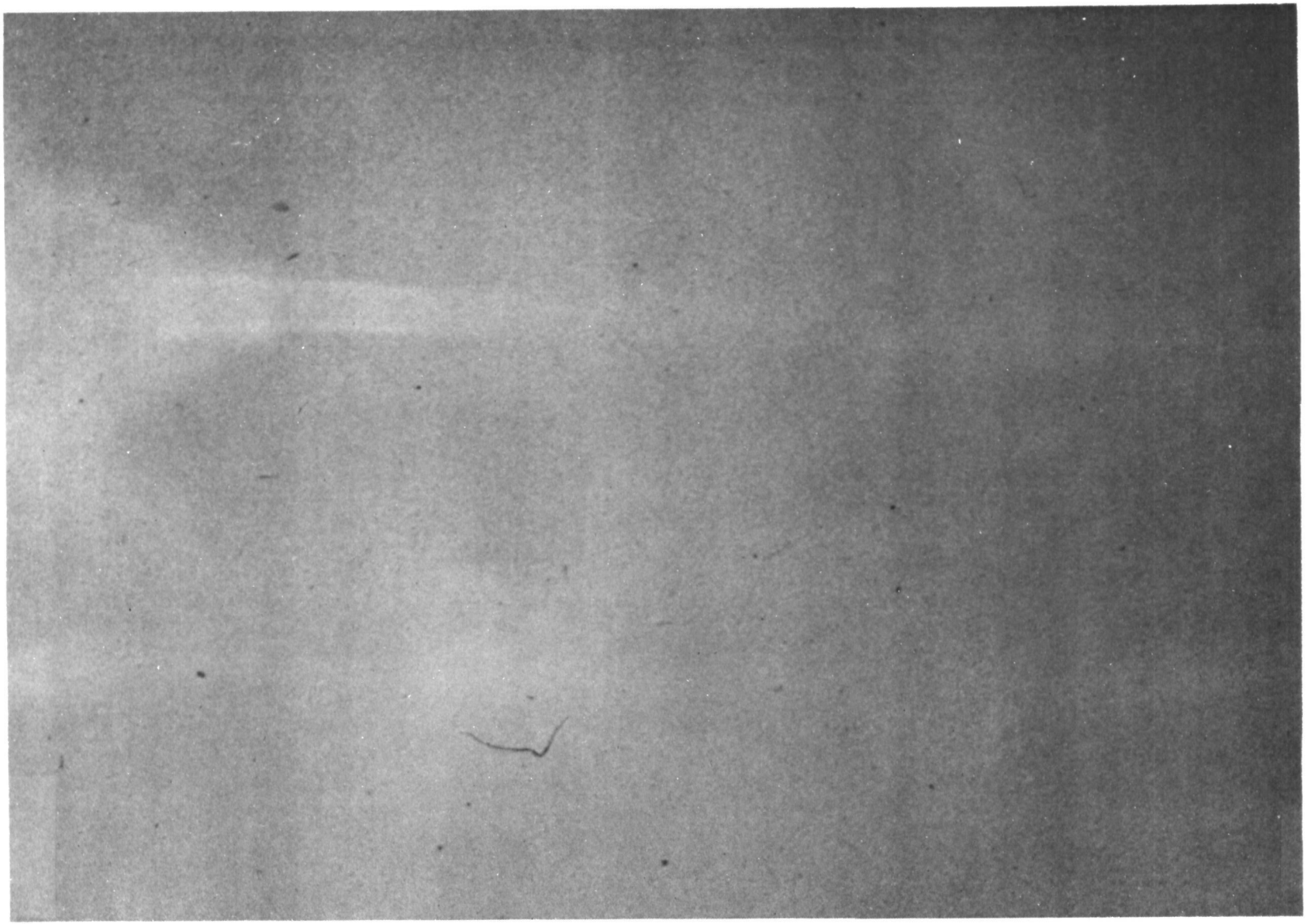

(e) Time = 25 seconds

Figure 22.- Continued.

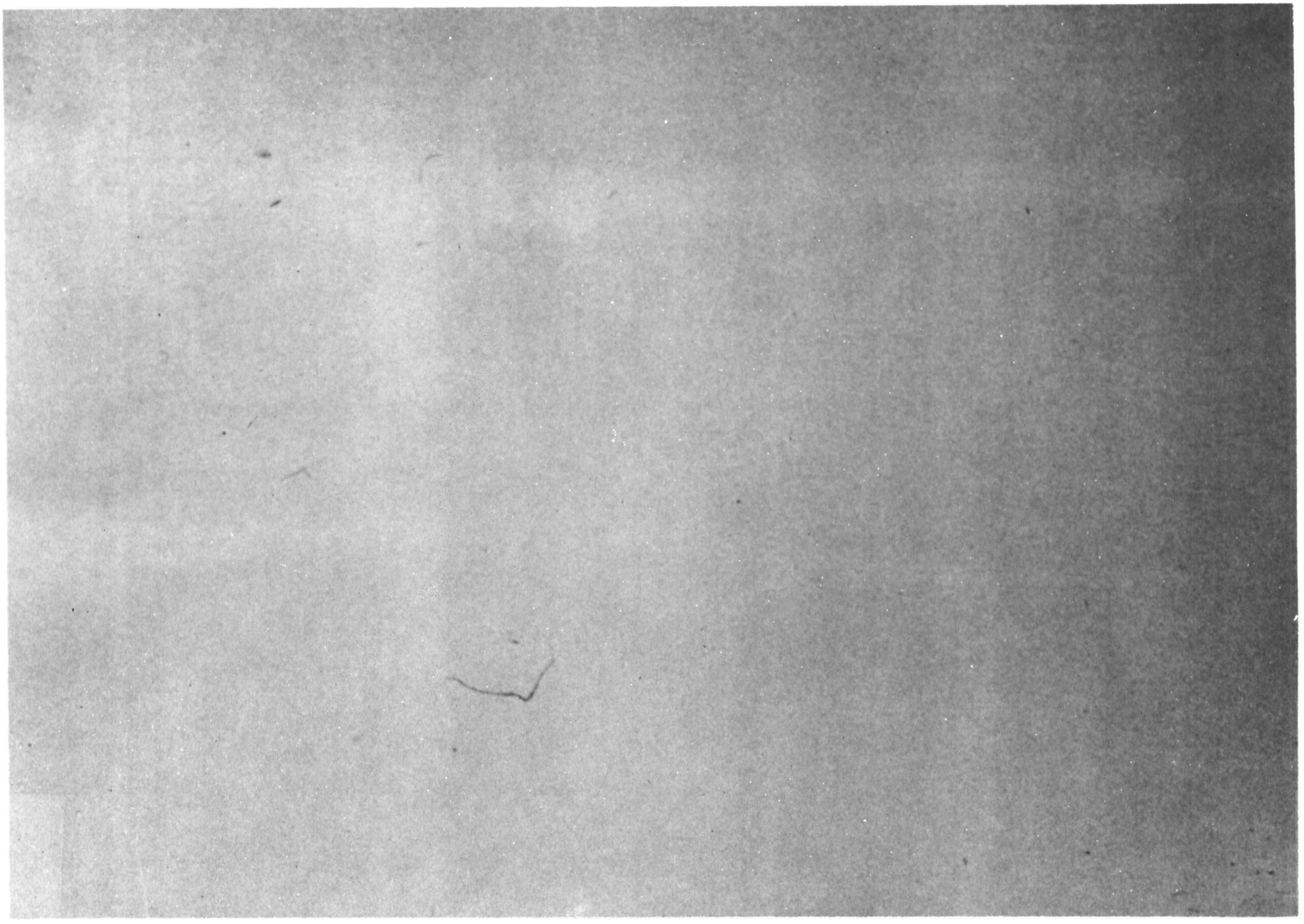

(f) Time = 30 seconds

Figure 22.- Continued.

(g) Time = 35 seconds

Figure 22.- Continued.

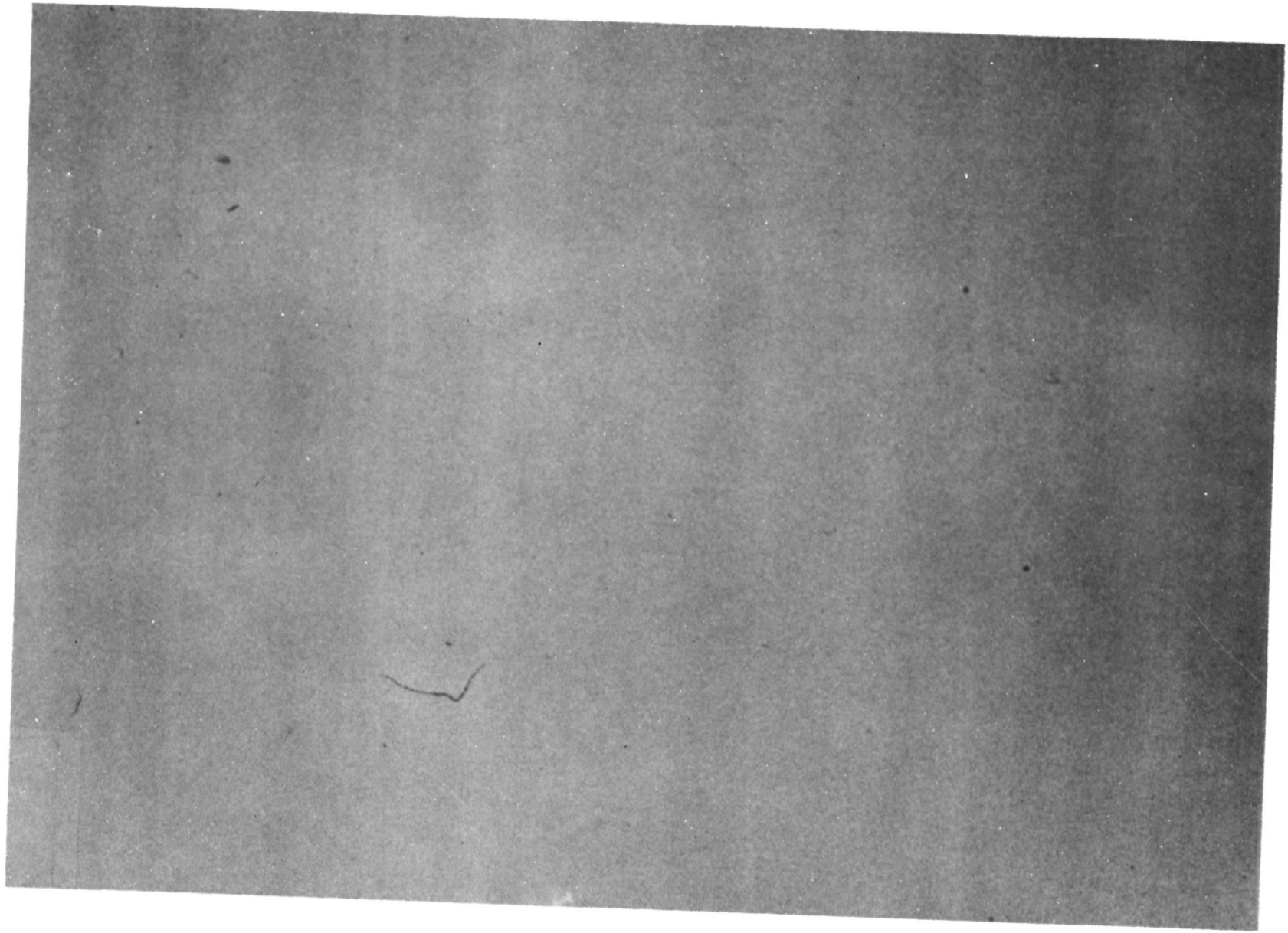

(h) Time = 40 seconds

Figure 22.- Concluded.

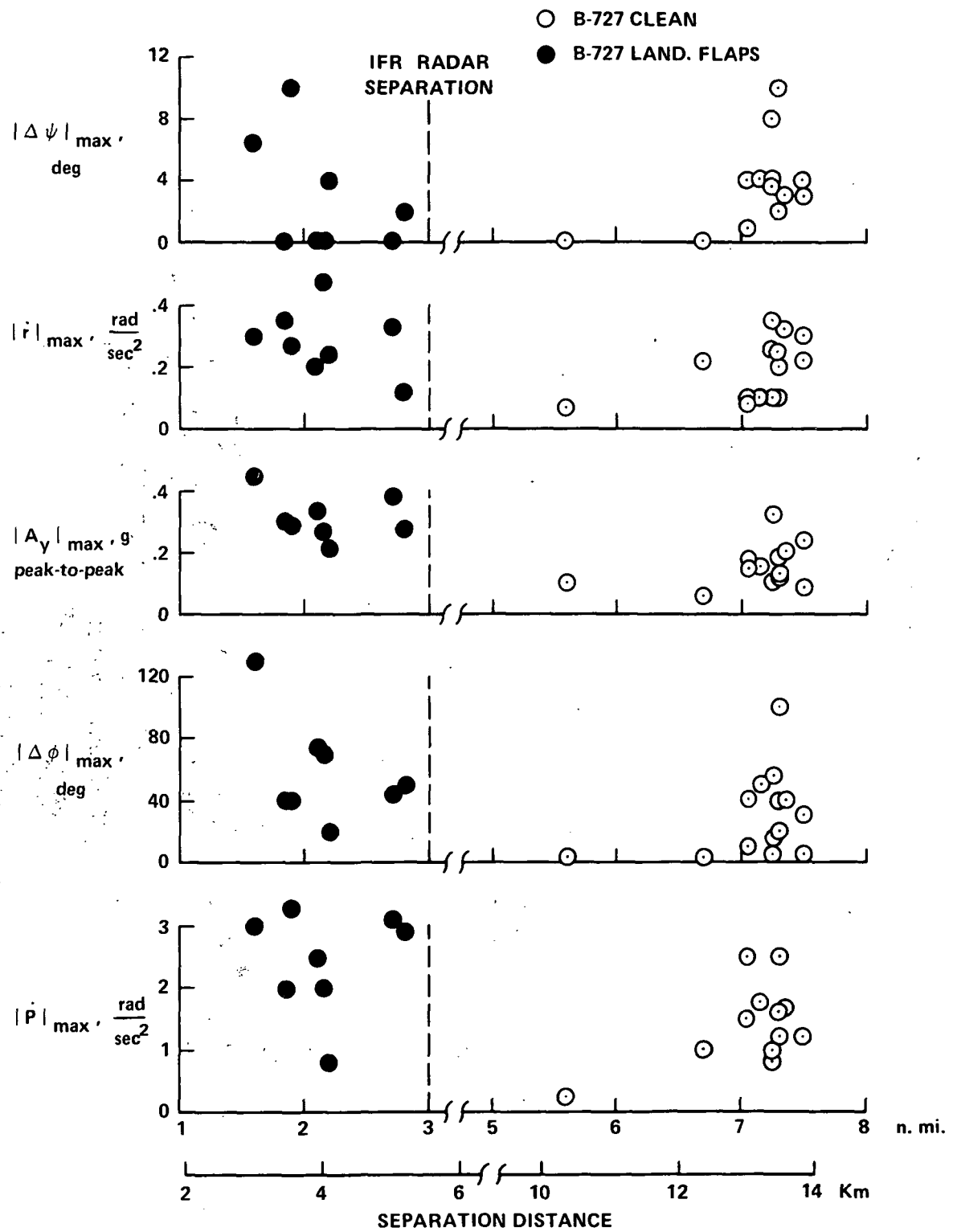

(a) Lateral-directional

Figure 23.- Effect of generator flap configuration on maximum Lear Jet excursions versus separation distance.

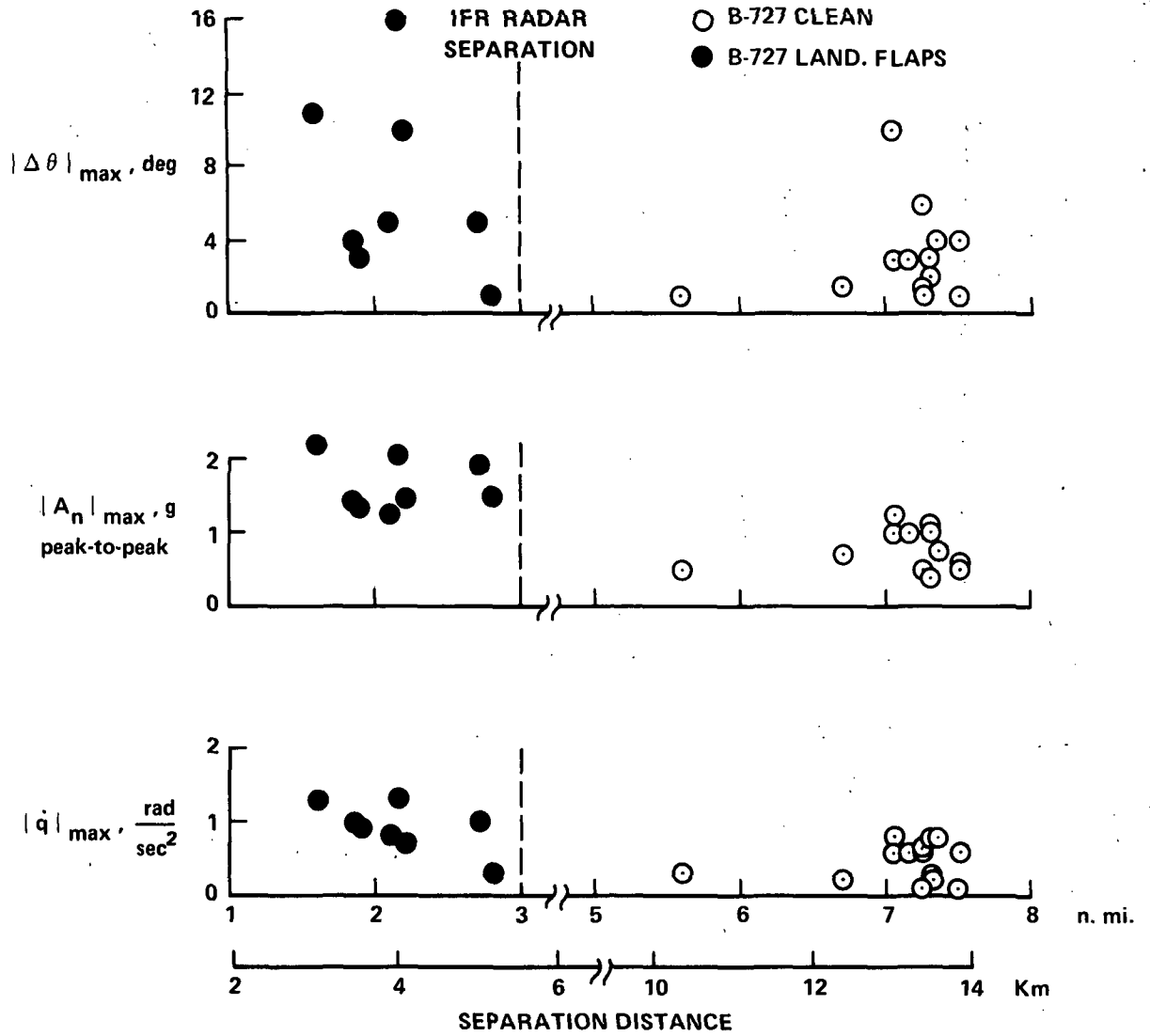

(b) Longitudinal

Figure 23.- Concluded.

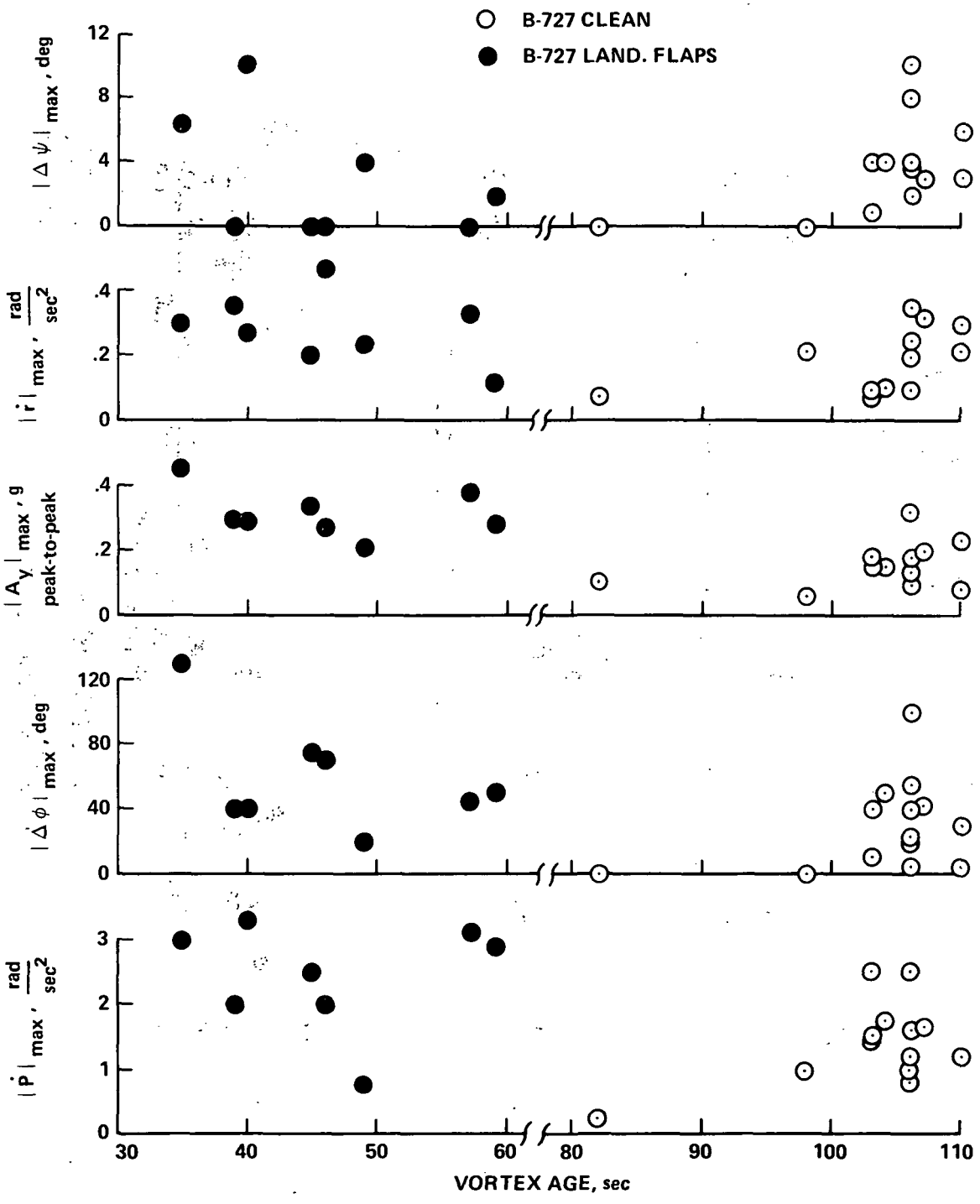

(a) Lateral-directional

Figure 24.- Effect of generator flap configuration on maximum Lear Jet excursions versus vortex age.

C.2

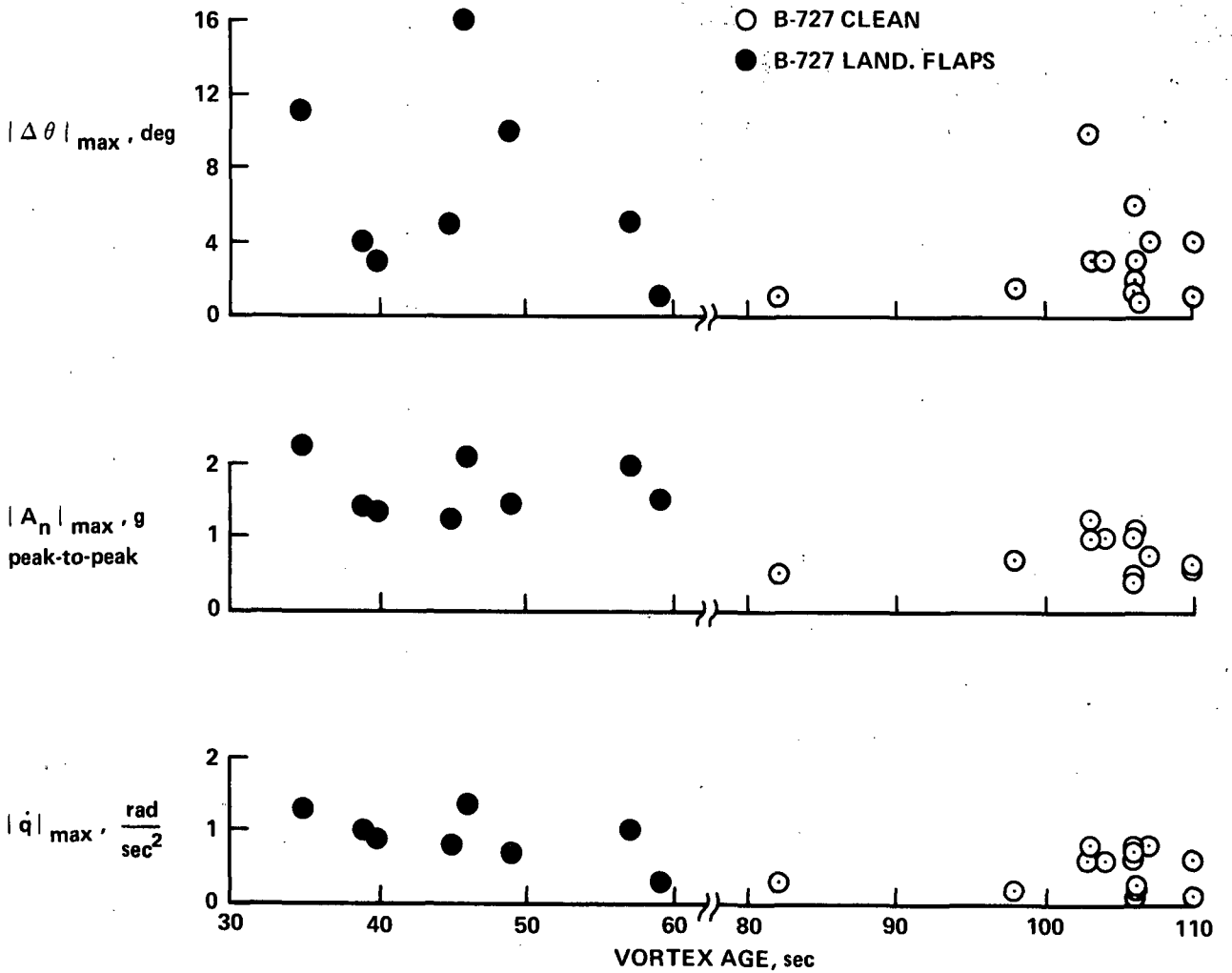

(b) Longitudinal

Figure 24.- Concluded.

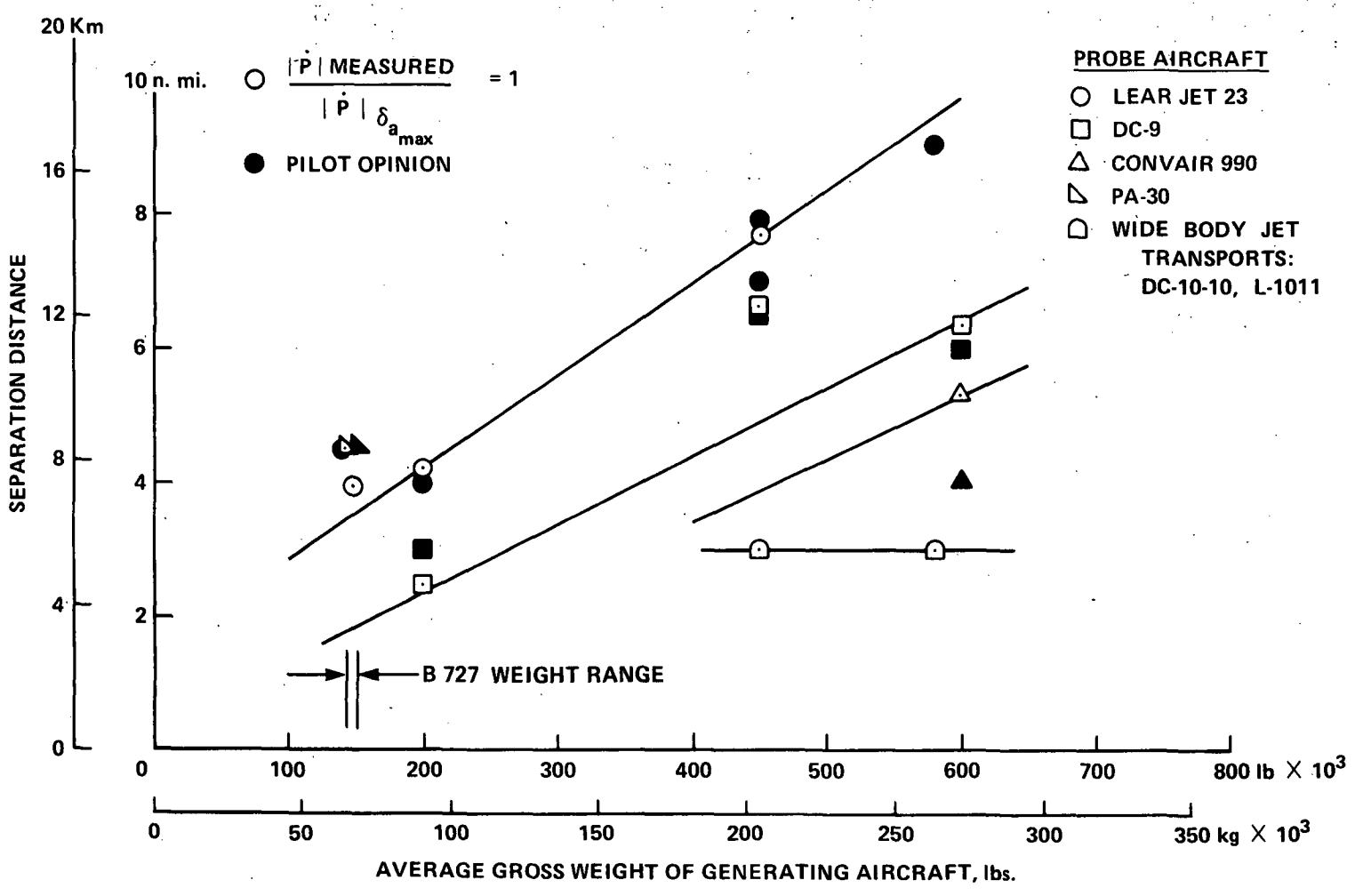

Figure 25.- Comparison of the minimum separation distances based on roll control criteria, for an operational encounter of the wake vortex of the Boeing 727 and other larger aircraft.

APPENDIX A

Lear Jet High Angle of Attack Response to Vortices

As noted during the discussion of Figure 6, the LR-23 is protected from stall by a stick shaker and pusher system. The system utilizes angle of attack vanes mounted on opposite sides of the forward fuselage to sense incipient aerodynamic stall, and acts through the autopilot to supply a low frequency buffet signal to the pilot through the control stick, followed by a command through the elevator control for an aircraft nose down attitude change.

The pilots noted stick shaker actuation during a number of encounters. Subsequent inspection of the airplane response data also revealed indications of stick pusher actuation which were consistent with high angle of attack measurements from the nose boom angle of attack sensor. To illustrate the significance of these high-angle-of-attack indications, Figure A-1, reproduced from Reference 4, shows pertinent stall characteristics of the LR-23. Angle of attack for maximum lift is near 13° to 15°, depending on flap deflection. At stall, rolling moments equal full aileron power, and side forces equivalent to about one-half rudder power, may be produced. Severe tail buffet, followed by elevator hinge moment reversal, is a further characteristic of the aircraft at maximum angle of attack.

Maximum angle of attack, as measured by sensors on the nose boom, for each encounter during the landing approach tests is summarized in Figure A-2. The data are plotted versus separation distance for convenience. Stick pusher actuation was noted on the response data for all points plotted at or above 12° angle of attack, indicating the fuselage angle of attack vanes were sensing flow angles consistent with the nose boom angle of attack measurement. Trim angle of attack for the landing approach flight condition was about 6° to 8°, and detailed examination of the response data strongly suggests the rapid buildup to high indicated angles of attack was due to vortex velocity gradients as the airplane entered the B727 wake.

Based on the wind tunnel data of Figure A-1, the high indicated angles of attack were sufficient to produce a momentary stall condition, which suggests a possible ambiguity regarding the airplane excursions following the wake encounter. The excursions could be generated by two inseparable effects; namely, asymmetric changes in the aerodynamic load distribution, or the normal reduction in flying qualities near stall.

Additional significance of the angle-of-attack effect on the encounter dynamics is shown on the next two figures, in terms of control power required to counter the angular accelerations generated by the wake. Figure A-3 presents the LR-23 lateral control derivative $C_{l_{\delta_a}}$ versus angle of attack. Also shown for comparison are the landing approach flight data,

converted point-by-point to an equivalent $C_{l_{\delta_a}}$ required to balance the measured maximum roll acceleration with full aileron. The data are plotted at maximum angle of attack for each encounter. In general, this figure presents a picture of increasing severity of encounter linked with decreasing control power, as angle of attack increases toward the stall.

A similar comparison of elevator control power versus the measured pitch excursions is presented in Figure A-4. Here also the trend is toward larger pitching accelerations, approaching maximum control authority, at the higher angles of attack.

In summary, it may be postulated from the foregoing material that velocity gradients in the B727 wake at spacings used for current operations are of sufficient magnitude to produce a momentary stall environment for the LR-23. In addition, the excursions that result may derive from a combination of factors more complex than simple asymmetric span loading changes on the wing.

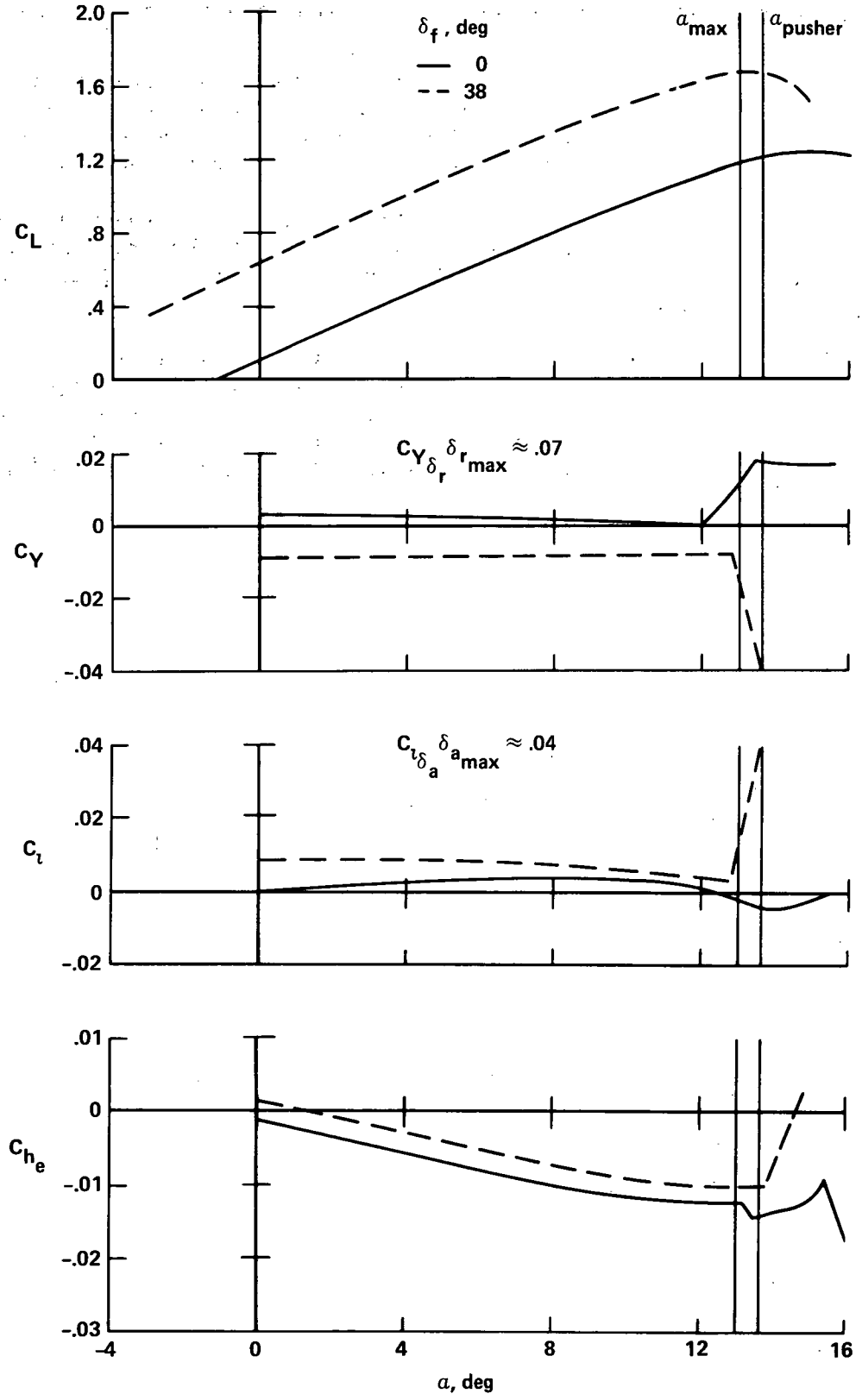

Figure A-1.- Lear Jet aerodynamics.

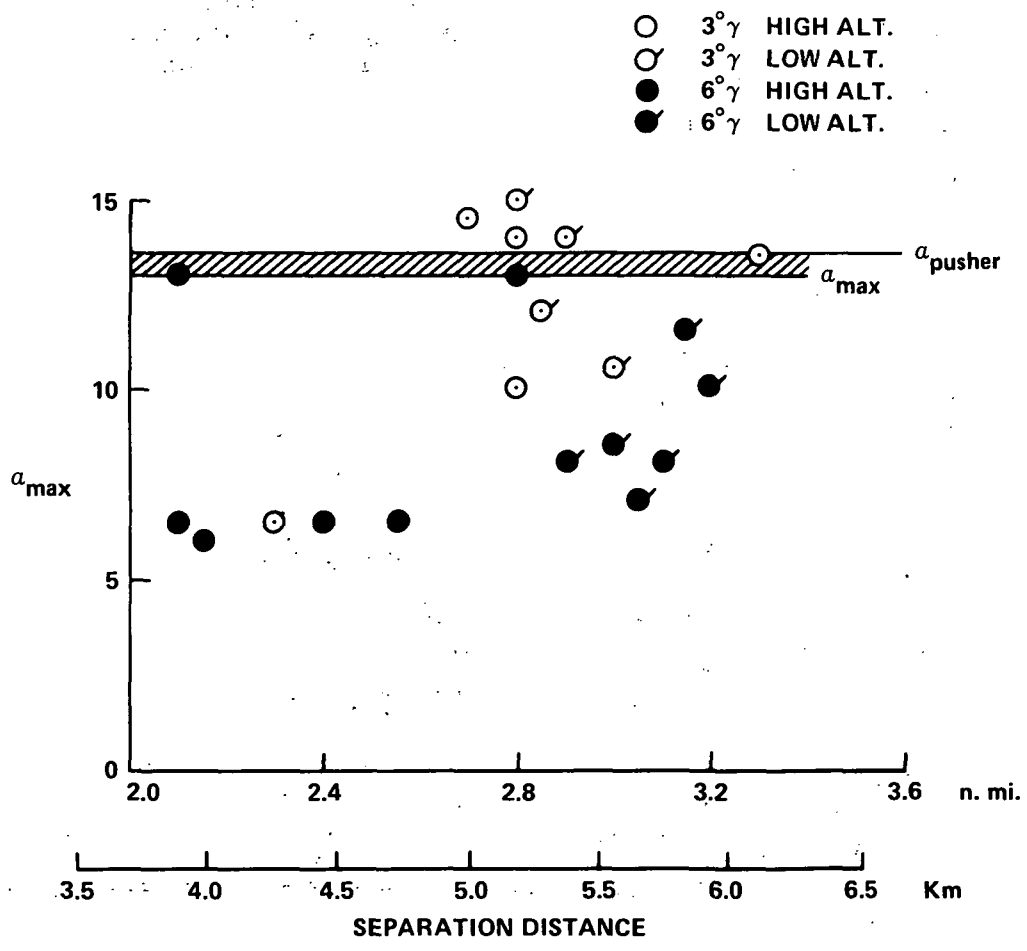

Figure A-2.- Maximum angle of attack measured on the Lear Jet at vortex encounter during landing approaches.

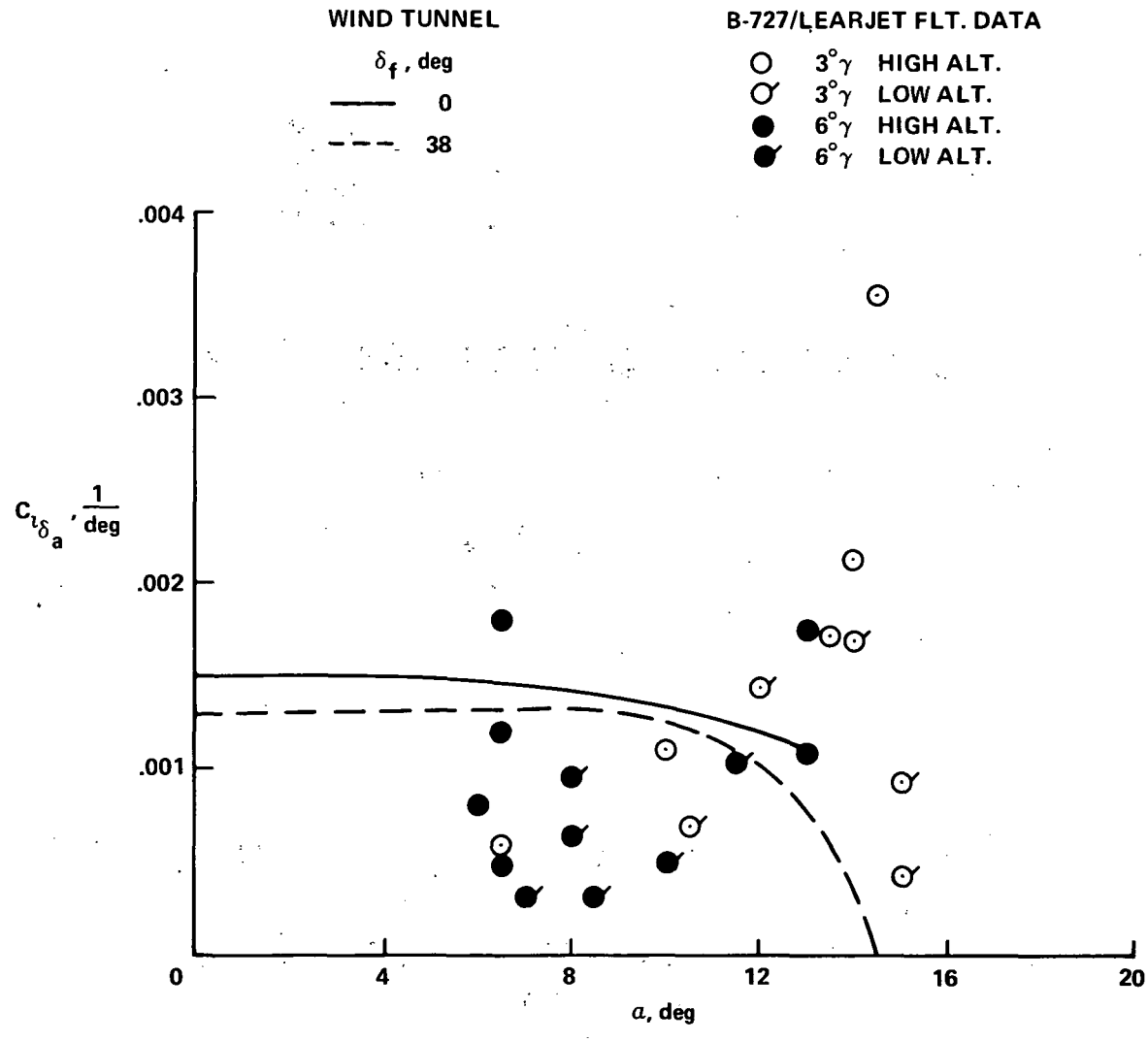

Figure A-3.- Angle of attack effect on Lear Jet lateral control power versus equivalent lateral control power required to counter vortex induced angular accelerations in roll.

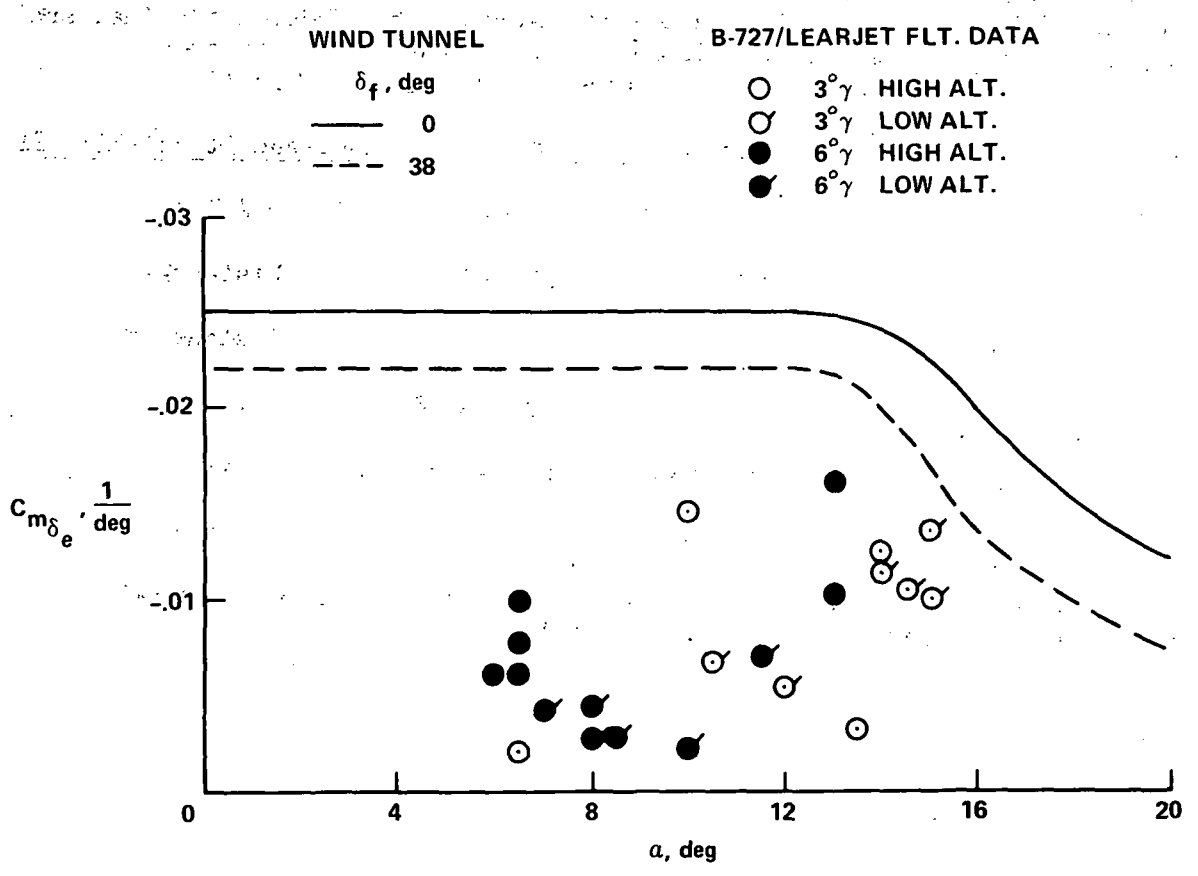

Figure A-4.- Angle of attack effect on Lear Jet longitudinal control power versus equivalent longitudinal control power required to counter vortex induced angular accelerations in pitch.

APPENDIX B

Vortex Location Mapping Data

As stated earlier, the relative difference of the probability of wake vortex encounter for the two types of approach profiles cannot be answered just from this flight test. Additional information would be required to do this. All of the vortex location data from this flight test are included in order to aid such a probability analysis. The vortex mapping system was described earlier and the tracking stations are shown in Figure 5. The vortex location data for the 14 mapping runs are presented. The data were obtained for five conventional approaches, five two-segment approaches to runway 22, and four take-off and climb-out cases using runway 04. The horizontal and vertical location of a cross section element of one of the vortex pairs is plotted for each of the four stations as a function both of (1) time after station passage, and (2) distance of the vortex element behind the B727 aircraft. The data were measured as a function of time, and calculated ground speed of the B727 was used to convert from time to distance in nautical miles. The figures are arranged as follows:

Figure	Flight Condition	Independent Parameter
B-1(a) - B-1(e)	Conventional Approaches	Distance
B-1(f) - B-1(j)	Two-Segment Approaches	Distance
B-1(k) - B-1(n)	Take-offs	Distance
B-2(a) - B-2(e)	Conventional Approaches	Time
B-2(f) - B-2(j)	Two-Segment Approaches	Time
B-2(k) - B-2(n)	Take-offs	Time

In these figures indicated airspeeds are tabulated and the wind directions are referenced to magnetic north.

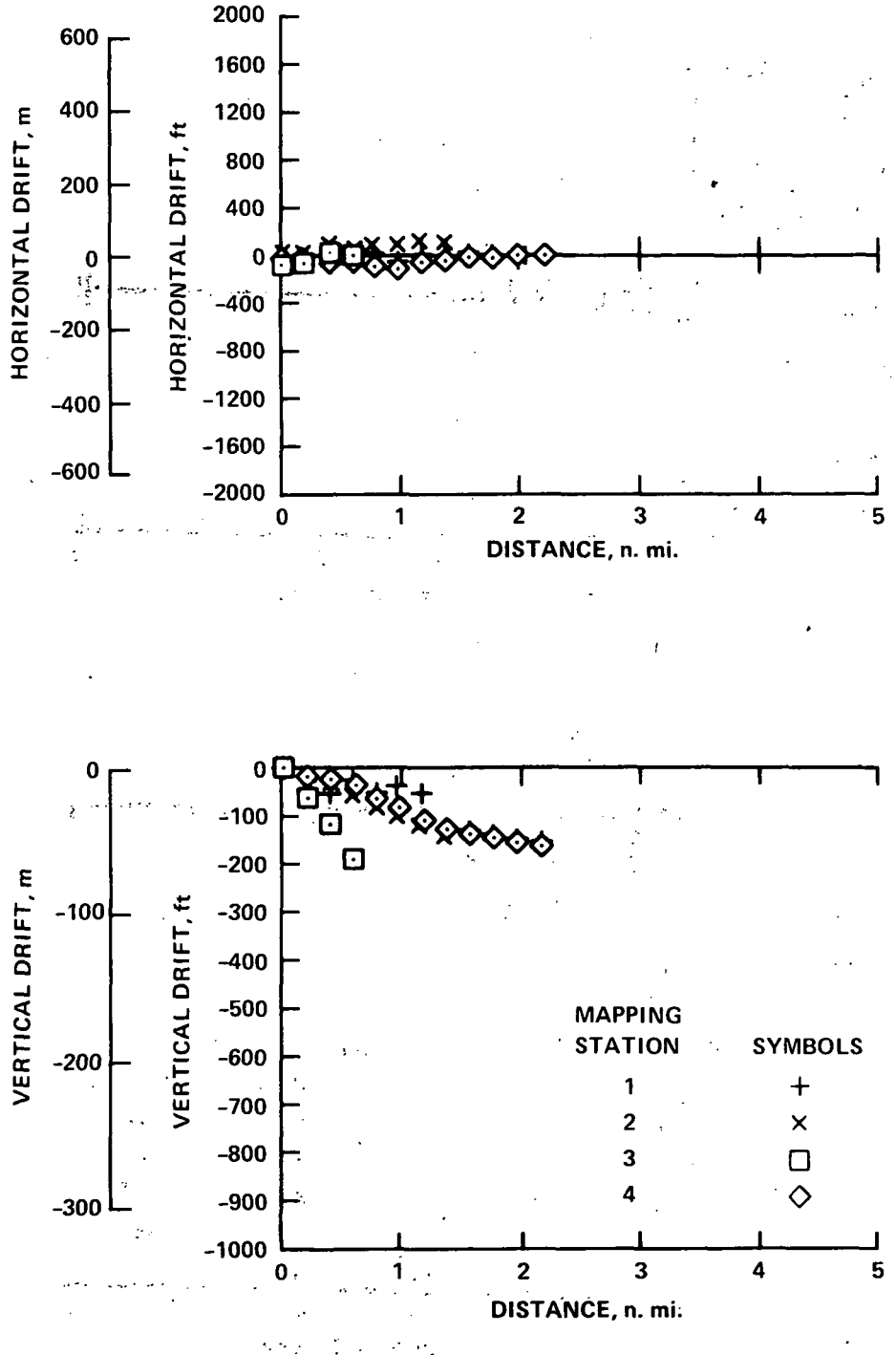

(a) Conventional approach; flaps = 30°; airspeed = 135 kts.; weight = 64,000 kg. (141,500 lbs.); winds = calm; turbulence = smooth

Figure B-1.- Vortex location behind a B727 aircraft.

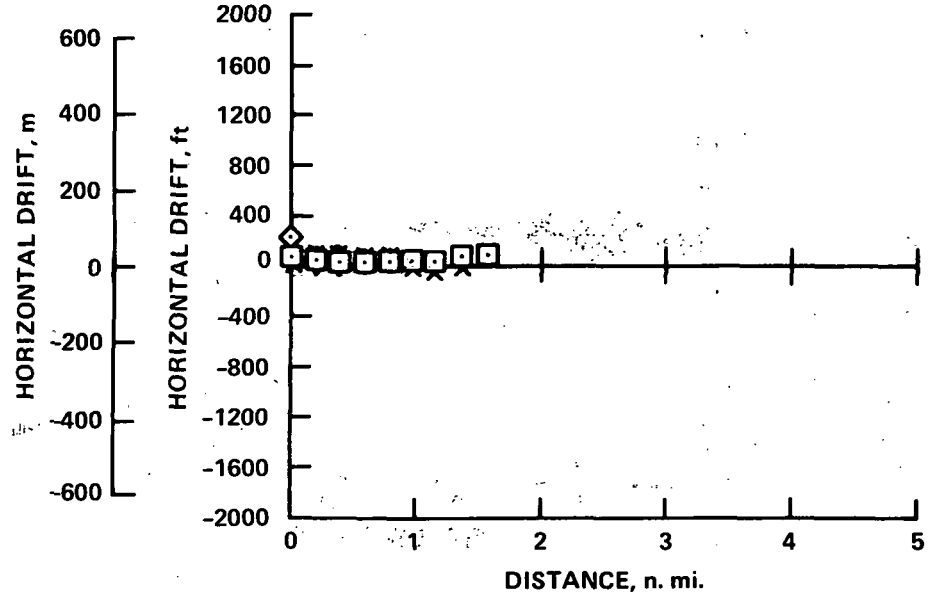

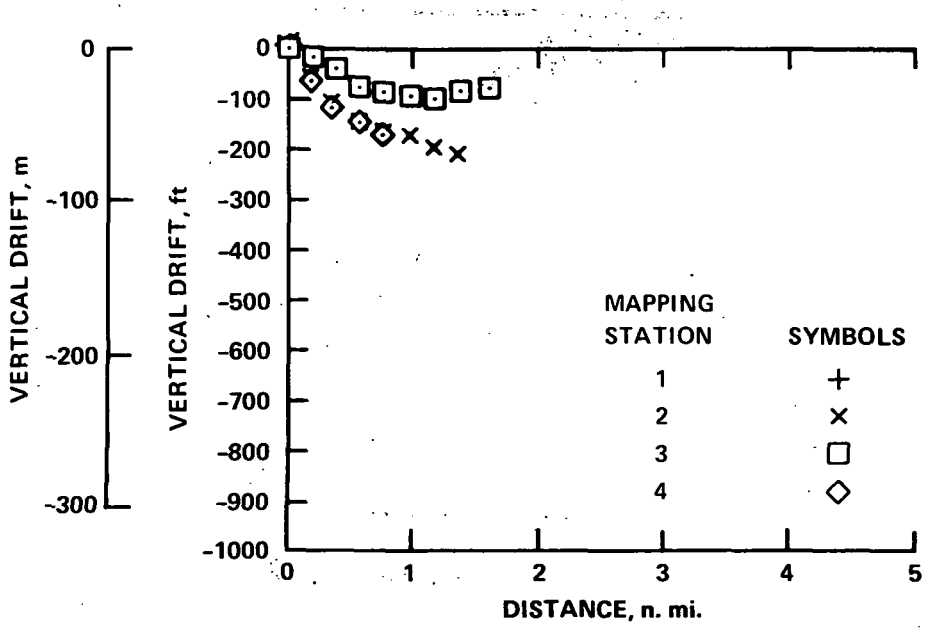

(b) Conventional approach; flaps = 30°; airspeed = 132 kts.; weight = 66,000 kg. (146,000 lbs.); winds = 240° at 12 kts.; turbulence = light-moderate

Figure B-1.- Continued.

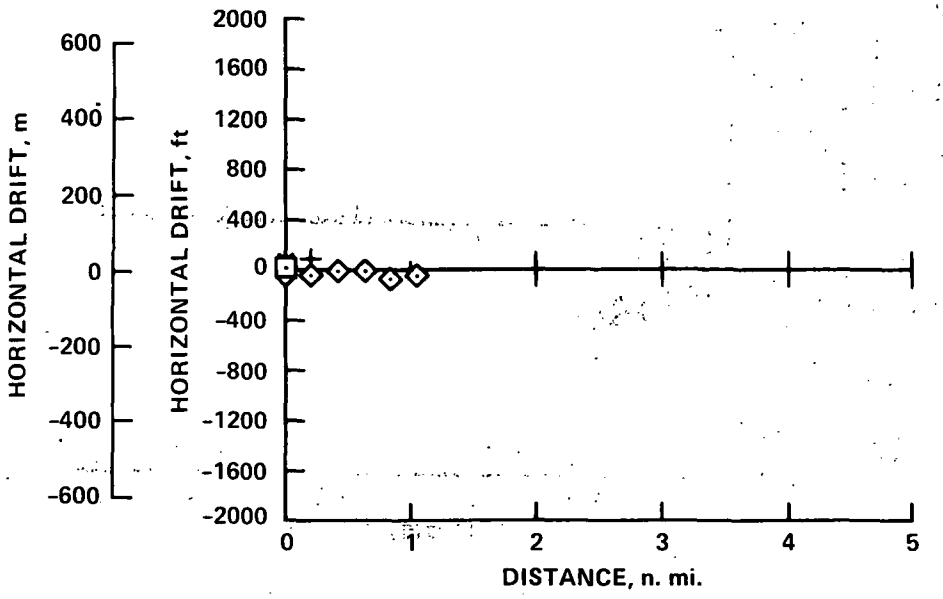

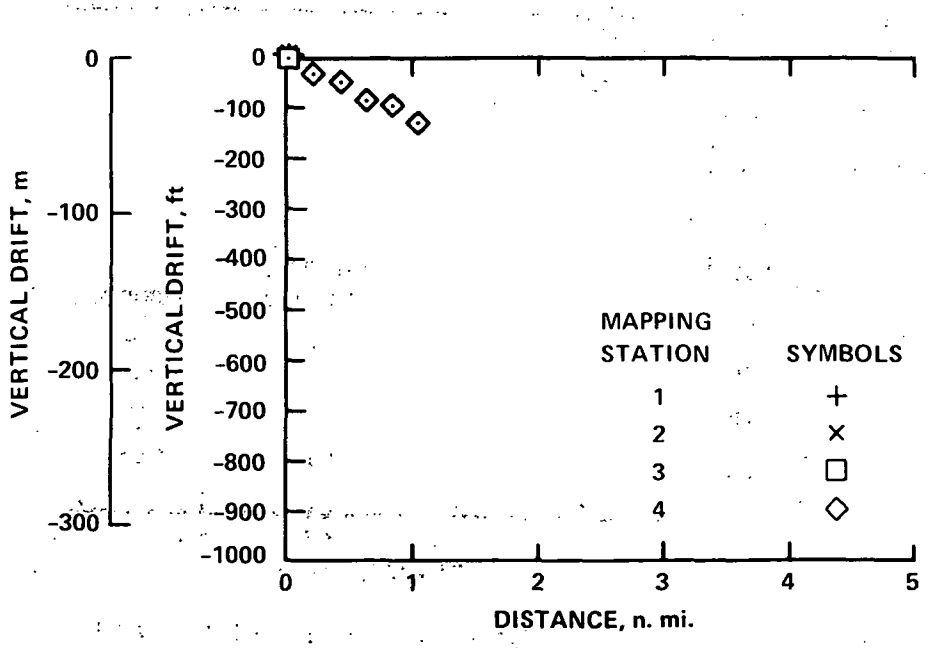

(c) Conventional approach; flaps = 30°; airspeed = 145 kts.; weight = 68,000 kg. (150,000 lbs.); winds = 230° at 5 kts.; turbulence = light

Figure B-1.- Continued.

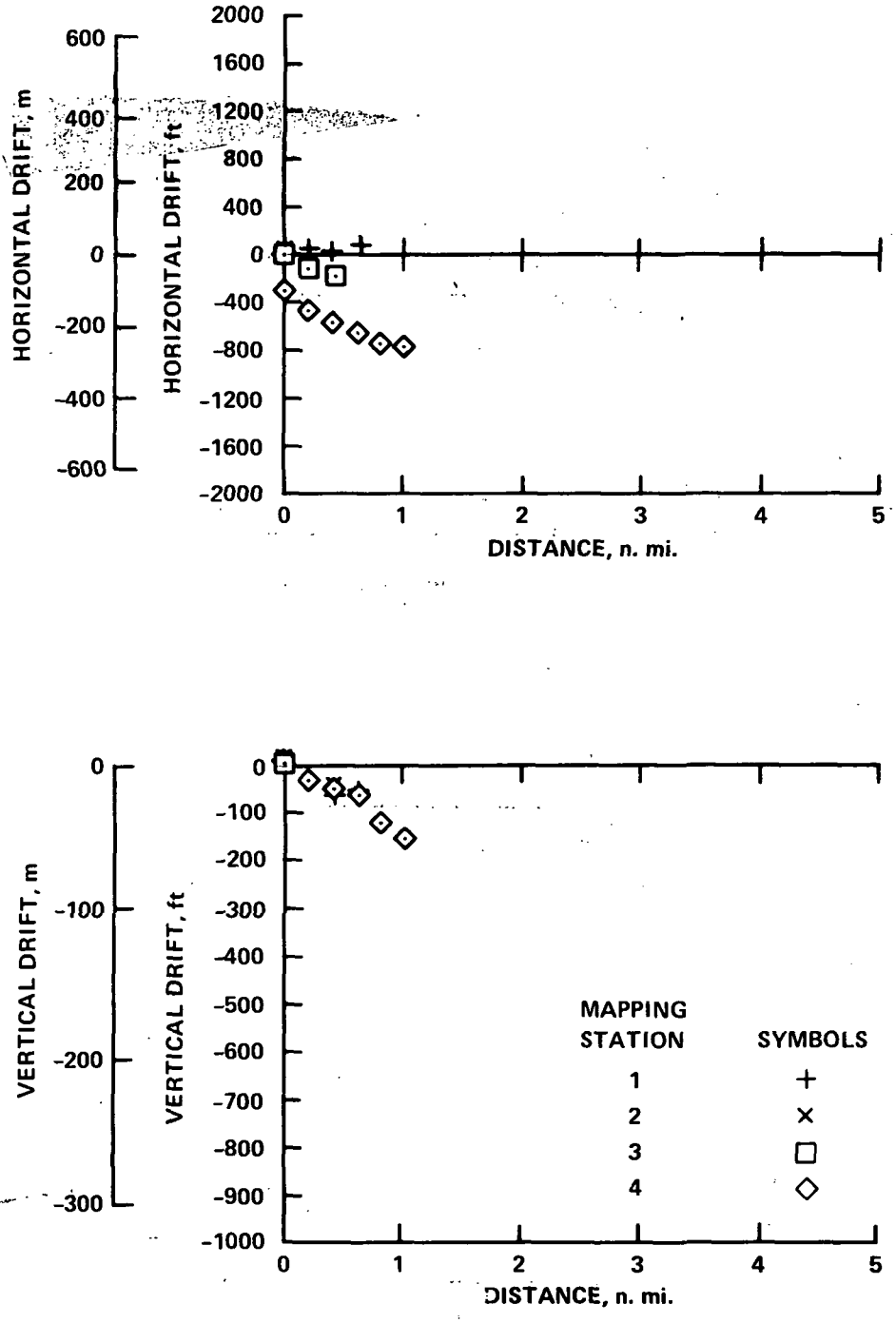

(d) Conventional approach; flaps = 30°; airspeed = 140 kts.; weight = 64,500 kg. (141,500 lbs.); winds = 240° at 10 kts.; turbulence = light-moderate

Figure B-1.- Continued.

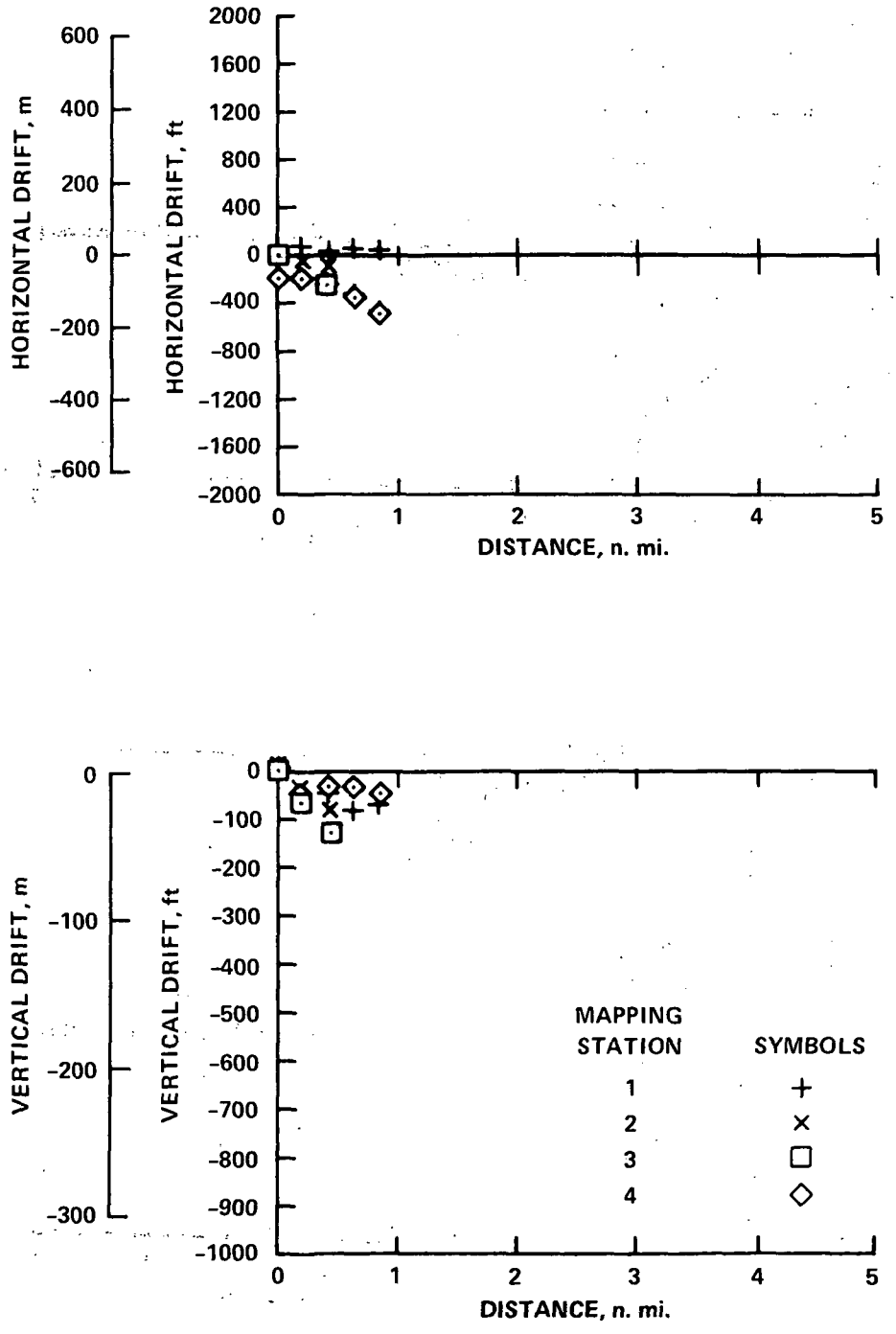

(e) Conventional approach; flaps = 30°; airspeed = 145 kts.; weight = 67,000 kg. (148,000 lbs.); winds = 230° at 8 kts.; turbulence = light-moderate

Figure B-1.- Continued.

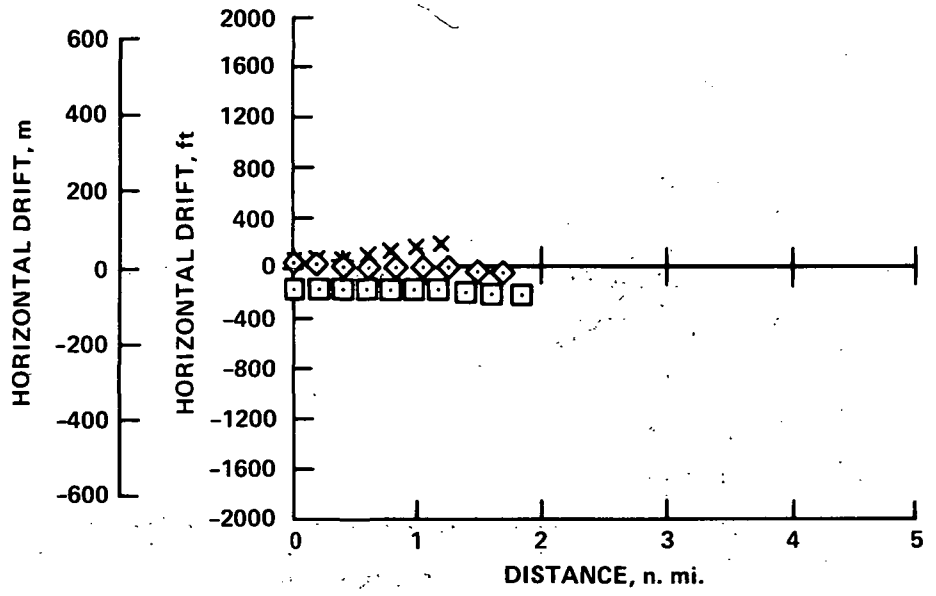

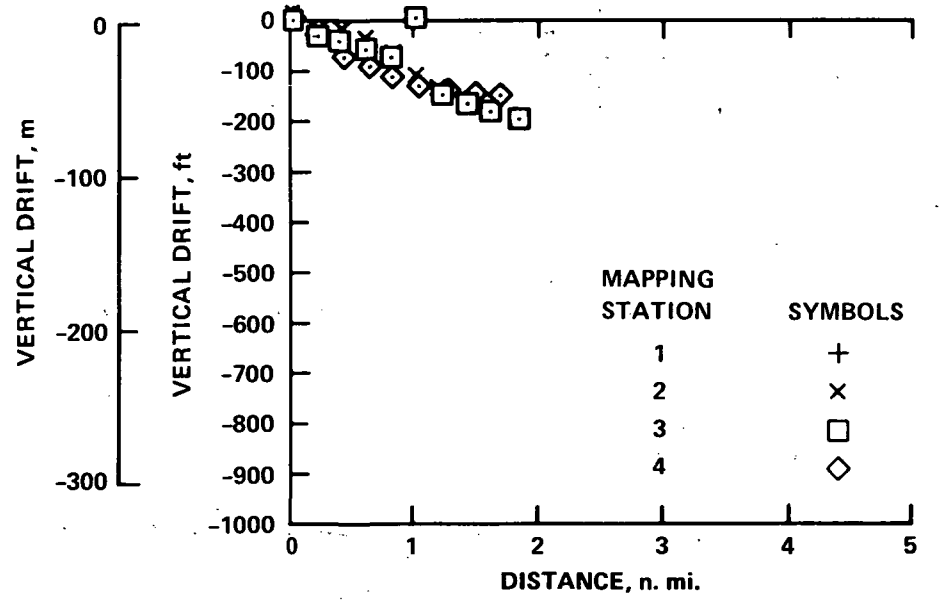

(f) Two-segment approach; flaps = 30°; airspeed = 138 kts.; weight = 69,000 kg. (151,500 lbs.); winds = calm; turbulence = smooth

Figure B-1.- Continued.

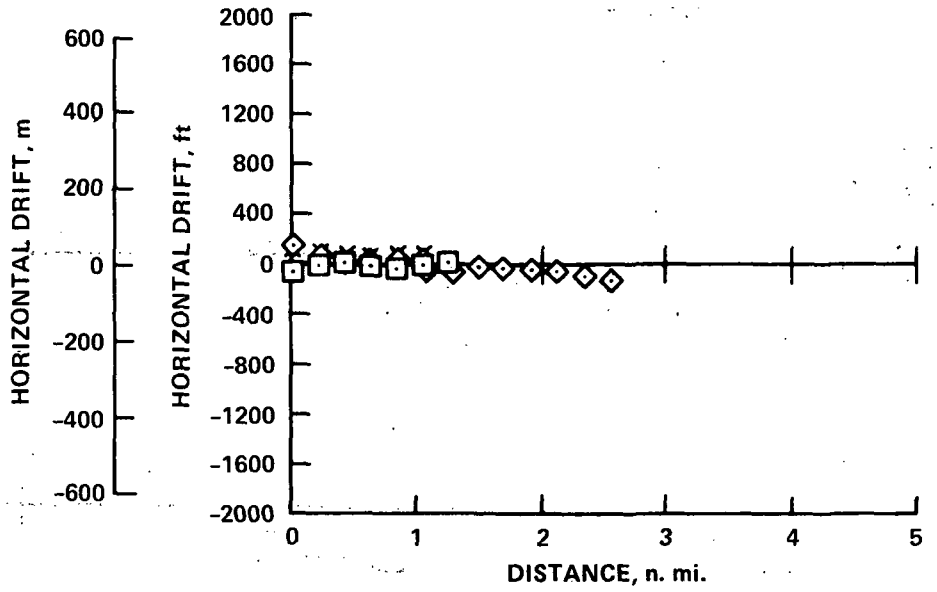

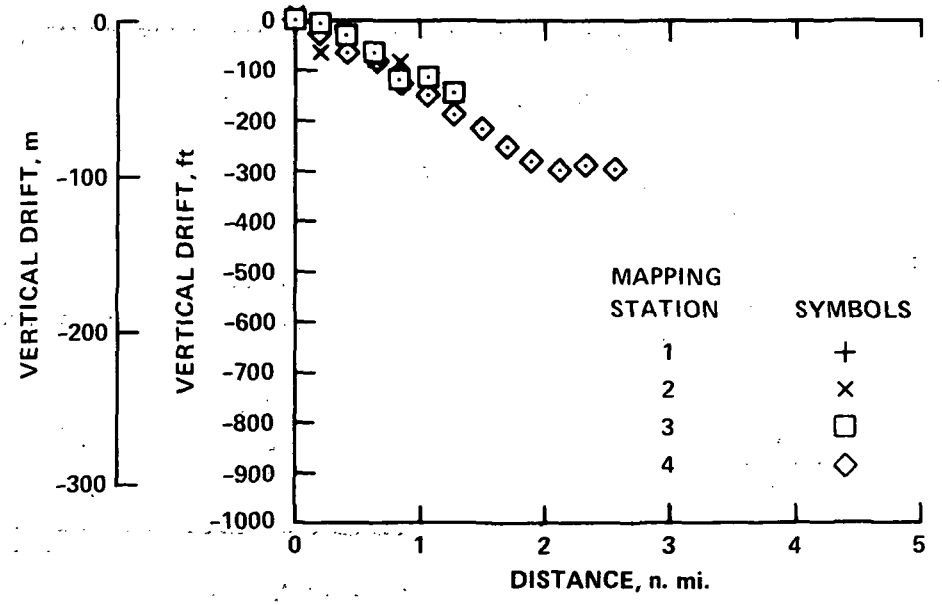

(g) Two-segment approach; flaps = 30°; airspeed = 144 kts.; weight = 67,000 kg. (148,000 lbs.); winds = 240° at 12 kts.; turbulence = light-moderate

Figure B-1.- Continued.

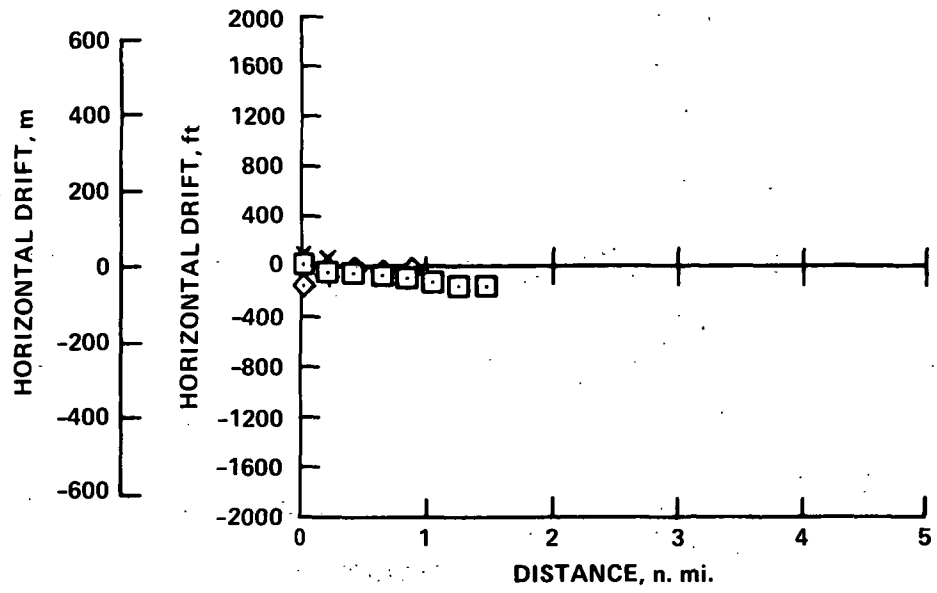

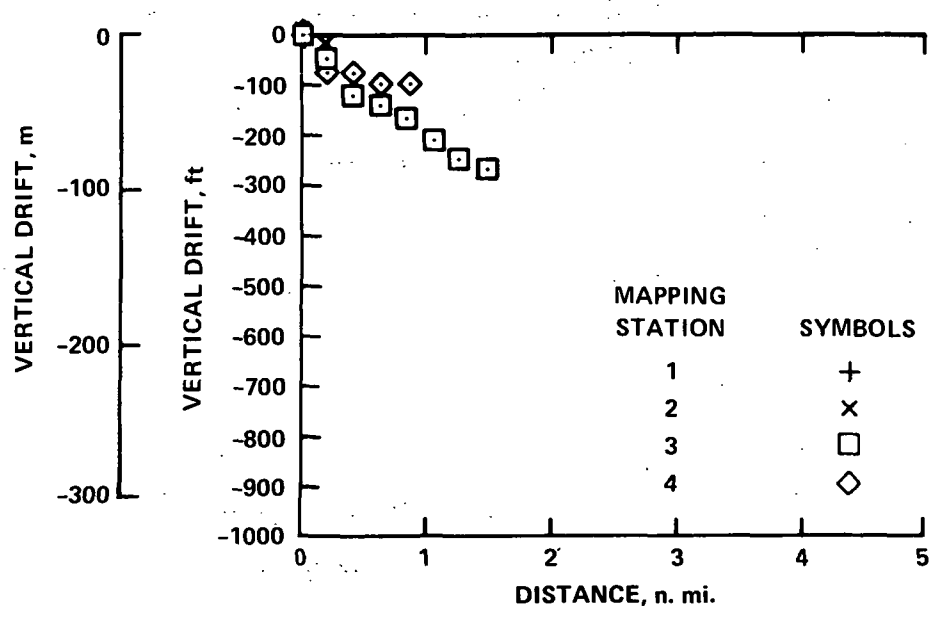

(h) Two-segment approach; flaps = 30°; airspeed = 144 kts.; weight = 68,000 kg. (150,000 lbs.); winds = 230° at 5 kts.; turbulence = light

Figure B-1.- Continued.

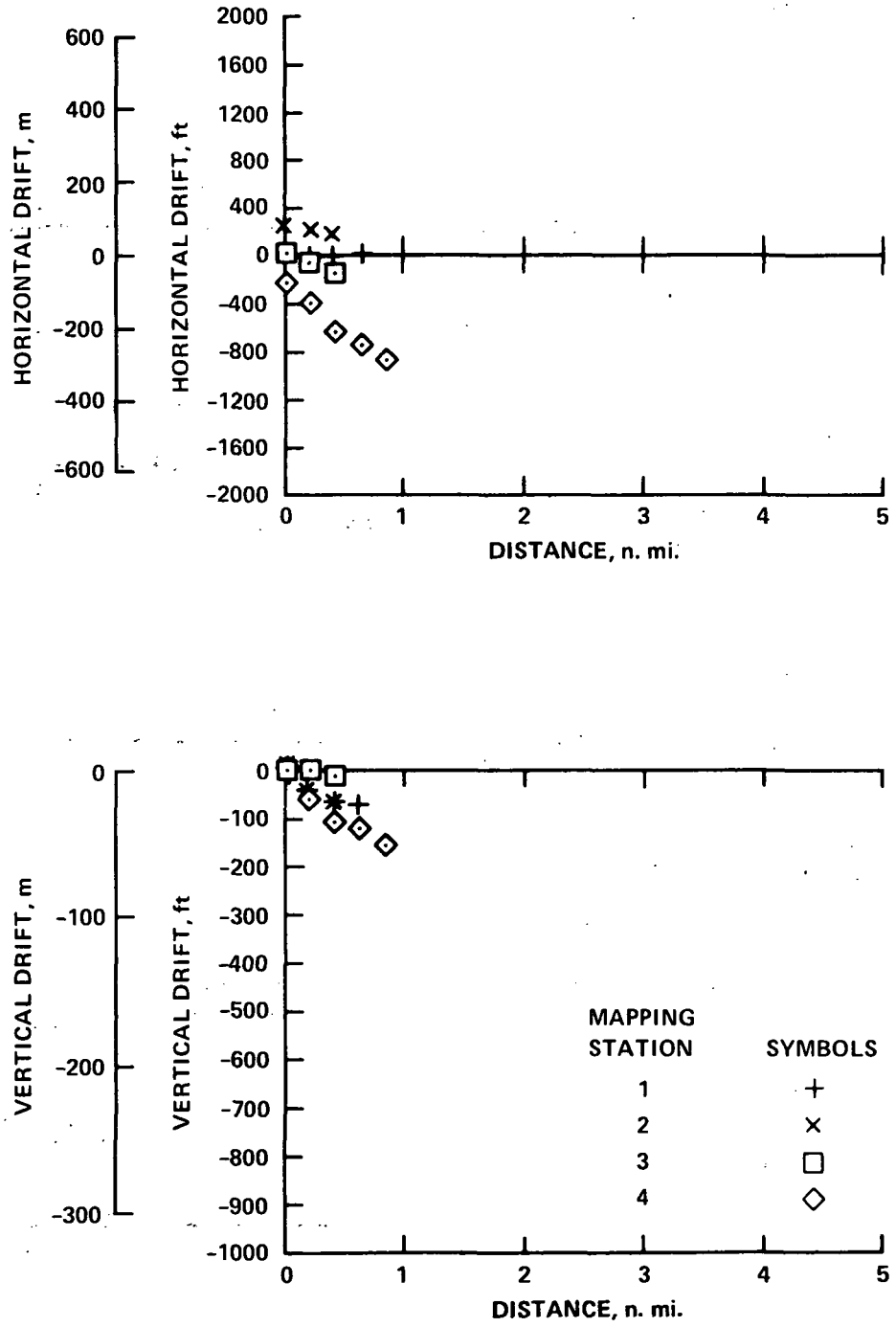

(i) Two-segment approach; flaps = 30°; airspeed = 145 kts.; weight = 65,500 kg. (144,000 lbs.); winds = 235° at 9 kts.; turbulence = light-moderate

Figure B-1.- Continued.

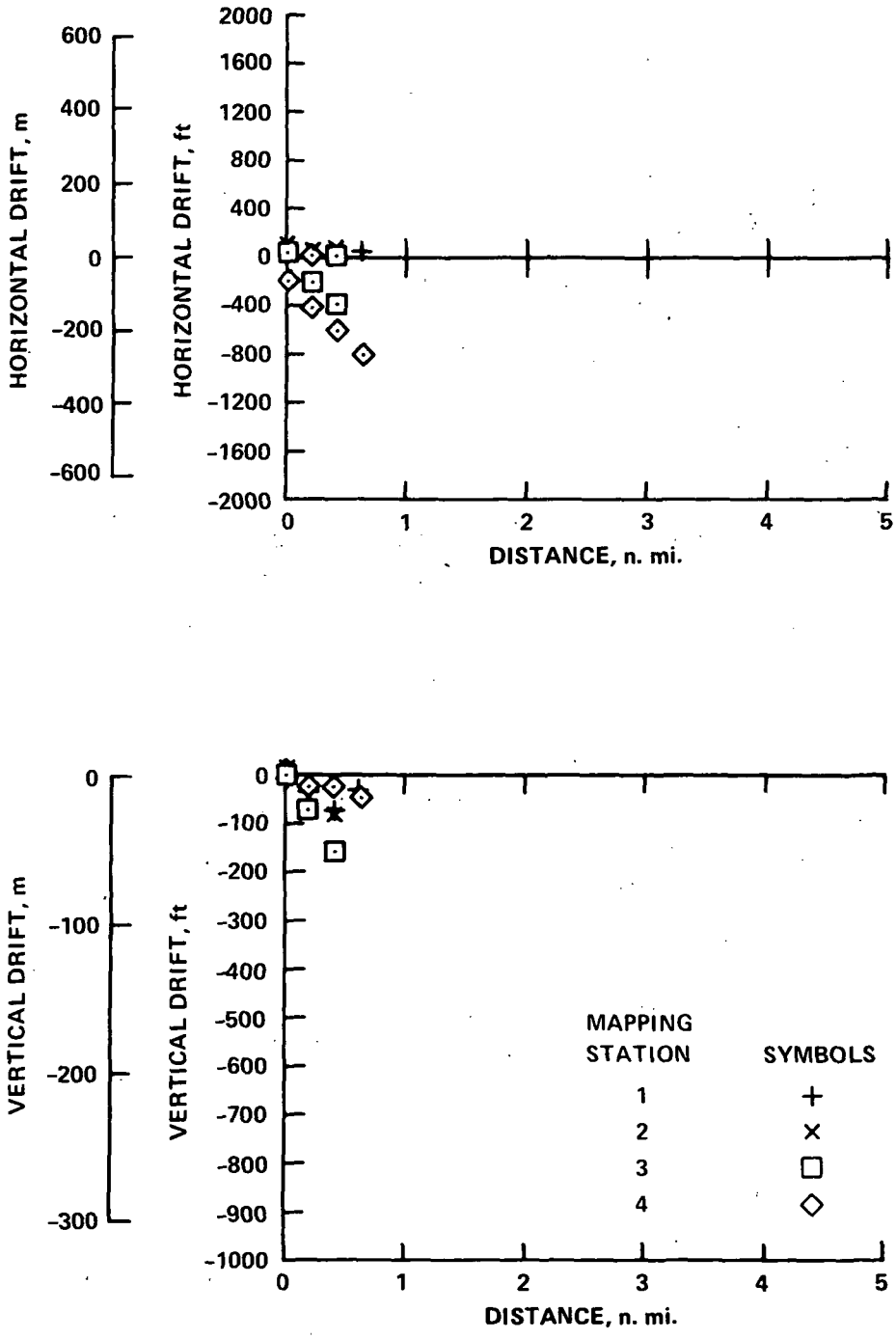

(j) Two-segment approach; flaps = 30°; airspeed = 145 kts.; weight = 69,000 kg. (151,500 lbs.); winds = 160° at 4 kts.; turbulence = light

Figure B-1.- Continued.

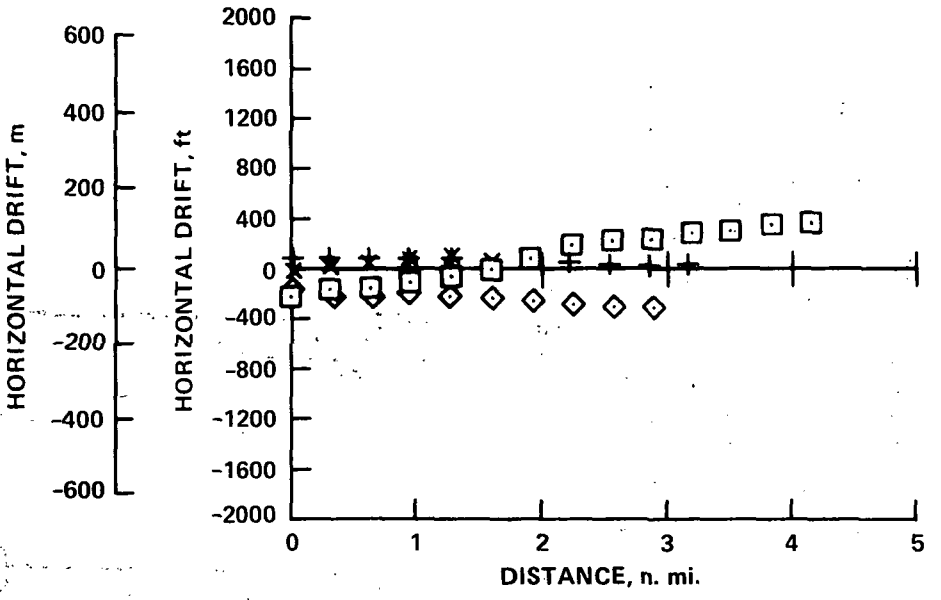

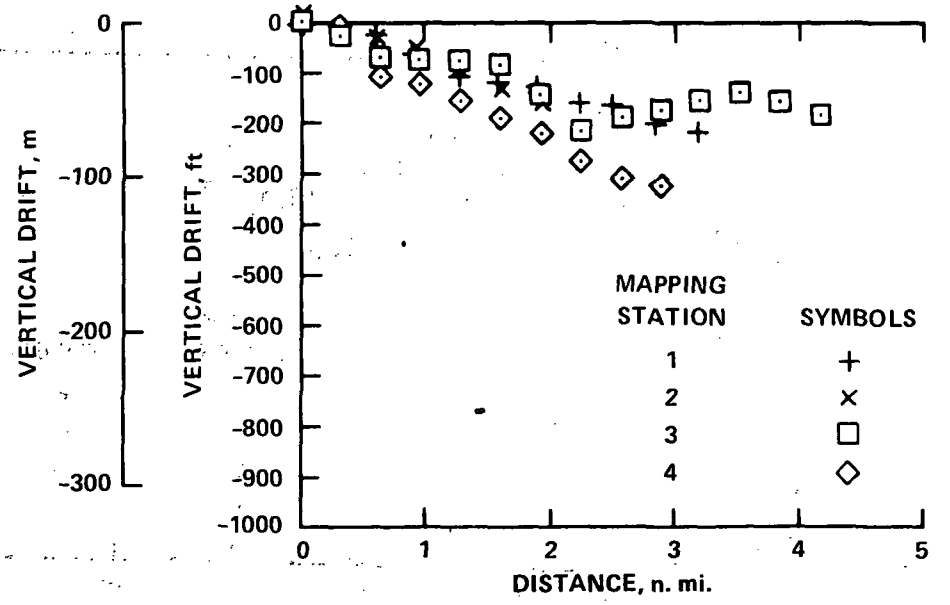

Figure B-1.- Concluded.

(k) Takeoff; flaps = 15°; airspeed = 220 kts.; weight = 69,000 kg. (153,000 lbs.); winds = calm; turbulence = smooth

Figure B-1.- Continued.

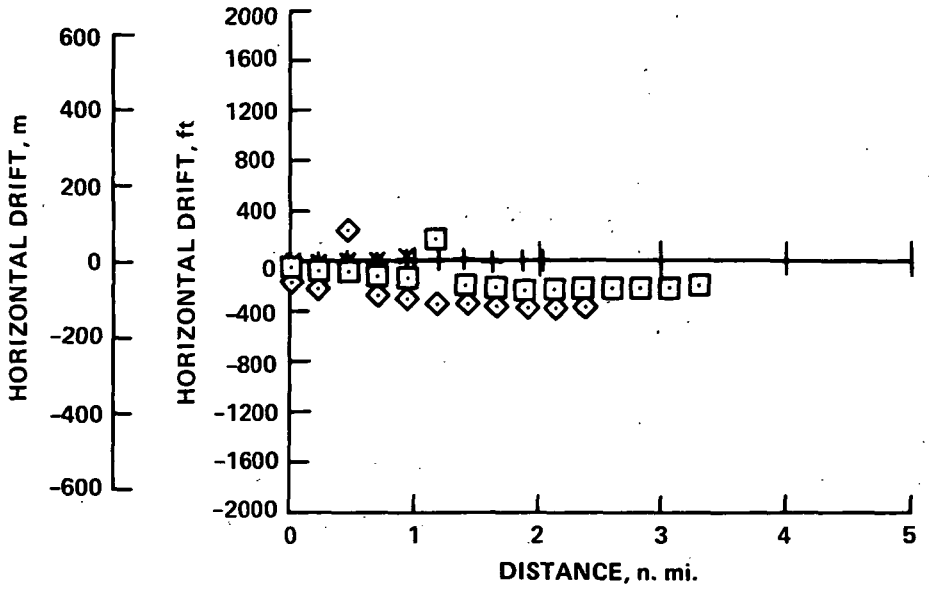

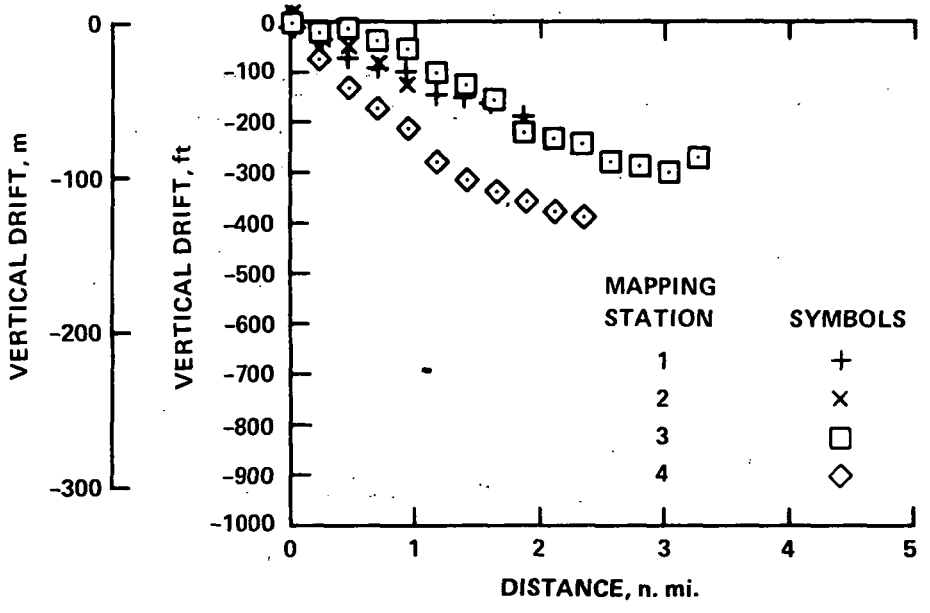

(1) Takeoff; flaps = 15°; airspeed = 160 kts.; weight = 70,000 kg. (159,000 lbs.); winds = 160° at 4 kts.; turbulence = light

Figure B-1.- Continued.

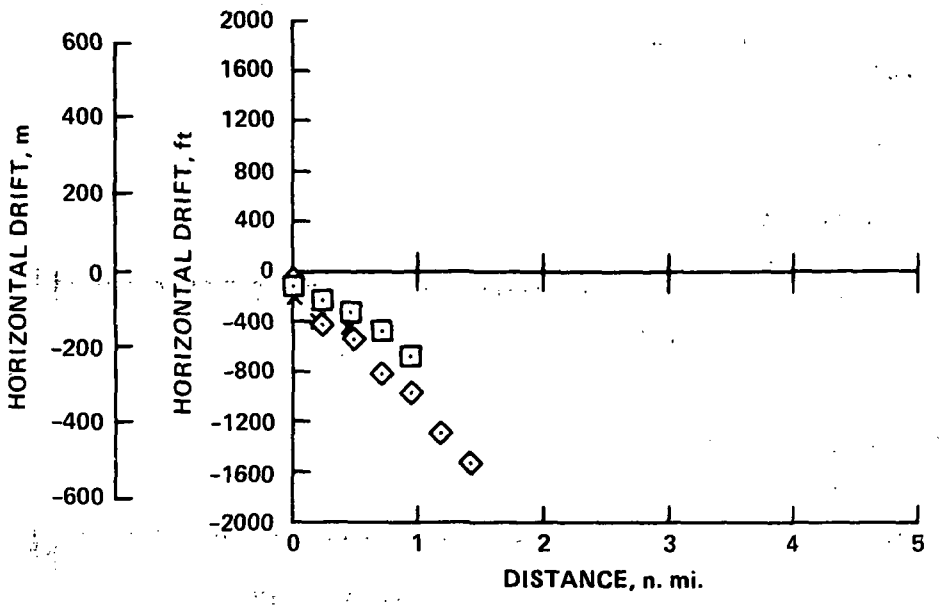

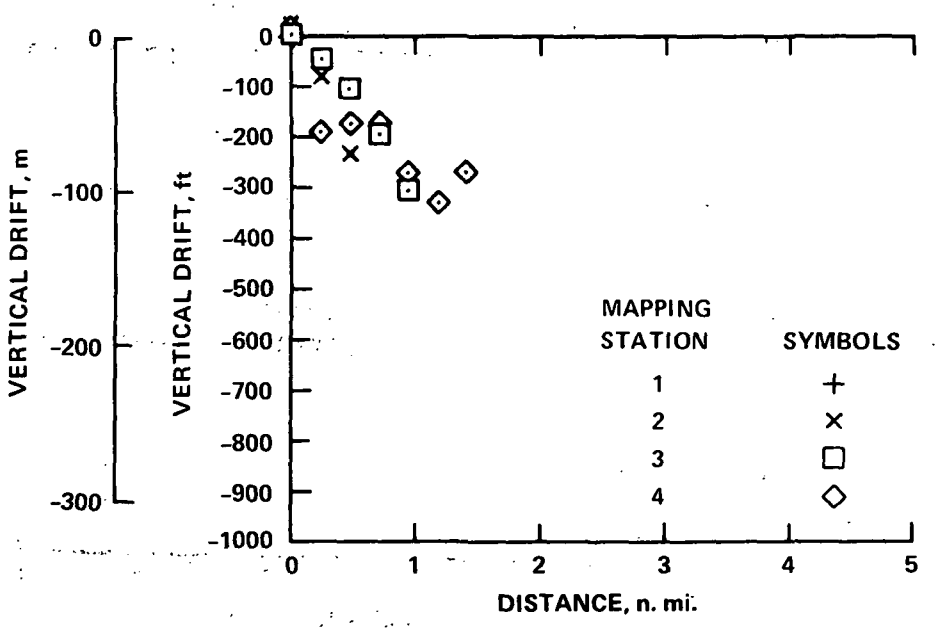

(m) Takeoff; flaps = 15°; airspeed = 160 kts.; weight = 66,000 kg. (145,500 lbs.); winds = 230° at 8 kts.; turbulence = light

Figure B-1.- Continued.

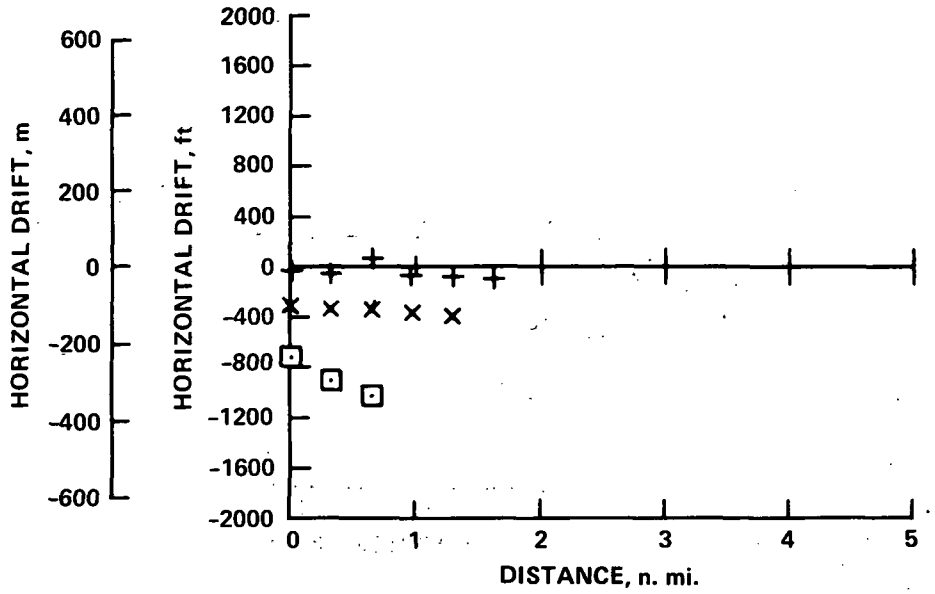

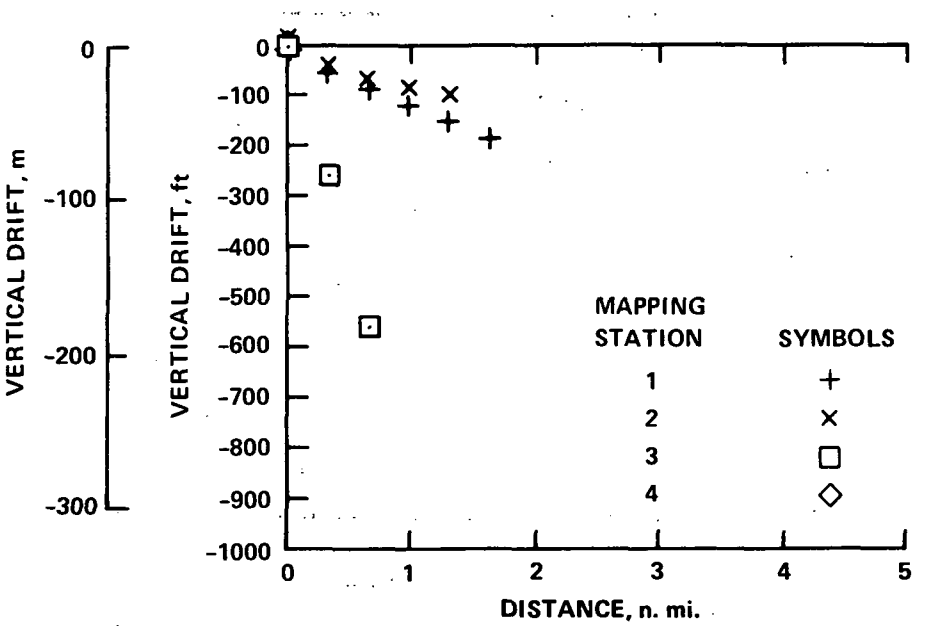

(n) Takeoff; flaps = 15°; airspeed = 200 kts.; weight = 69,000 kg. (155,000 lbs.); winds = 160° at 4 kts.; turbulence = light

Figure B-1.- Concluded.

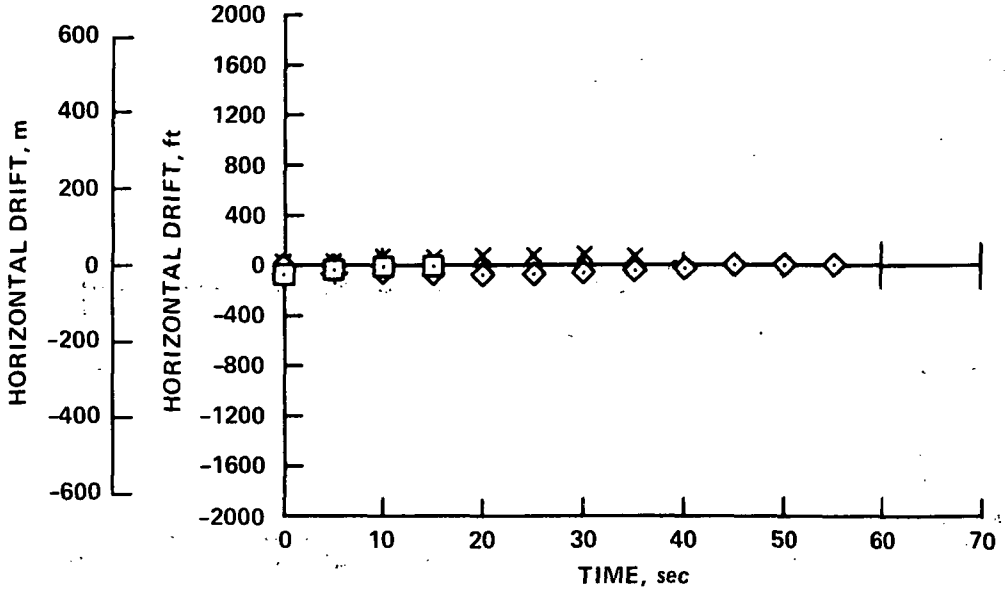

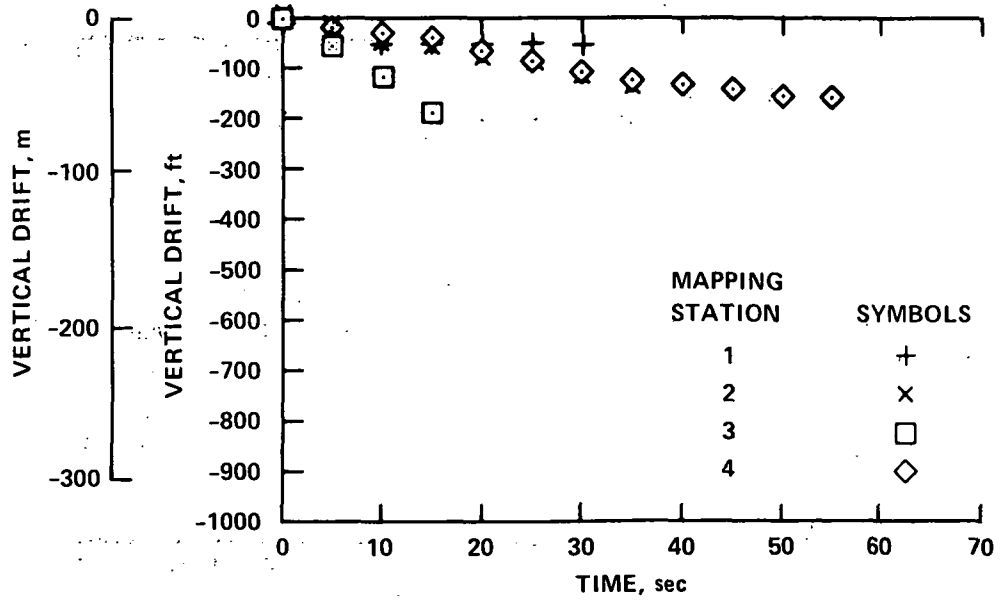

(a) Conventional approach; flaps = 30°; airspeed = 135 kts.; weight = 64,000 kg. (141,500 lbs.); winds = calm; turbulence = smooth

Figure B-2.- Vortex location after B727 passage.

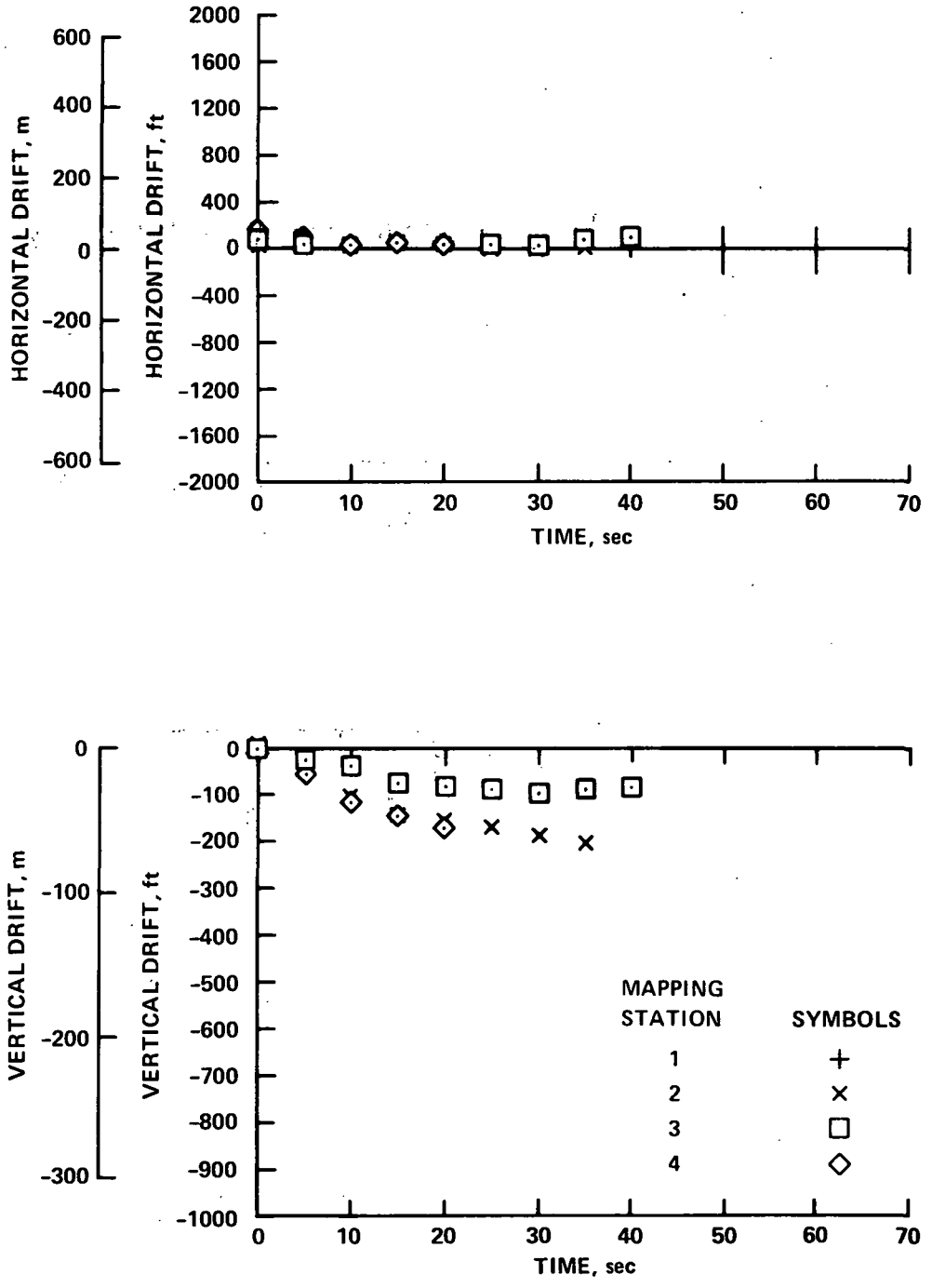

(b) Conventional approach; flaps = 30°; airspeed = 132 kts.; weight = 66,000 kg. (146,000 lbs.); winds = 240° at 12 kts.; turbulence = light-moderate

Figure B-2.- Continued.

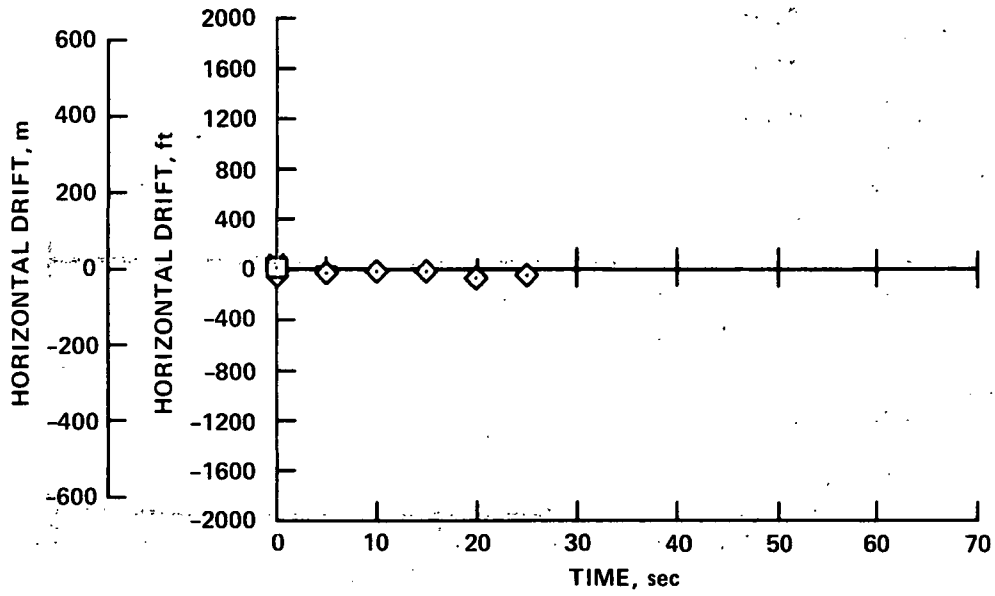

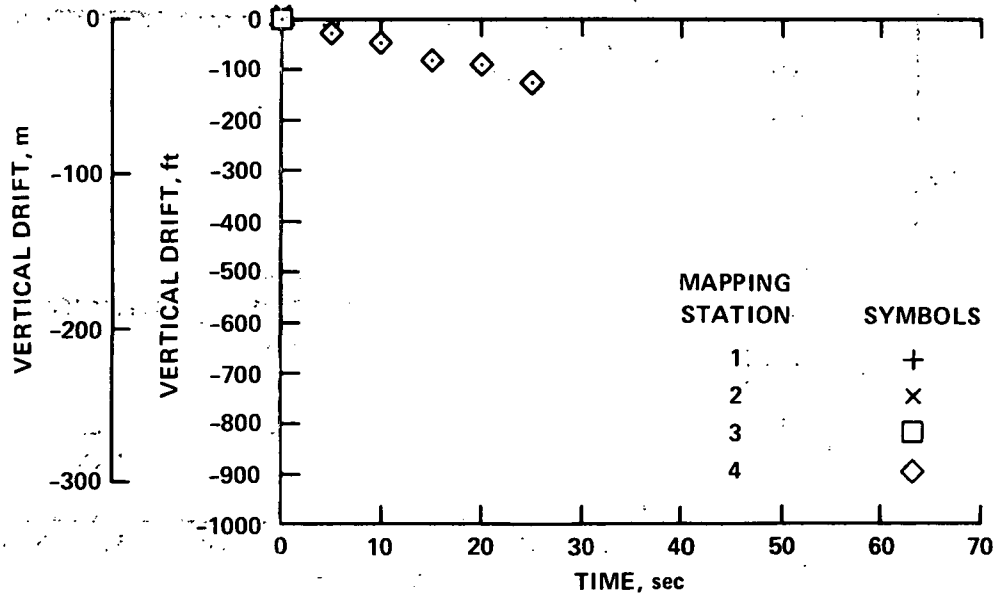

(c) Conventional approach; flaps = 30°; airspeed - 145 kts.; weight = 68,000 kg. (150,000 lbs.); winds = 230° at 5 kts.; turbulence = light

Figure B-2.- Continued.

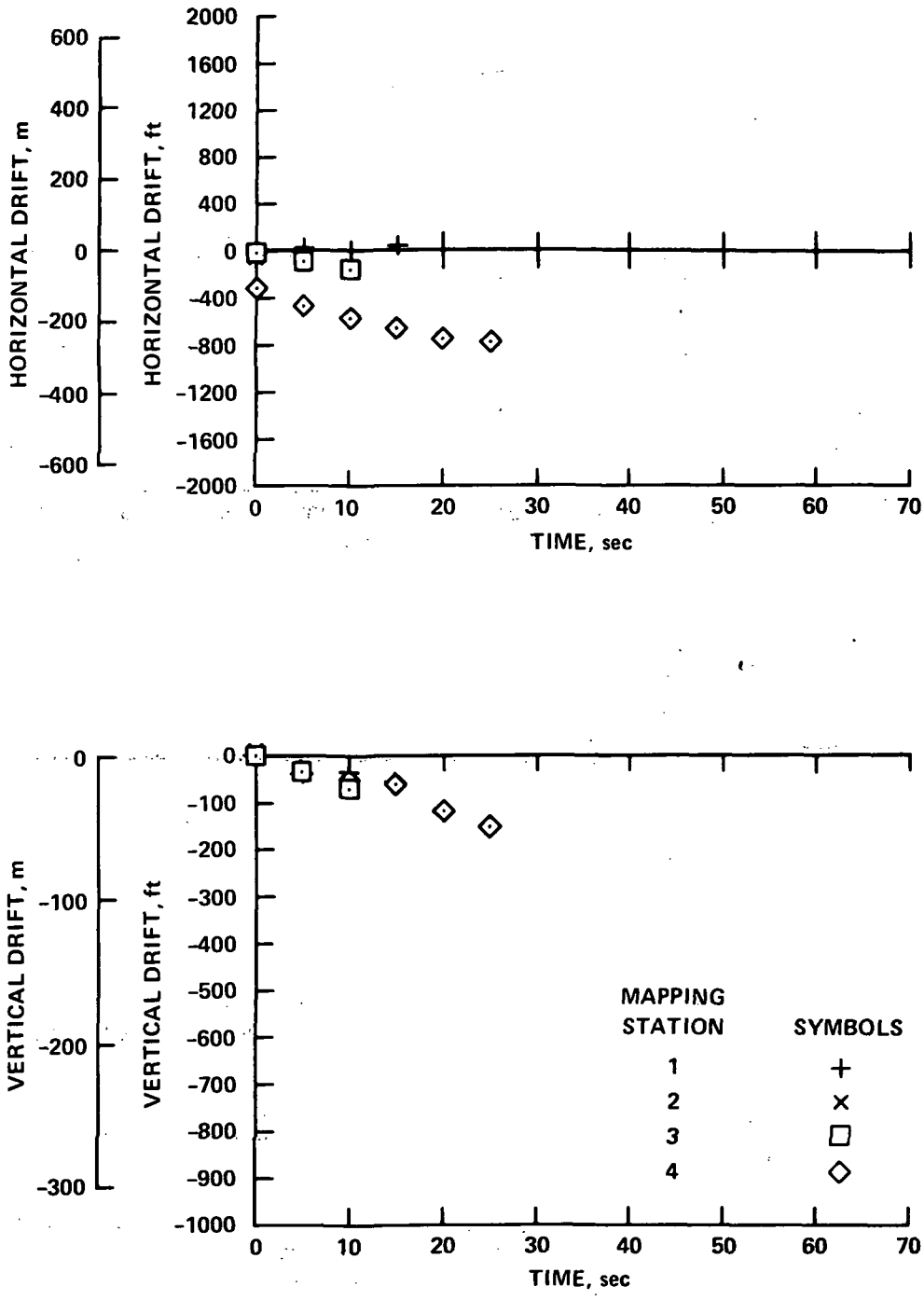

(d) Conventional approach; flaps = 30°; airspeed = 140 kts.; weight = 64,500 kg. (141,500 lbs.); winds = 240° at 10 kts.; turbulence = light-moderate

Figure B-2.- Continued

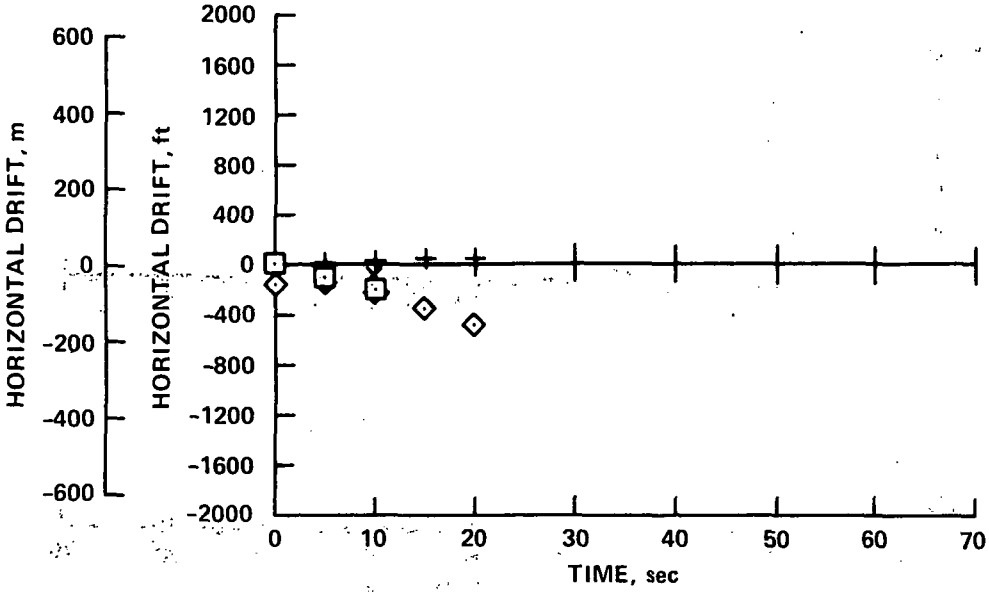

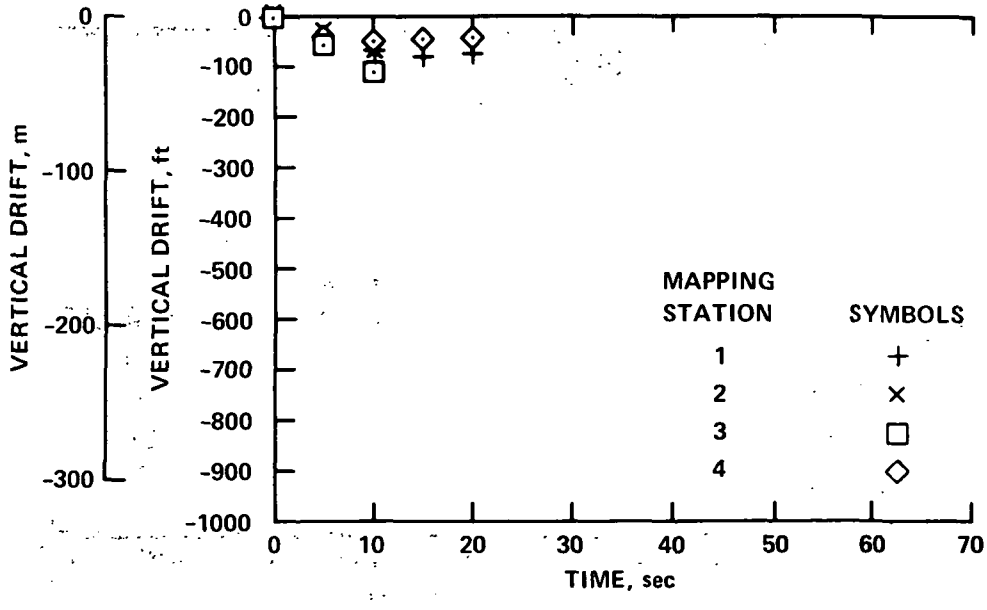

(e) Conventional approach; flaps = 30°; airspeed = 145 kts.; weight = 67,000 kg. (148,000 lbs.); winds = 230° at 8 kts.; turbulence = light-moderate

Figure B-2.- Continued.

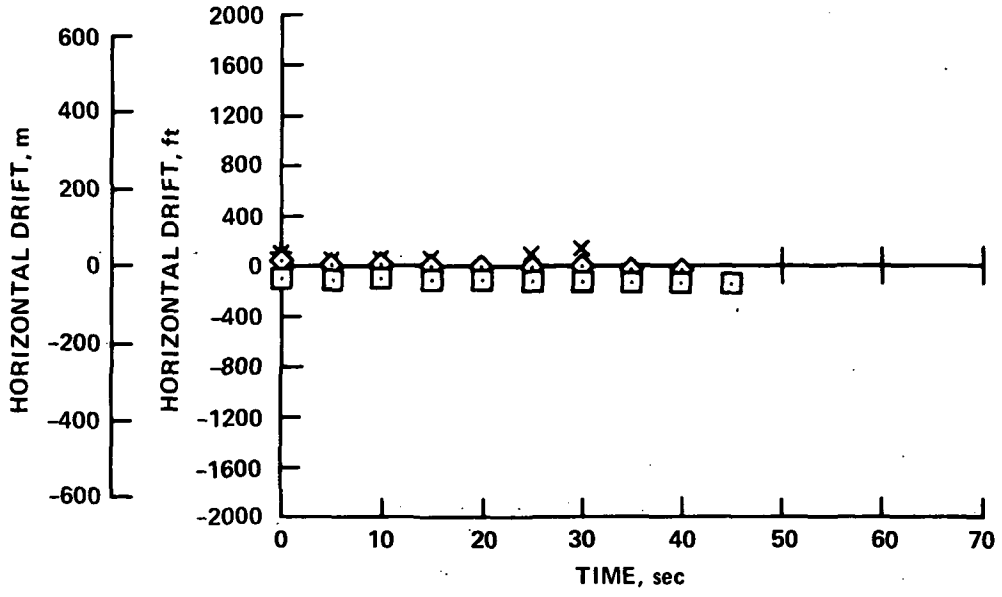

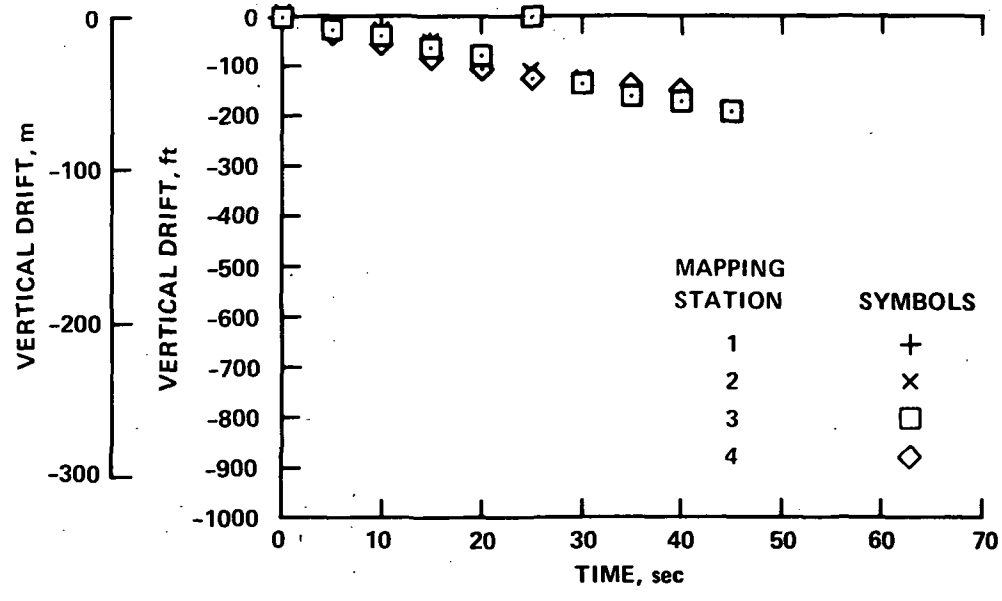

(f) Two-segment approach; flaps = 30°; airspeed = 138 kts.; weight = 69,000 kg. (151,500 lbs.); winds = calm; turbulence = smooth

Figure B-2.- Continued.

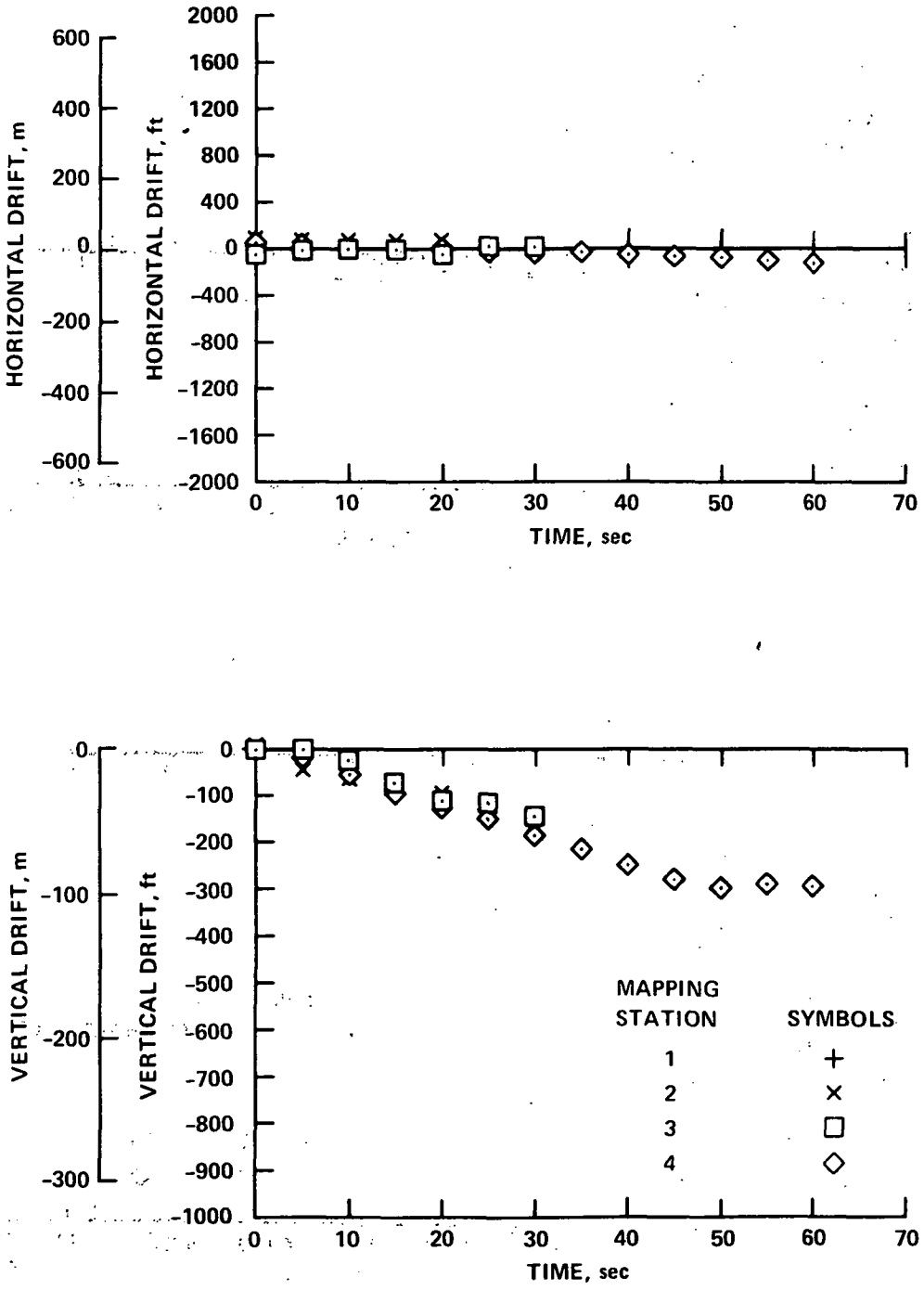

(g) Two-segment approach; flaps = 30°; airspeed = 144 kts.; weight = 67,000 kg. (148,000 lbs.); winds = 240° at 12 kts.; turbulence = light-moderate

Figure B-2.- Continued.

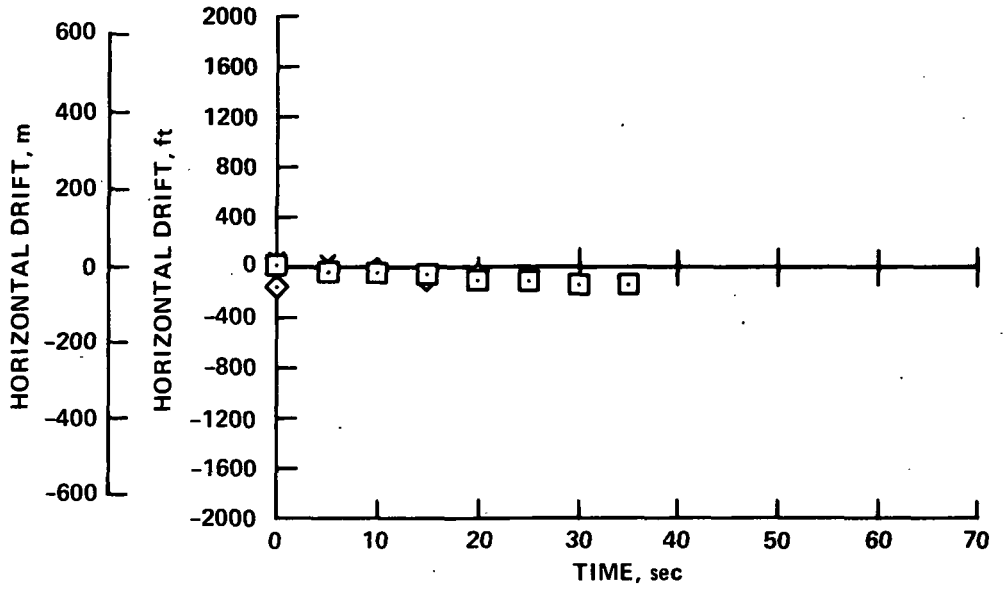

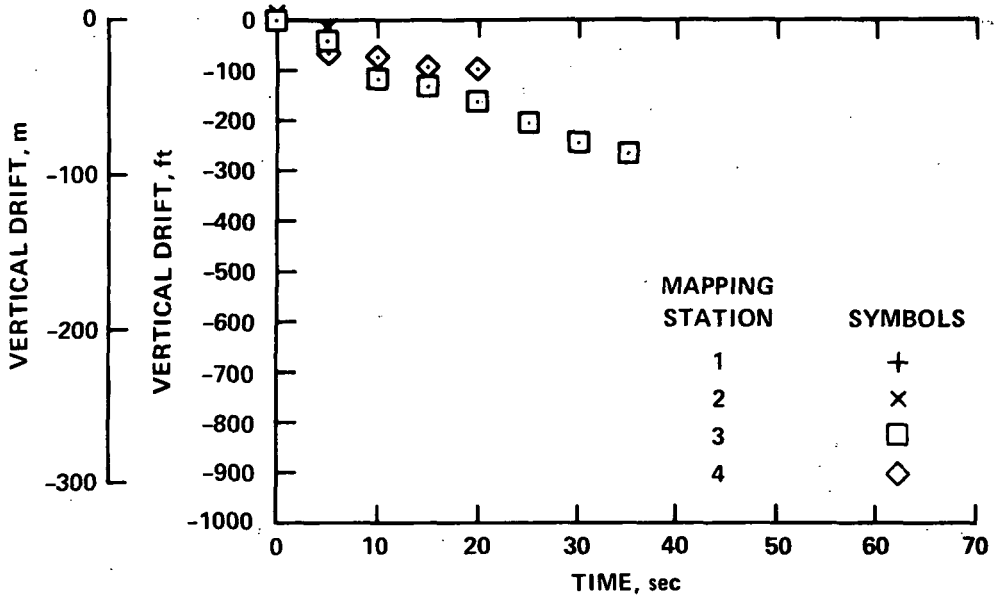

(h) Two-segment approach; flaps = 30°; airspeed = 144 kts.; weight = 68,000 kg. (150,000 lbs.); winds = 230° at 5 kts.; turbulence = light

Figure B-2.- Continued.

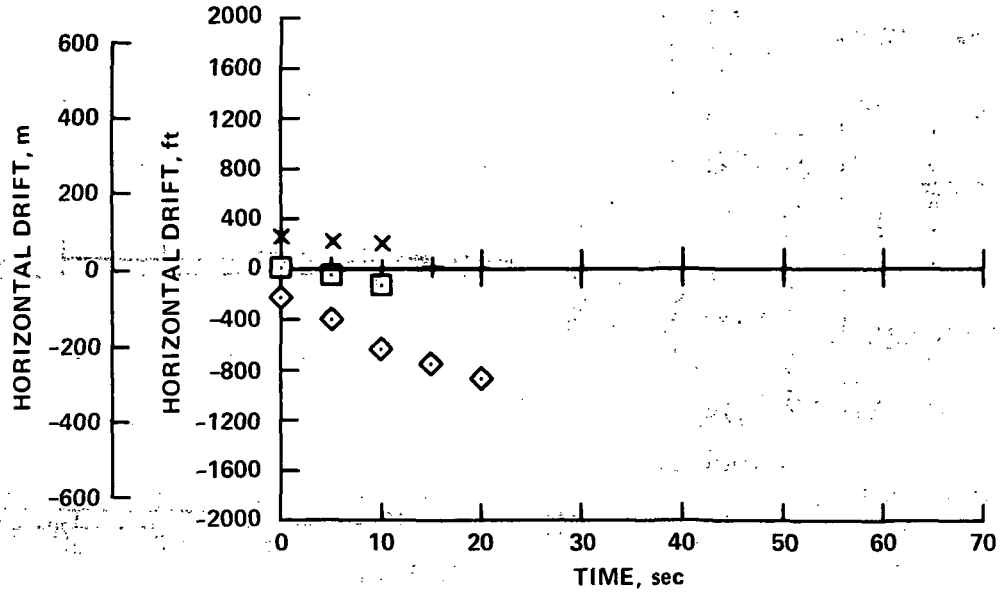

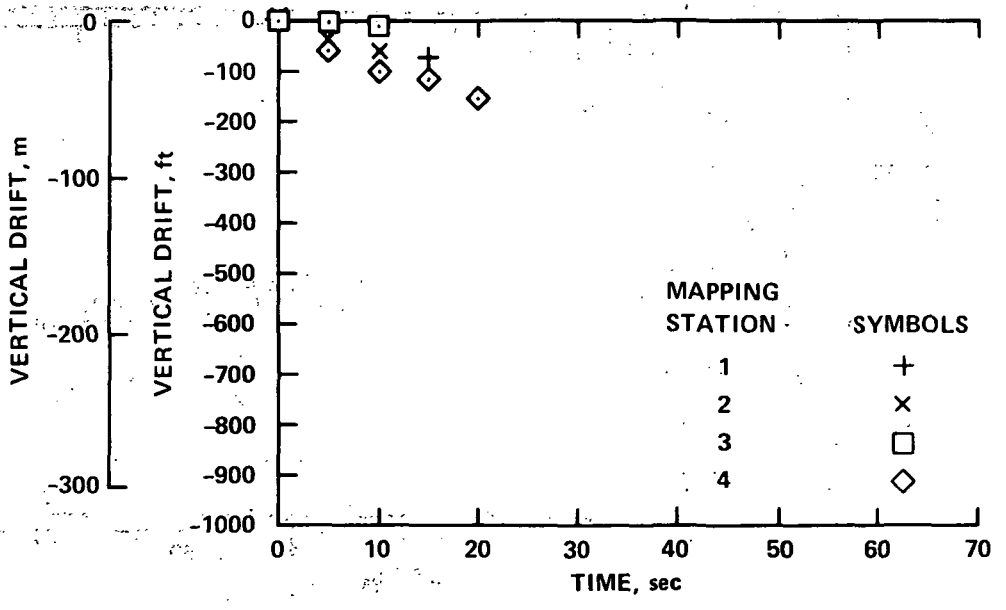

(i) Two-segment approach; flaps = 30°; airspeed = 145 kts.; weight = 65,500 kg. (144,000 lbs.); winds = 235° at 9 kts.; turbulence = light-moderate

Figure B-2.- Continued.

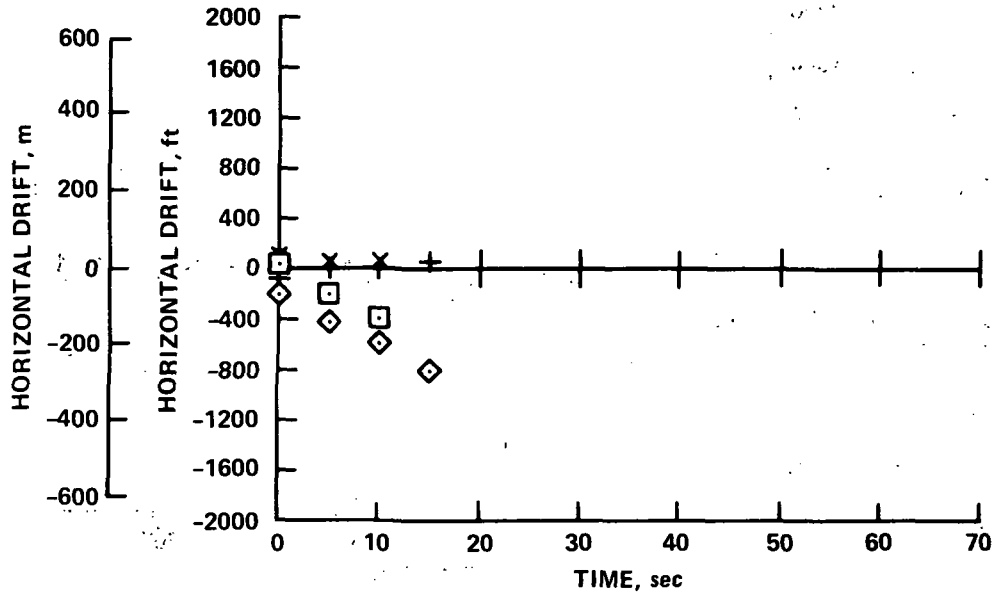

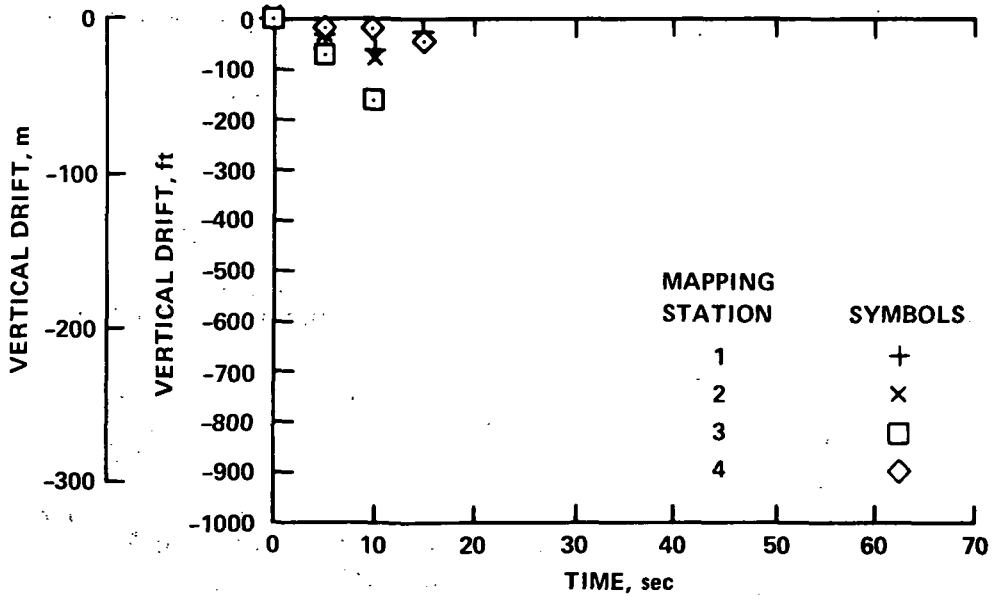

(j) Two-segment approach; flaps = 30°; airspeed = 145 kts.; weight = 69,000 kg. (151,500 lbs.); winds = 160° at 4 kts.; turbulence = light

Figure B-2.- Continued.

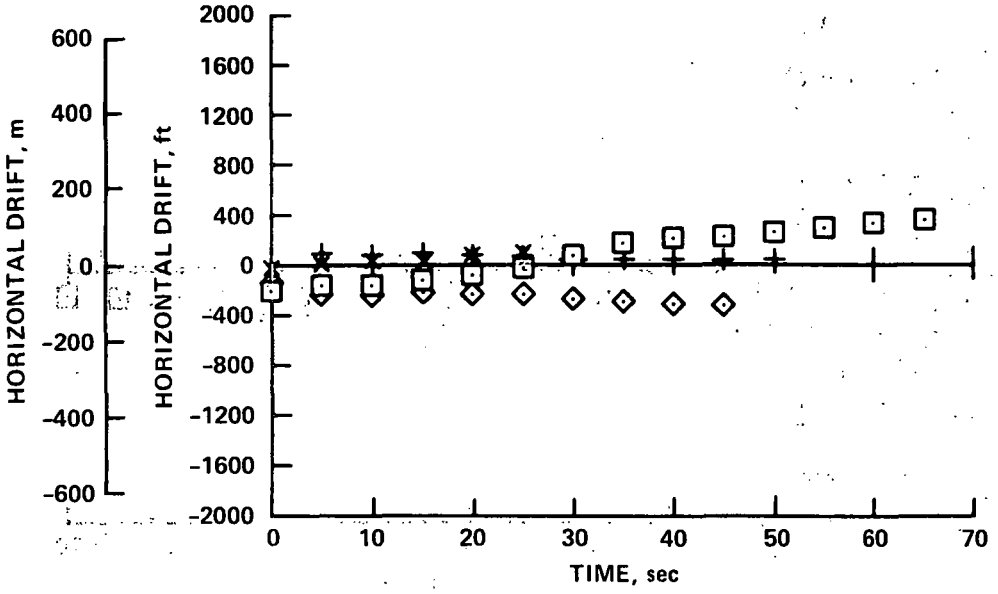

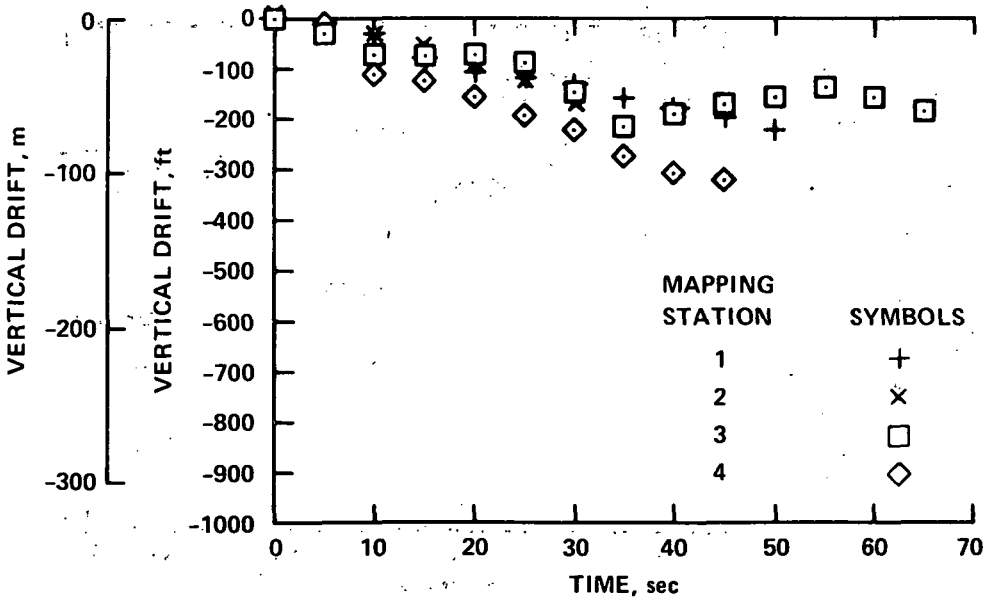

(k) Takeoff; flaps = 15°; airspeed = 220 kts.; weight = 69,000 kg. (153,000 lbs.); winds = calm; turbulence = smooth

Figure B-2.- Continued.

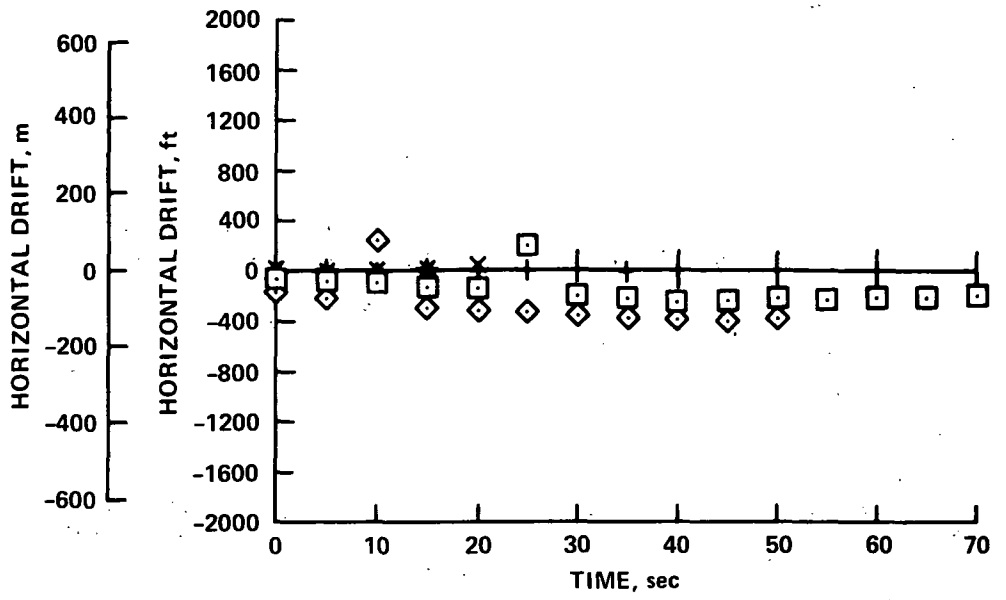

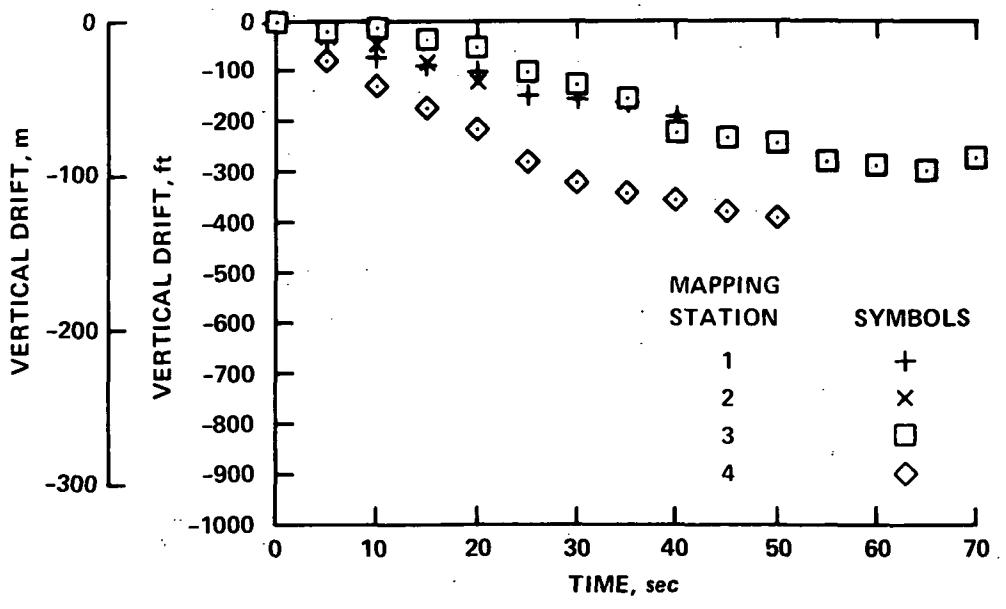

(1) Takeoff; flaps = 15°; airspeed = 160 kts.; weight = 70,000 kg. (159,000 lbs.); winds = 160° at 4 kts.; turbulence = light

Figure B-2.- Continued.

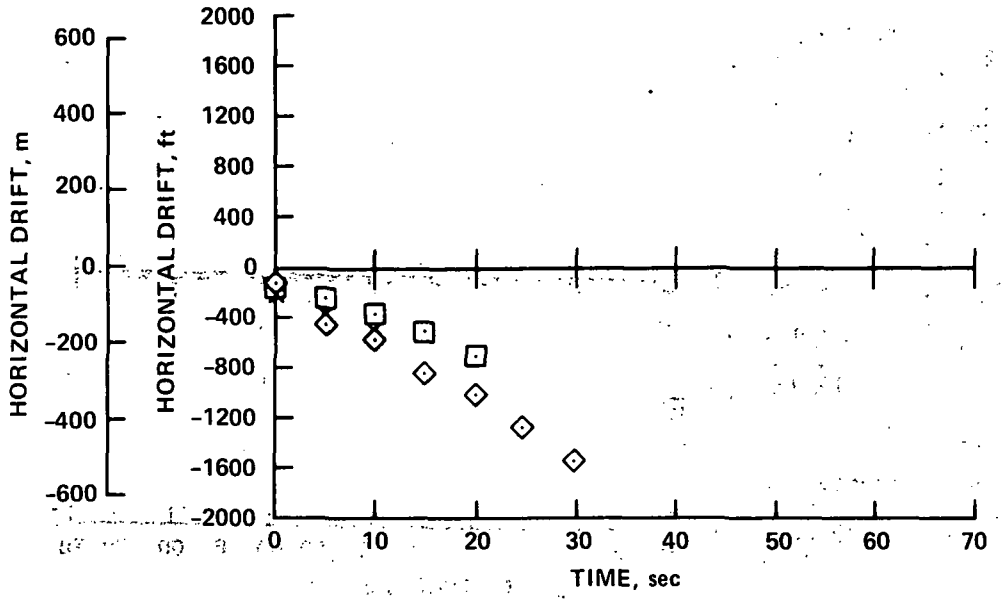

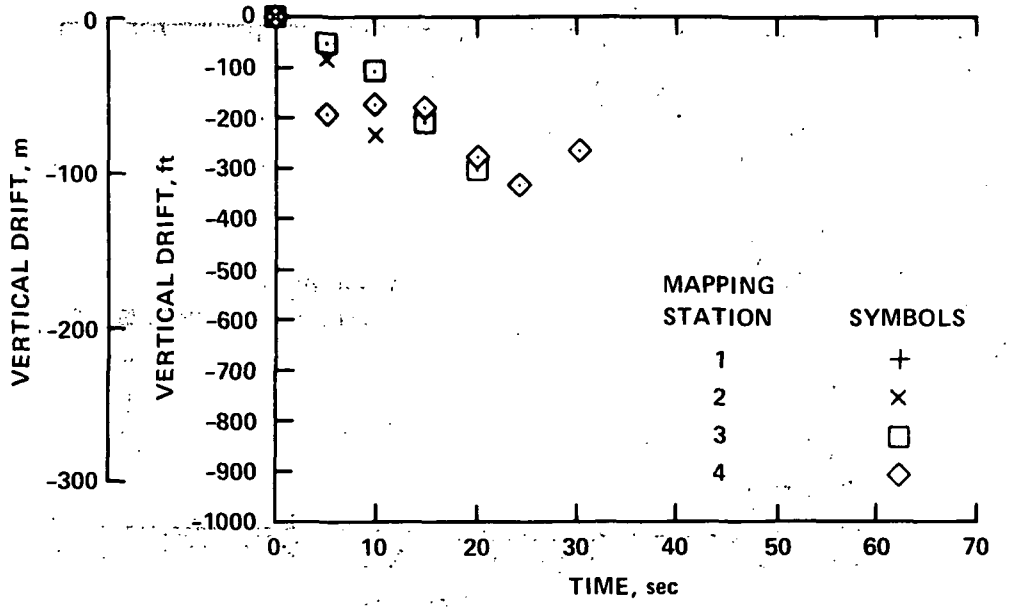

(m) Takeoff; flaps = 15°; airspeed = 160 kts.; weight = 66,000 kg. (145,500 lbs.); winds = 230° at 8 kts.; turbulence = light

Figure B-2.- Continued.

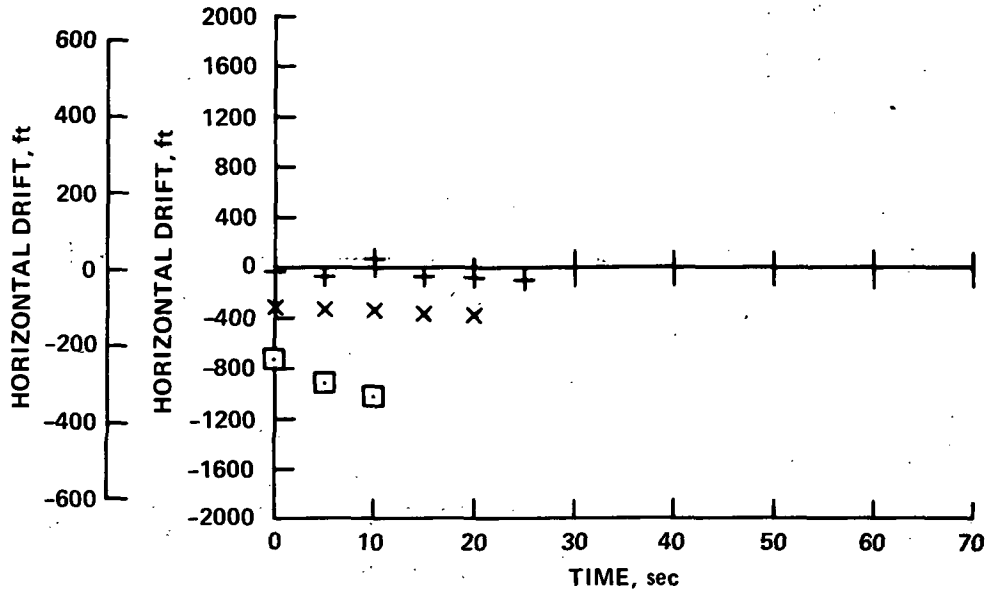

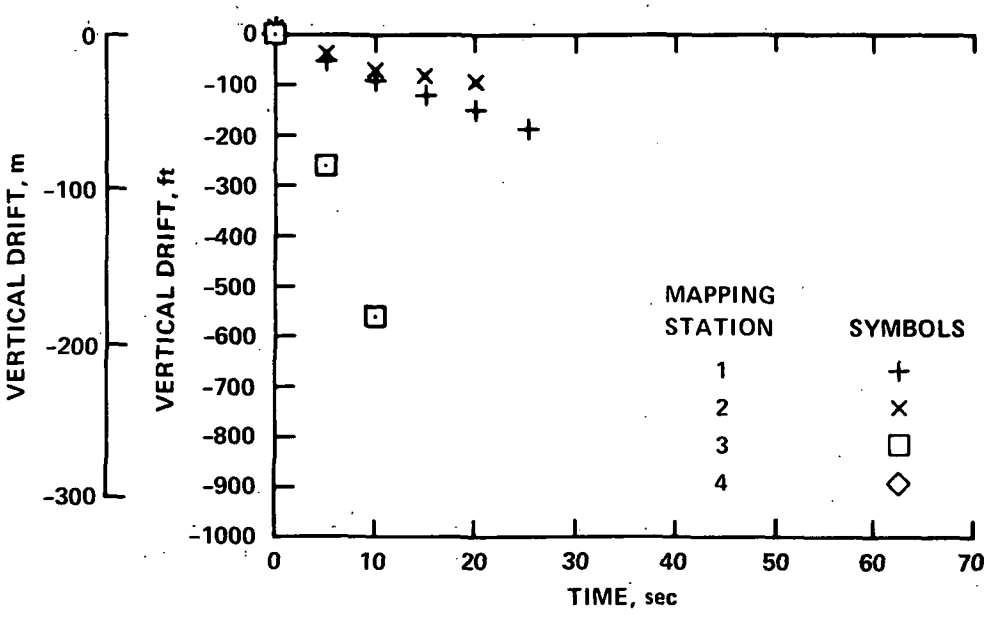

(n) Takeoff; flaps = 15°; airspeed = 200 kts.; weight = 69,000 kg. (155,000 lbs.); winds = 160° at 4 kts.; turbulence = light

Figure B-2.- Concluded.